

AD-A057 933

BENDIX CORP BALTIMORE MD COMMUNICATIONS DIV  
DESIGN, FABRICATION, AND TESTING OF A BRASSBOARD MODEL ATCRBS B--ETC(U)

F/G 17/7

JUN 78 A L BROCKWAY, J B KUHL, P J WOODALL

DOT-TSC-769

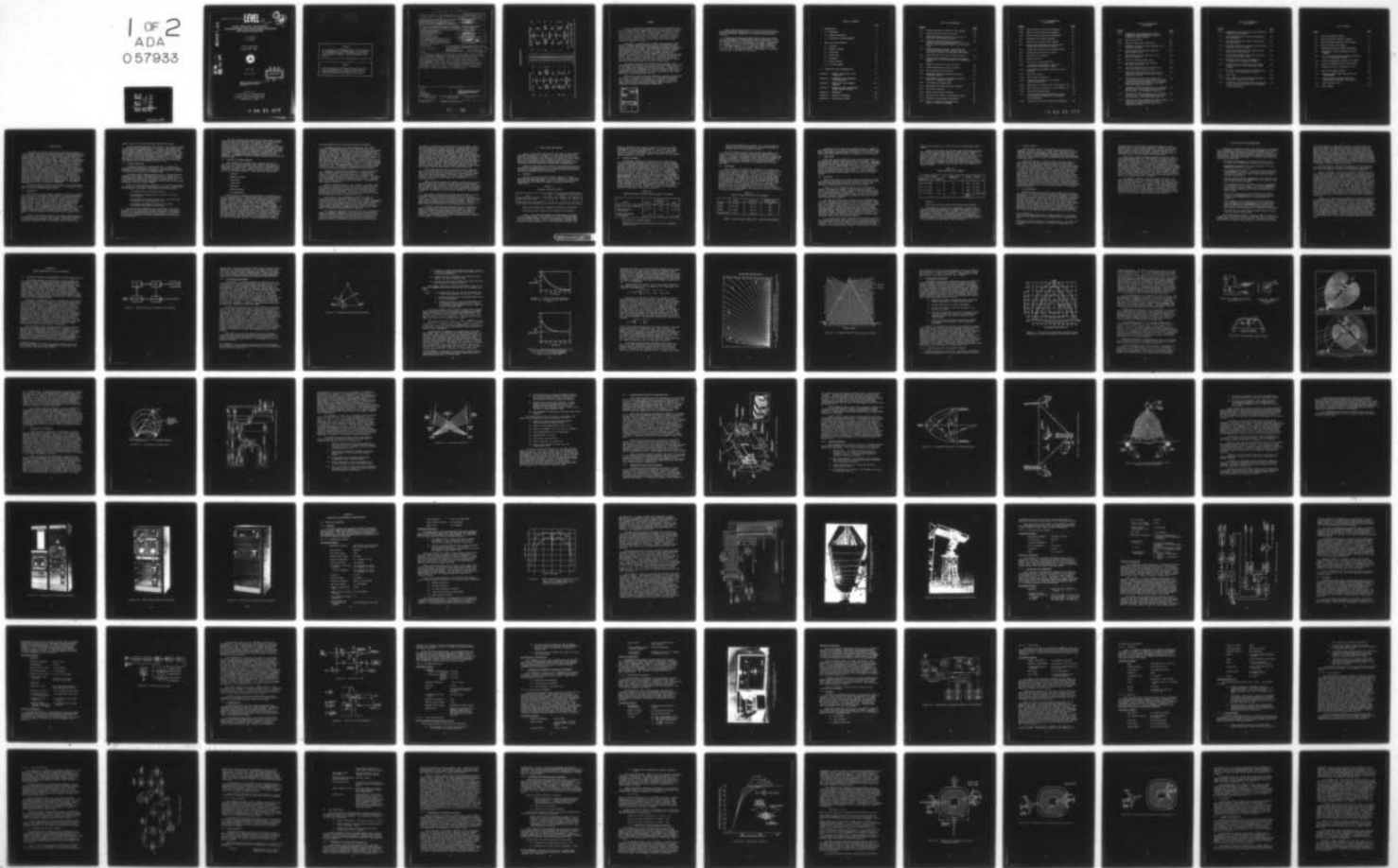
UNCLASSIFIED

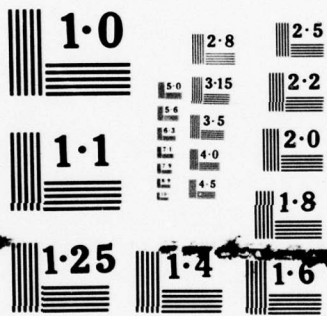
BENDIX-489A09A

FAA-RD-78-63

NL

1 of 2  
ADA  
057933





NATIONAL BUREAU OF STANDARDS  
MICROCOPY RESOLUTION TEST CHART

REPORT NO. FAA-RD-78-63

# LEVEL

III

A051148

13  
#2  
JC

## DESIGN, FABRICATION, AND TESTING OF A BRASSBOARD MODEL ATCRBS BASED SURFACE TRILATERATION DATA ACQUISITION SUBSYSTEM

A.L. Brockway  
J.B. Kuhl  
P.J. Woodall

Bendix Corporation  
East Joppa Road  
Baltimore MD 21204



JUNE 1978

FINAL REPORT

DDC  
AUG 23 1978

E

DOCUMENT IS AVAILABLE TO THE U.S. PUBLIC  
THROUGH THE NATIONAL TECHNICAL  
INFORMATION SERVICE, SPRINGFIELD,  
VIRGINIA 22161

Prepared for  
U.S. DEPARTMENT OF TRANSPORTATION  
FEDERAL AVIATION ADMINISTRATION  
Office of Research and Development  
Washington DC 20590

ADA 057933

AD No.  
DDC FILE COPY

78 08 21 003

NOTICE

This document is disseminated under the sponsorship of the Department of Transportation in the interest of information exchange. The United States Government assumes no liability for its contents or use thereof.

NOTICE

The United States Government does not endorse products or manufacturers. Trade or manufacturers' names appear herein solely because they are considered essential to the object of this report.

88052070A

DDC LIFE COB

NO 0A

8 08 21 008

14 BENDIX-489A09A

1. Report No. 18 FAA-RD-78-63	2. Government Accession No. 19 FAA-RD, TSC.	3. Recipient's Catalog No. 78-63, FAA-78-7
4. Title and Subtitle 6 DESIGN, FABRICATION, AND TESTING OF A BRASSBOARD MODEL ATCRBS BASED SURFACE TRILATERATION DATA ACQUISITION SUBSYSTEM	5. Report Date 11 June 1978	6. Performing Organization Code
7. Author 10 A.L./Brockway, J.B./Kuhl P.J./Woodall	8. Performing Organization Report No. DOT-TSC-FAA-78-7 Bendix 489A09A	9. Performing Organization Name and Address 15 Bendix Corporation* Communications Division East Joppa Road Baltimore MD 21204
12. Sponsoring Agency Name and Address U.S. Department of Transportation Federal Aviation Administration Office of Research and Development Washington DC 20590	10. Work Unit No. (TRAIS) FA821/R8113	11. Contract or Grant No. DOT-TSC-769
15. Supplementary Notes *Under contract to:	13. Type of Report and Period Covered 9 Final Report June - Dec 1977	14. Sponsoring Agency Code
16. Abstract Field test results are emphasized in this report, which also contains background information on Airport Surface Traffic Control (ASTC) and the contract objectives. The National Aviation Facilities Experimental Center (NAFEC) field test series conclusively proved the technical feasibility of an Air Traffic Control Radar Beacon System (ATCRBS) based Airport Surface Traffic Control sensor system. Operational Data Acquisition Subsystem (DAS) performance projections developed to date as a result of the National Aviation Facilities Experimental Center test series are presented, and a recommendation for pursuit of Contract Option 2 is substantiated.		
17. Key Words ASTC ATCRBS Transponder Surveillance	18. Distribution Statement DOCUMENT IS AVAILABLE TO THE U.S. PUBLIC THROUGH THE NATIONAL TECHNICAL INFORMATION SERVICE, SPRINGFIELD, VIRGINIA 22161	
19. Security Classif. (of this report) Unclassified	20. Security Classif. (of this page) Unclassified	21. No. of Pages 186
		22. Price

402 895

Lee



PREFACE

The U.S. Department of Transportation gave the responsibility to the Transportation Systems Center (TSC) for development of airport surface traffic control (ASTC) systems required to meet the present and future needs of the FAA and airport users. The primary objective of Contract DOT-TSC-769 is to establish the feasibility of an ATCRBS based trilateration data acquisition subsystem for airport surface traffic surveillance. This report is the final report on Task 2B of that contract, fabrication field testing of the ASTC brassboard equipment at NAFEC.

Analysis<sup>1,2</sup> indicated that a system using a spatial combination of ATCRBS sidelobe suppressions and interrogations will satisfy all major ASTC sensor requirements in the FAA's Upgraded Third Generation ATC system. The GEOSCAN<sup>®</sup>(for Geographic Scanning) technique developed by Bendix forms the basis for such a system. Using GEOSCAN, discrete aircraft on an airport surface can be selectively interrogated. ATCRBS transponder replies from addressed aircraft can then be processed to locate and identify the target. The trilateration process (i.e. measuring time-of-arrival of the reply at three or more stations) can be used to provide data to compute aircraft location, while aircraft identity can be obtained by decoding pulses in the reply signal train.

The NAFEC test series from August through November 1975, demonstrated that GEOSCAN works and proved the technical feasibility of the ATCRBS based surface trilateration concept. Compatibility of this system with ATCRBS/ARTS III and NAS Stage A systems was investigated during the NAFEC test series and results show that ATC operational system performance will not be degraded by the implementation of ATCRBS based ASTC systems.

Although the NAFEC tests were successful and most encouraging, the scope of the tests was limited due to the NAFEC environment. It is clear, therefore, that Option 2 to Contract DOT-TSC-769, which requires testing of the Brassboard system at a relatively high traffic density operational airport (Logan, Boston), is necessary and should be undertaken immediately.

ACCESSION for		
NTIS	Write Section	<input checked="" type="checkbox"/>
DDC	Duff Section	<input type="checkbox"/>
UNANNOUNCED		<input type="checkbox"/>
JUSTIFICATION.....		
BY.....		
DISTRIBUTION/AVAILABILITY CODES		
Dist. AVAIL. and/or SPECIAL		
A		

This contract was administered by the TSC Airport Surface Surveillance Section under John W. O'Grady and was conducted by the ATC Engineering Department of the Bendix Communications Division.

During the course of the NAFEC test program, many people at TSC (Cambridge), FAA/NAFEC and at Bendix contributed to its successful completion. In particular, the authors wish to thank M. J. Moroney of TSC for his direction and support throughout the program. Also, the contributions and helpful comments of J. L. McCormick (Bendix), J. D. Vinatieri (MITRE, Bedford), Dr. R. D. Kodis (TSC), Harry Jackson (FAA/NAFEC), Dr. S. Ross (S. Ross & Co.) and those many others, too numerous to enumerate properly here, are sincerely appreciated.

SEARCHED		INDEXED
<input checked="" type="checkbox"/>	SEARCHED	INDEXED
<input type="checkbox"/>	SEARCHED	INDEXED
<input type="checkbox"/>	SEARCHED	INDEXED
SERIALIZED		FILED
APR 19 1964		FBI - BOSTON
FBI - BOSTON		APR 19 1964
FBI - BOSTON		APR 19 1964
FBI - BOSTON		APR 19 1964
FBI - BOSTON		APR 19 1964

## TABLE OF CONTENTS

	PAGE
1. INTRODUCTION	1
1.1 BACKGROUND	1
1.2 PROGRAM OBJECTIVES	2
1.3 OVERVIEW OF ACCOMPLISHMENTS	3
2. NAFEC FIELD TEST RESULTS	7
2.1 ACCURACY	7
2.2 SURFACE COVERAGE	8
2.3 RESOLUTION	9
2.4 UPDATE RATE	10
2.5 MULTIPATH	10
2.6 VEHICLE EFFECTS	12
2.7 RF INTERFERENCE	12
3. CONCLUSIONS AND RECOMMENDATIONS	15
APPENDIX A SUMMARY DESCRIPTION OF DAS OPERATION	17
APPENDIX B BRASSBOARD DAS PERFORMANCE CHARACTERISTICS	49
APPENDIX C NAFEC FIELD TEST PROGRAM SUMMARY	107
APPENDIX D SUMMARY OF WORK ACCOMPLISHED UNDER CONTRACT OPTION 1	167
APPENDIX E REFERENCES	169
APPENDIX F REPORT OF INVENTIONS	171
APPENDIX G DEFINITION OF TERMS	173

## LIST OF ILLUSTRATIONS

<u>FIGURE</u>		<u>PAGE</u>
A-1	System Functional Information Flow Diagram	18
A-2	Generalized TOA Position Location	20
A-3	Predicted Standard Deviation In TOA Due to Noise Only As a Function of S/N	22
A-4	Predicted Standard Deviation in TOA As a Function of S/N with Beam Bending ( $\sigma_b = 1.8$ ns) and Non Range Dependent Errors ( $\sigma_f = 10.2$ ns) Fixed	22
A-5	Idealized Total Path Loss (Free Space Plus Vertical Multipath Fade) Contours from an Interrogator Antenna 18 Feet Above the Surface	24
A-6	Predicted TOA Error Vector Versus Position	25
A-7	Single Triad Trilateration Accuracy Contours Estimated For a Two Mile Baseline Trilateration System	27
A-8	ATCRBS Interrogation Characteristics	29
A-9	ATCRBS ASR/ARSR SLS Antenna Patterns	29
A-10	Basic Geoscan Antenna Pattern	29
A-11	Suppressor Station Transmission Showing Suppressed Regions	30
A-12	Interrogator Station Transmission Showing Additional Suppressed Regions	30
A-13	Interrogator Coverage Zones	32
A-14	Brassboard DAS Simplified Block Diagram	33
A-15	System Scan Geometry	35
A-16	Master Station Trailer Details	38
A-17	Brassboard DAS Layout for Maximum Coverage	40
A-18	Brassboard DAS Equipment Deployment	41
A-19	Typical Brassboard Equipment Siting (Detail of Stations Enlarged)	42

LIST OF ILLUSTRATIONS  
(continued)

<u>FIGURE</u>		<u>PAGE</u>
A-20	Master Station Electronics Equipment	45
A-21	Slave Station Electronics Equipment	46
A-22	Receive Station Electronics Equipment	47
B-1	Brassboard DAS Antenna Patterns	51
B-2	Phased Array Antenna Block Diagram	53
B-3	Phase Array Antenna During Construction Showing Horn and Monopole Details	54
B-4	Phased Array Antenna During Range Testing	55
B-5	Transmitter Module Block Diagram	58
B-6	Receiver Block Diagram	61
B-7	Basic PAE Circuit	63
B-8	PAE Circuit Timing Waveforms	63
B-9	Calibration Transponders (Left) and Instrumented Transponder (Right)	67
B-10	Instrumented Transponder Simplified Block Diagram	69
B-11	Data Flow Concept	75
B-12	Interrogator Resolution	81
B-13	Geoscan Cell Coverage of Two Close Proximity Aircraft	83
B-14	Same Cell as in Figure B-13, but Steered $.25^\circ$	84
B-15	Same Cell as in Figure B-14, but Steered $.25^\circ$	85
B-16	Track Width Versus Range	88
B-17	Angular Relationships between the $P_2$ and $P_1$ Patterns as Determined by Transponder SLS Performance	88
B-18	Track Width and Cell Size Control Segments	89

LIST OF ILLUSTRATIONS  
(continued)

<u>FIGURE</u>		<u>PAGE</u>
B-19	Transponder Valid Suppression Decode Probability (Normal Distribution about Referenced Points Assumed)	92
B-20	Peak Angle Defined	103
B-21	Range at Which First Peak Occurs	103
C-1	Benchmark Positional Errors Compared With Predicted Accuracy	114
C-2	Raw DAS Data Vs Theodolite Track For Moving Target Test	117
C-3	Positional Error and Velocity During Moving Target Test	118
C-4	Portion of Moving Target Track	120
C-5	Two Target Resolution Test Results. DAS Tape 0205, File 5	121
C-6	Two Target Resolution Tests at Point A2 (Test on 8/22/75; $P_2/P_1 = 6$ dB)	125
C-7	Two Target Resolution Tests at Point A2 (Regions within which each Target replies with $P_2/P_1 = 6$ dB)	127
C-8	Reply Count for Four Scans Versus Pairs of Steering Directions from Master and Slave Stations Steering Increments of 0.25 Degrees Gulfstream Aircraft Located at Point B84 (Data from Tape 3339, File 9)	129
C-9	Histogram of Reply Probability for the Master Station with a Gulfstream Aircraft at Point B84 and $P_2/P_1 = 7$ dB (Tape 3339, File 9)	130
C-10	Histogram of Reply Probability for the Slave Station with a Gulfstream Aircraft at Point B84 and $P_2/P_1 = 3$ dB (Tape 3339, File 9)	132
C-11	Histogram of Reply Probability for the Master Station with a Test Vehicle 100 Feet Southwest of Point B84 and $P_2/P_1 = 5$ dB (Tape 3339, File 9)	133

LIST OF ILLUSTRATIONS  
(continued)

<u>FIGURE</u>		<u>PAGE</u>
C-12	Brassboard DAS Interrogation Cell Boundaries (Operation at Boresight)	137
C-13	Projected Operational Sensor Interrogation Cell Boundaries	139
C-14	Projected Operational Sensor Interrogation Cell Boundaries	140
C-15	Multipath Search Area (Shaded) and Multipath Evaluation Points at NAFEC	143
C-16	Calibration Photo Log Video Showing 10 dB Step in Input Attenuation	144
C-17	Master Station Reply Video Form Test Point MB Showing Multipath Levels	146
C-18	Multipath Levels Versus Percentage of Coverage Area as Measured at NAFEC	146
C-19	Probability of at Least Two Out of Three Valid ID's Based on Multipath Data Taken at NAFEC	148
C-20	F1 Pulse and the Resulting Multipath Signal From MIO, 1 Microsecond per Division	148
C-21	NAFEC Tower	149
C-22	Total Number of Interrogations Required to Achieve 200 Updates per Second	154
C-23	Probability of Achieving a Given Update Rate ( $n_T n_U$ ) Versus Round Reliability and Number of Reinterrogations	156

## LIST OF TABLES

<u>TABLE</u>		<u>PAGE</u>
2-1	POSITION LOCATION ACCURACY	7
2-2	POWER REQUIRED TO ACHIEVE COVERAGE	8
2-3	MULTIPLE TARGET RESOLUTION TEST SUMMARY	9
2-4	NAFEC MULTIPATH DATA SUMMARY	11
B-1	INTERROGATION TRACK SEGMENT PARAMETERS	90
B-2	INTERROGATION TRACK PARAMETERS FOR EACH SEGMENT	91
B-3	1.5 to 2 NMI TRACK WIDTH SEGMENT PROJECTION FOR THE OPERATIONAL SYSTEM	91
B-4	LOCATION INDEPENDENT RECEIVER SITE ERRORS	95
B-5	LOCATION DEPENDENT RECEIVER SITE ERRORS	95
B-6	REFERENCE SIGNAL TO NOISE RATIO (S/N) .	97
C-1	NAFEC TEST PROGRAM SUMMARY	112
C-2	RESULTS OF NAFEC FIELD TEST BENCH MARK MEASUREMENTS	115
C-3	POSITION ERROR FOR TEST VEHICLE AND CALIBRATION TRANSPONDER MEASUREMENTS	119
C-4	NAFEC MULTIPATH DATA	145
C-5	TEST SCHEDULE	157

## 1. INTRODUCTION

This report covers work performed by the Bendix Communications Division (BCD) through January 1976 under Contract DOT-TSC-769 for the design, fabrication and field testing of a brassboard model ATCRBS based trilateration data acquisition subsystem (DAS) for Airport Surface Traffic Control (ASTC). This work is an integral part of the on-going ASTC program being conducted for the Department of Transportation (DOT), Federal Aviation Administration (FAA), by the Transportation Systems Center (TSC). In order to establish the technical feasibility of a surveillance technique for Airport Surface Traffic Control based on the Air Traffic Control Radar Beacon System (ATCRBS), a brassboard model of the Data Acquisition Subsystem (DAS) was designed and built by Bendix. This brassboard system contains the equipment necessary to selectively interrogate, detect, and record the position and identity of vehicles on the airport surface. This is accomplished by use of the GEOSCAN, (acronym for Geographic Scanning) interrogation technique and by means of time-of-arrival (TOA) measurements made at three sites on ATCRBS transponder replies from target vehicles. The DAS was field tested at NAFEC to verify the feasibility and performance capability predicted by theoretical analysis.<sup>2</sup>

This report contains results of the NAFEC field tests along with a digest of data previously reported<sup>1,2,3</sup> by Concept Analysis Task 1 A, and DAS Hardware Design Task 2A.

### 1.1 BACKGROUND

ASTC is one of the nine major programs in the FAA's upgraded third generation ATC system (UG3RD) aimed at improving performance, safety and cost. The UG3RD will provide for all-weather surveillance, guidance and control of increased numbers of aircraft to meet the needs of the 1980's and 1990's. The National Aviation System Plan for Fiscal Years 1976-1985 calls for "establishing modern airport surface guidance and air traffic detection and control aids." As the technology arm of the Department of Transportation (DOT), Transportation Systems Center (TSC) was given responsibility for undertaking the ASTC R&D program under the Airport Safety and Facilities Support Branch (ARD-420), Airport Division, Systems Research and Development Service (SRDS) of the FAA.

Contract DOT-TSC-769, awarded to the Bendix Communications Division by the TSC called for the "design, fabrication and testing of a brassboard model ATCRBS based surface trilateration data acquisition subsystem" which, if feasible, would be used as the

sensor input in the Advanced Surface Surveillance System.

The major problem arising from the use on the airport surface of existing ATCRBS transponders is the mutual interference caused by overlapping transponder replies. A solution was invented by Bendix using a method of discrete transponder interrogation that takes advantage of existing attributes of the ATCRBS system. This new concept, GEOSCAN is essentially a form of bistatic interrogation tailored to provide time/space addressability. This system can elicit a reply from one surface aircraft at a time. Aircraft positions can then be determined using trilateration techniques and identity also can be obtained from the reply.

## 1.2 PROGRAM OBJECTIVES

The major objective of this program was to evaluate the feasibility and operational potential of an ATCRBS based surface trilateration data acquisition subsystem (DAS) through the design, fabrication and testing of a brassboard model.

The beacon based systems program is one of several programs underway at TSC aimed at developing technology to support an integrated ASTC system. The fabrication and testing of the brassboard system was considered a key effort because identity of aircraft is required and the equipment must function in the airport environment with the existing ATCRBS.

Given the constraints of operating in the airport environment and meeting the operational requirements stipulated in Exhibit One of the Contract, the aims of this contract can be stated as:

- . To measure how well the DAS performed;
- . To evaluate the compatibility of the DAS with other ATC functions;
- . To ascertain the effects of multipath, fruit and other interference on DAS performance; and
- . To determine the extent to which line-of-sight interference degraded DAS performance.

The DAS was not configured in an operational form so the evaluation of its operational potential was based on analytical studies as validated by empirical data obtained by field testing. The data base established from field test results was used in developing preliminary performance characteristics for an operational ASTC DAS.

The basic contract was organized into three tasks; Concept Analysis, Hardware Development and a NAFEC Field Testing Program. Three optional tasks were also included for the purpose of gathering additional test data at operational airports. This program proceeded in parallel with a TSC ASTC system study defining the requirements of a complete surface surveillance system.<sup>4</sup> The brassboard equipment was simplified as much as possible to minimize costs and development time. It resembles an operational DAS only with respect to the basic RF processes of interrogation and reception. A summary description of DAS operation is given in Appendix A and Appendix B gives performance characteristics for the brassboard DAS.

### 1.3 OVERVIEW OF ACCOMPLISHMENTS

This program was initiated with a contract award on 10 June 1974. The concept analysis study, Task 1A, was started at that time and a draft report based on contract requirements was submitted on 1 August 1974.<sup>1</sup> That report was revised at TSC's request to address critical technical issues on which the feasibility of the concept depends.<sup>2</sup> These seven key issues were:

- . ACCURACY
- . SURFACE COVERAGE
- . RESOLUTION
- . UPDATE RATE
- . MULTIPATH
- . VEHICLE EFFECTS
- . RF INTERFERENCE

Task 1A Concept Analysis was completed on 30 November 1974 with the submission of an Interim Design Report<sup>3</sup> which included an initial hardware design. Authorization was received from TSC in December 1974 to proceed with Task 2A, brassboard hardware fabrication. The Critical Design Review (CDR) of the brassboard hardware was held on 22 January 1975. The brassboard system, which is discussed in detail in Section 4., consists of three transportable stations together with additional test equipment and instrumentation used to calibrate test vehicles. Two of the stations contain an interrogator and a null steering phased array antenna. The third station contains a TOA receiver to complete the three station trilateration network. The three stations are interconnected by microwave links for the transmission of timing and steering data, and the transfer of test data to a single recorder at the Master Station. A voice communications network

was established for test control and direction purposes.

The Master Station has a Test Control Unit (TCU) which controls the sequencing and timing of interrogations, reply reception, and antenna scanning. This unit is manually programmed to conduct each test. Steering and interrogation commands are supplied in real time to the remote, or slave interrogator station via the microwave link. Three TOA counters and identity (ID) decoders are present in the Master station to measure signals from each receiver. These data are recorded in digital form on a high speed magnetic tape recorder along with DAS steering information and interrogation timing data. TOA and identity data can also be read out on a display in the Master station. The tapes recorded during each test were supplemented by test engineer observations (engineer's log). Processing of tapes was accomplished off-line at TSC using software programs developed under this contract.

Physically, each station consists of a trailer with an AC power generator, heating air conditioning, an antenna support tower, a DAS antenna, a microwave data link, communications antennas as required, and a DAS electronics equipment rack containing equipment required at that particular station. The system is transportable and requires neither permanent (e.g., concrete pads) site preparation nor electrical-mechanical interfaces with other airport facilities.

Task 2B required testing of the brassboard at NAFEC. Also included were the test planning, test analysis, data processing and software development. To meet the program schedule, the planning and software development work were conducted while the hardware was being fabricated. The Task 2B software CDR was held at TSC on 12 March 1975 at which time the software programs were demonstrated in the TSC computer facility.

Installation of the brassboard at NAFEC was begun on 7 August 1975 and the system was operational on 14 August in accordance with the test plan. The field test program was designed to gather field test data in each of the identified key technical areas. Tests were performed first using fixed targets, then single moving targets, and finally multiple targets. Test vans instrumented with beacon transponders were used in early tests. Later in the series, FAA aircraft were employed.

Five ATCRBS interference evaluation tests were conducted at NAFEC to assess the compatibility of the DAS with the existing ATCRBS environment. The DAS was synchronized to operate in the dead time of the NAFEC ASR-4 (as it would be in an operational system) to preclude interference with this operational site. During the first interference evaluation test, the DAS PRF was

set equal to the ASR-4's (approximately 380 per seconds) and the DAS was periodically turned on and off as the DAS power output was increased from minimum to maximum. Observers were stationed at the Philadelphia and Washington-National TRACONS and at the Islip-New York and Leesburg - Virginia, ARTCC's to record any sign of interference with ATC operations. These observers also obtained ARTS III data extraction tapes and NAS Stage A COMDIG and DART printouts to quantitatively evaluate effects of the DAS on ATRBS performance. Controller comments during the tests also were collected. The last interference evaluation was performed on November 18, 1975 between 6PM and midnight at DAS PRF's of 380, 760 and 1520 per second. These data were taken to magnify any effect the DAS might have on the ATRBS environment. The highest PRF exceeds expected requirements of an operational DAS.<sup>4</sup>

Forty-eight DAS tests were planned and 42 were completed prior to the conclusion of the NAFEC series on 18 November 1975. Each test usually required a four-hour period with one and sometimes two tests being conducted each day. Test scheduling was planned so that, when possible, the ASTC Program would not conflict with other on-going NAFEC test activities, i.e., (MLS, ILS, B-CAS, etc.).

Bendix provided personnel to operate and maintain the brass-board equipment and to perform DAS data processing and analysis. The test team which scheduled, coordinated and performed the brass-board tests at NAFEC consisted of TSC, NAFEC and Bendix personnel as described in Appendix C. This team was augmented by controllers at terminal and enroute sites during the conduct of interference tests.

The GEOSCAN interrogation sequence was performed in a pre-programmed manner and reply data was recorded for post test analysis. The reply data was processed off-line to generate discrete target reports for each interrogation-reply round containing target position measurements and decoded identity. Expected operational performance was predicted from specific test data and from extrapolated statistical data developed from the tests.

A wealth of test data was obtained during the NAFEC field tests to evaluate the seven key technical issues. A good percentage of these data was redundant, provided a data base for comparing similar performance characteristics under varying conditions. These data were analyzed to answer questions concerning concept feasibility and system performance and a synopsis of the results is presented here.

## 2. NAFEC FIELD TEST RESULTS

Results of the field test program show that the basic ATCRBS Trilateration approach is feasible. In the seven key technical areas of investigation, the NAFEC test results were within acceptable tolerance limits of the analytically predicted values. There was never an indication that the DAS as a whole or any of its functional subsystems had basic shortcomings or performance limitations which would jeopardize an operational implementation.

While the results are very positive, they should not be misconstrued as a demonstration of a prototype operational DAS since the basic brassboard system was only a test tool used to evaluate feasibility as defined by the key issues.

### 2.1 ACCURACY

Position location accuracy obtained within the triangle formed by the three stations is as shown in Table 2-1. This table was generated from measurements made at 26 discrete surface points supplemented by more than 1000 samples acquired during moving target tests.

TABLE 2-1  
POSITION LOCATION ACCURACY

Data	Jitter ( $1\sigma$ )	Bias Error (RMS)	Total Error ( $1\sigma$ )
NAFEC Test Data (Raw) <sup>a</sup>	6.5 ft.	39.1 ft.	39.6 ft.
NAFEC Test Data (Corrected) <sup>b</sup>	6.5 ft.	10.8 ft.	12.6 ft.

<sup>a</sup>Data as recorded without applying calibration corrections.

<sup>b</sup>Known bias errors removed using calibration correction.

Jitter is the sample-to-sample error measured at one point in the coverage region. The bias error is the difference between the mean measured position and the true position, averaged (RMS) over the coverage region. Factors contributing to the bias error include long term variations in: received signal strength, time

delay in the data links, geometric dilution of precision (GDOP), multipath and clock count quantization. It can be noted that the NAFEC 1 $\sigma$  accuracy measurement of 12.6 feet is in good agreement with the Task 1A predicted value of 14.7 feet and the 3 $\sigma$  position accuracy of 39.6 feet compares favorably with the contract design objective of 100 feet.

## 2.2 SURFACE COVERAGE

The surface coverage of an ASTC DAS must be sufficient to elicit replies from any point of interest on the airport surface. In order to generate accurate position estimates from the replies received at the three trilateration stations, the siting of these stations at NAFEC was established so that 87% of all runways/taxiways was within the triangle formed by the station locations. Continuous coverage - up to 1.5 nmi range for test vehicles and 1.3 nmi for aircraft (limited by the runway layout) - was provided within this region. Moving target test data showed that line-of-sight blockage, caused by VORTAC and MLS NAVAID structures, did not prevent this continuous coverage. In order to meet the nominal reply criteria of the U.S. National Standard<sup>a</sup>, a transponder should reply at least 90% of the time when he received interrogation signal strength at the transponder's antenna output is -71 dBm. Surface coverage of an ASTC DAS is achieved wherever the vector sum of the direct path and the reflected path (vertical multipath) signals exceeds this value. Table 2-2 indicates the transmitted peak power required to achieve this condition.

TABLE 2-2  
POWER REQUIRED TO ACHIEVE VARIOUS RANGES OF COVERAGES

System	Power <sup>a</sup>	Aircraft Antenna Heights	Range
NAFEC Data Point (Measured)	31.6 W	3 feet	1.13 nmi
NAFEC Data Point (Calculated)	29.1 W <sup>b</sup>	3 feet	1.13 nmi
Operational System (Calculated)	44.8 W <sup>b,c</sup>	4 feet	2.0 nmi

<sup>a</sup> Peak effective radiated power

<sup>b</sup> Assuming an aircraft antenna gain of 0 dB and a shadowing loss of -10 dB

<sup>c</sup>The projected operational antenna has a larger horizontal aperture and vertical directivity, giving an increase in antenna gain of on the order of 10 dB.

The test results indicate that coverage requirements for a range of two nautical miles can reasonably be predicted for an operational DAS with the additional gain provided by an operational antenna. It appears, furthermore, that line-of-sight blockage and airport configuration limitations will be greater influences, in determine the location and number of DAS sites required for coverage of an airport, than the range limitations of the DAS equipment.

### 2.3 RESOLUTION

The resolution of an ASTC DAS is defined as its ability to elicit from a target of interest a reply that is not garbled by an interfering reply from another aircraft in close proximity as occurs at operational airports. The objective was to achieve 97% probability of an ungarbled reply from one of two aircraft separated by 200 feet. The NAFEC tests proved that the GEOSCAN technique could meet this objective. This was achieved by generating an interrogation cell whose center was positioned within 20 feet of the target of interest at any range out to 1.5 nautical miles. The size of the cell was adjusted by controlling the antenna aperture size (16 or 6 elements) and the  $P_2/P_1$  power ratio to provide for cell sizes ranging from 50' x 50' at .5 nm to 600' x 600' at 1.2 nm. By this means, the resolution capability indicated in Table 2-3 was achieved.

TABLE 2-3  
MULTIPLE TARGET RESOLUTION TEST SUMMARY

	Range	Separation	Probability of Correct Reply
NAFEC	1.1 nmi	130 ft.	85%
NAFEC	0.85 nmi	150 ft.	95%
NAFEC	0.5 nmi	150 ft.	>99%
Operational	2.0 nmi	150 ft.	95%

<sup>a</sup>NAFEC - measured data; Operational - predicted performance.

In addition to the two-target resolution tests, a number of other tests were run on targets to determine the reply probability versus the antenna steering angle for various  $P_2/P_1$  ratios. These tests substantiate that the desired resolution could be achieved.

#### 2.4 UPDATE RATE

NAFEC test results showed that the 2 second update rate required by the contract could be furnished by the DAS. It should be remembered; however, that this has little meaning for Brassboard operations because a preprogrammed scanning sequence was used and interrogation of a target vehicle for tracking purposes was not within the capability of the DAS. Fruit and multipath did not limit the update rate even in the presence of three operating beacon interrogators (ASR-4, ASR-5, ASR-7). Round reliabilities of greater than 90% were obtained at an update rate of 10 per second.

#### 2.5 MULTIPATH

Vertical multipath in the ASTC surface environment would be manifested by fade loss without any troublesome distortion. This effect has been predicted by theory and while it would limit coverage, it would cause no other significant problems.

Lateral or "out of beam" multipath, with its long time delays, is a potential problem in the surface environment. It could be controlled by providing adequate radiation pattern gain and a proper processing circuit design. Test results showed that the Bendix peak amplitude estimator (PAE) circuit, with its high multipath tolerance, successfully overcame the multipath signal levels encountered at NAFEC.

The time-of-arrival (TOA) detection circuit performed as designed. Multipath signals at any amplitude with delays exceeding 100 nanoseconds had no effect on the TOA measurements. Likewise, the identity (ID) detection circuit, functioned as designed when the multipath signals were 3 dB or more below the direct (desired) signal. Careful searches were made along the NAFEC runway/taxiway network within the DAS coverage region for severe multipath signals. Multipath signals affecting the DAS were detected by signal processing in the receiver PAE circuit, since the sector omni (120°) receiving antennas at all stations intercepted any and all multipath signals present.

In an operational system, multipath discrimination could be greatly enhanced by the simple addition of a sum-beam network to the phased array antenna in order to form a narrow beam pattern on receive. Also, as only one or two out of three valid ID's are required in a tracking system, software algorithms can be used to

reduce the probability of a false ID to an insignificantly small number.

Analysis of multipath sources that were found indicated that the multipath signal levels obtained, at NAFEC would be typical of those in the runway/taxiway network at most airports. This conclusion is based on data from operations in the vicinity of the municipal terminal, the Air National Guard hangars and the ATC Tower. Problems did occur with loss and garble of IDs at the Master and Slave stations, but these were determined to be caused by a combination of digital and data link circuit malfunctions and not by multipath. Results from multipath tests are summarized in Table 2-4 below.

TABLE 2-4  
NAFEC MULTIPATH DATA SUMMARY

Multipath Signal		Coverage Area Affected	Effect on TOA	Effect on ID
Amplitude	Delay <sup>a</sup>			
>20 dB down	3 $\mu$ s	91%	None	None
-9 to -20 dB	1 $\mu$	8%	None	None
-3 to -9 dB	.1 $\mu$ s	1%	None	None
+3 to -3 dB	.2 $\mu$ s	0.01%	None Measurable	Measured <sup>b</sup>

<sup>a</sup>Typical

<sup>b</sup>Loss of ID at one of three sites during this condition.

From these test results it is reasonable to expect that an ATCRBS trilateration system could overcome the effects of multipath while maintaining accuracy, coverage, and update rate in any operational installation. Evaluation of limiting cases and the development of definitive quantitative measures of multipath performance with pattern gain discrimination and software/hardware tracking capability requires additional testing at typical operational airports as prescribed in contract Option 2.

## 2.6 VEHICLE EFFECTS

Aircraft test results<sup>5</sup> indicated there was some azimuth shadowing or signal loss due to line-of-sight blockage by aircraft appendages such as landing gear, flaps, etc. This signal loss value was found to be approximately 15 dB maximum with nominal values of 50 to 7 dB for the DC-6, Gulfstream I and Aero Commander aircrafts. These results agree with earlier Bendix tests on a 10:1 scale model B-707.

During DAS testing, a CB-580 aircraft was positioned at a point about 0.85 nmi from the Master Station and interrogator power set at the theoretical Minimum Triggering Level (MTL) value for a nominal transponder at that range plus 7 dB additional power for expected azimuth shadowing effects. The aircraft was rotated in place and round reliability greater than 90% was observed with a continuous update rate of about four samples per second during the complete turn. Vehicle effects did not interface with the acquisition of continuous data from a Gulfstream aircraft taxiing down runway 4-22 or from a Cessna 172 taxiing along runway 8-26. Vehicle effects for wide bodied aircraft (such as the B-747, L-1011, etc.) were not obtainable at NAFEC and would require testing at airports where such aircraft normally operate. Test data, however, indicate that with such aircraft the effects of azimuth shadowing on accuracy, update rate, and coverage could be reduced by providing higher receive pattern gain and by adding redundant interrogation and receive sites.

## 2.7 RF INTERFERENCE

ATCRBS interference evaluation tests showed that operating the DAS at a PRF of 1520 caused no measurable degradation of ATCRBS performance. <sup>a,6</sup> This result was verified by observers and from the analysis of data extraction tapes from Philadelphia, Washington-National and NAFEC.<sup>b</sup> In addition, the DAS was synchronized with the NAFEC operational ASR-4. When the ASTC PRF was increased to 1520 the interrogation/suppression count in the NAFEC region almost reached the point where a statistical inference could be made of the effect on the ATCRBS round reliability by ASTC operations. Additional tests are required, however, to validate the theoretical prediction of the impact of the ASTC operations, it is expected that a DAS PRF of 2280 per second or higher would have to be used.

---

<sup>a</sup>The projected operational PRF for O'Hare Airport for 100 surface vehicles during peak hours with reinterrogations is approximately 1400.

<sup>b</sup>Observers in ARTC at Islip, N.Y. and Leesburg, Va., also reported no interference and NAS Stage A printouts, corroborating the findings.

TSC measurements of the ATCRBS surface environment at Logan (Boston) and at Chicago O'Hare Airports <sup>7,8</sup> showed that an ASTC DAS operating at the required operational PRF will not adversely affect ATCRBS systems in the region. Similar findings were developed at Los Angeles, although some additional data must be gathered before a firm conclusion can be drawn there.

These tests tended to confirm results from previous TSC investigation which show that ASTC operations would not interfere with normal ATCRBS functions. For instance, transponders were activated in all moving aircraft on the surface during tests at Logan and O'Hare Airports. This would be a requirement for an ASTC system. Results of these tests were favorable to operational ASTC system deployment. In addition, TSC measurements of the ATCRBS environment on the surface at Logan, O'Hare and Los Angeles International Airports support the contention that ASTC system, operating at required PRF's, probably will not affect ATCRBS in those areas. Airborne ATCRBS environment tests, which TSC has scheduled for these airports will lead to more conclusive assessments of the impact of an operational ASTC on ATCRBS.

The impact of ATCRBS on the DAS at NAFEC was minor. The NAFEC environment, with three operating ASR's, is severe from a fruit generation standpoint. For this reason, DAS receiver sensitivity was reduced 10 dB. This would not have been necessary if the brassboard had a real-time computer to set independent range gates based on expected target range. In any case, round reliabilities greater than 85% were achieved consistently and 90% or greater was typical of the measurements. For operational systems it should be noted that clear identity would not be needed at all three receivers thereby reducing further fruit effects.

### 3. CONCLUSIONS AND RECOMMENDATIONS

The primary objective of Phase I of this contract, demonstration of technical feasibility of an ATCRBS based DAS, was successfully accomplished. Data acquired during the NAFEC field test series are in agreement with the results of earlier concept analytical studies. The technology required to support the concept is available and functions as required. The following key technical points were established.

- . Trilateration accuracy, was measured to be 38.1 feet,  $3\sigma$ , well within the contract objective of 100 feet,  $3\sigma$ .
- . Resolution was measured at a reply probability  $>97\%$  for vehicles separated by 150 feet.
- . DAS coverage was measured to 1.13 nm for aircraft with an antenna height of 3 feet. Interrogator power required at this range validates the theory for operational system coverage requirements.
- . Aircraft target tracking (update rate) was confirmed over the available NAFEC test area up to 1.13 nm maximum range up to a rate of 10 per second.
- . DAS performance was not adversely affected by multipath in the NAFEC test environment. This can be attributed to the multipath rejection capability of the brassboard system and the relatively clear ASTC multipath environment at NAFEC.
- . There was no problem with signal blockage and fading caused by vehicle effects for aircraft types available at NAFEC, i.e., Convair 580, DC-6, Gulfstream and Cessna 172.
- . The brassboard was tested beyond projected operational PRF's without causing interference to local ASR systems either at NAFEC or at surrounding sites. These tests show that synchronization of the ASTC system with the local ASR may not be necessary for operational deployments.
- . The tests did not reveal any DAS system technical limitations or inherent shortcomings.

The brassboard DAS program is ready for Phase II testing in higher density operational airport environments and some steps have already been initiated in this direction. Included in contract DOT-TSC-769 are optional tasks calling for field testing at Logan

and O'Hare Airports. These tests could not have been undertaken until NAFEC tests were completed because of concern relative to generating ATCRBS interference which might impact ATC operations. Results of NAFEC interference tests, however, combined with environment measurements at Logan, O'Hare and Los Angeles, show clearly that an operational ATCRBS trilateration system at these airports, operating at the projected PRF's, will not create measurable ATCRBS interference nor ARTS III degradation. It is reasonable to conclude that the brassboard can be operated as necessary to acquire further test data to support ATCRBS Trilateration operational potential and performance, without interfering with the present ATCRBS environment or adversely affecting airport operations.

Contract Option 1, covering test planning and DAS hardware augmentation design for the Logan and O'Hare tests, was exercised on 15 May 1975, details of which are discussed in Appendix D.

Option 2 includes a provision for hardware modification which will improve the ability of the brassboard in the area of real-time control and processing. The added capability is necessary at operational airports where the traffic density cannot be structured and controlled purely for test purposes. A DAS with real-time data presentation would allow data to be examined as it is taken, thereby permitting early detection and correction of system faults. A real-time tracking capability must be included to acquire preprocessed data in quantities necessary to evaluate the complex inter-relationships between vehicle effect, multipath, resolution (a function of transponder characteristics), etc. Post processing all data in its new state is prohibitably expensive, requiring approximately one hour of machine processing time to reduce and analyze one minute of brassboard DAS data. More important it severely limits evaluation of the contribution the system can make in aiding real operational situations.

Finally, now that technical feasibility is clearly established it is appropriate to begin consideration of an operational sensor equipment configuration. This raises a host of new considerations relative to such matters as increasing sensor capability (extended range and coverage, different modes of interrogation and measurement, beacon system growth to DABS, etc.), interfaces with terminal ATC facilities, and controller displays, surface automation applications (e.g., intersection control, runway occupancy estimation, etc.), control algorithms and system architecture, and many others which have not been addressed to date. These questions need to be addressed in the context of realizing a return in operational benefits from the investment made in this highly successful feasibility demonstration.

## APPENDIX A

### SUMMARY DESCRIPTION OF THE DAS OPERATION

#### A.1 TECHNIQUES REQUIRED FOR IMPLEMENTING AN ATCRBS BASED ASTC DAS

The overall operation of the present airborne ATCRBS and future ASTC system may be described by the closed loop depicted in Figure A-1 below. Transponder replies are received and processed by the DAS which passes data to the display system. There it is combined with data from the ASTC Data Base to produce a visual display of aircraft position(s), identity and movement (track) to the controller. He makes decisions as to aircraft status using this and other ATC inputs and issues directions to the aircraft via VHF voice radio. As the aircraft responds, the steady stream of replies revises the display accordingly, updating visual information being supplied the controller. Note the single direction of the information flow.

Although an interrogation signal is transmitted from the DAS to the aircraft, its only function is to generate the reply which is then processed for data. ATCRBS uses the simple "track while scan mode" of gathering data. Interrogations are transmitted over a narrow beam which is sequentially scanned by a constantly rotating antenna. Replies are generated by all aircraft in the coverage volume. Each target generates a string of replies (typically 18) which are processed for range from the interrogator, identity code, and the centroid of the "hit run", designating probable true azimuth. There is no feedback to the interrogator for modifying the interrogation process by either the control/display system or the controller. The interrogation function is independent of relative target positions or velocities. This is possible in the airborne system since normal aircraft separations usually allow replies to be received in an azimuth and range, time ordered sequence without mutual interference.

The performance of the airborne system is totally unacceptable within the dense target environment of an airport since targets must be separated by at least 3.5 to 7 degrees in azimuth and more than 1.68 nautical miles in range to prevent reply overlap and garble.\* The method of position measurement is equally unacceptable since target density prevents the sliding window method of angle measurement and the two way range measurement has a specified precision of only +1000 feet. Even the generally accepted one sigma value of 300 feet provided operationally is

\* Based on Standard FAA ATCRBS Interrogator antenna performance and a two way range of 20.3 microseconds for a reply plus 0.45 microseconds reply pulse width, nominal.

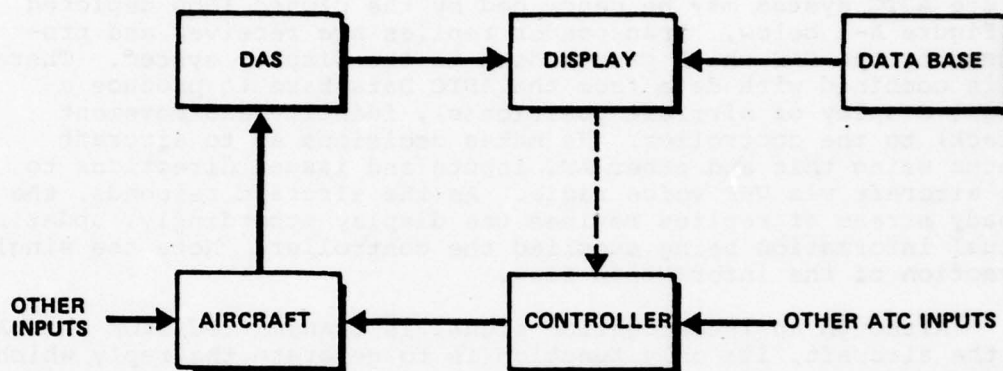


Figure A-1. System Functional Information Flow Diagram

unacceptable Projected operational ASTC and DAS accuracy requirements call for measuring position to a one sigma accuracy of 25 feet and resolving aircraft separated by distances of the order of 175 feet through selective interrogation. These requirements are to be satisfied using the trilateration position measuring system and the GEOSCAN interrogation system as described below.

#### A.1.1 Trilateration Technique

Trilateration is a process whereby the position of an RF transmitter may be located by measuring the Time of Arrival (TOA) of the signal it emits at three separate receiving sites. In this application TOA differences ( $\Delta$ TOA) are used for position determination. The three TOAs are measured, and the  $\Delta$ TOAs ( $T_2 - T_1$ , etc.) are computed. Each pair of TOA measurements describes a hyperbolic line of constant  $\Delta$ TOA ( $T_2 - T_1 = K$ , etc.) which passes between the two respective stations and is symmetrical about the baseline between them, as in Figure A-2. The intersection of two such hyperbolas fixes the point of transmission since it is the only point which can generate that particular pair of  $\Delta$ TOAs. The third  $\Delta$  TOA is not independent of the other two since  $(T_1 - T_2) + (T_2 - T_3) + (T_3 - T_1) = 0$  and therefore it provides no additional information. However, three TOAs from three separate sites are required to develop two  $\Delta$ TOAs.

Extensive work has been done on this technique of position location by MITRE, RAND and others.\* Their work generally deals with a cluster of sites with the target emitter at ranges far outside the three station triangle. Under these conditions severe measurement errors occur as range increases and are most severe along baseline extensions. For a particular pair of TOA measurements, the error limits lead to a pair of confocal hyperbolas that bound the true position locus. The intersection of two such regions produces a hyperbolically bounded zone within which the target transmitter must be, rather than its precise location. Since the boundary hyperbolas diverge as they recede from their common focus, the position uncertainty for given errors will be greater at some points than at others. This reduction in accuracy or error magnification as a function of location in the system geometry is referred to as GDOP (for Geometric Dilution of Precision).

Under Task 1A, Bendix has analyzed the TOA measurement process<sup>2</sup> and has found that the target position accuracy called for by the ASTC system requirements can reliably be met by a properly designed trilateration DAS. This procedure can be summarized as follows:

\*L. H. Wegner, "On the Accuracy Analysis of Airborne Techniques for Passively Locating Electromagnetic Emitters", RAND Corporation, Report R-722-PR, (June 1971).

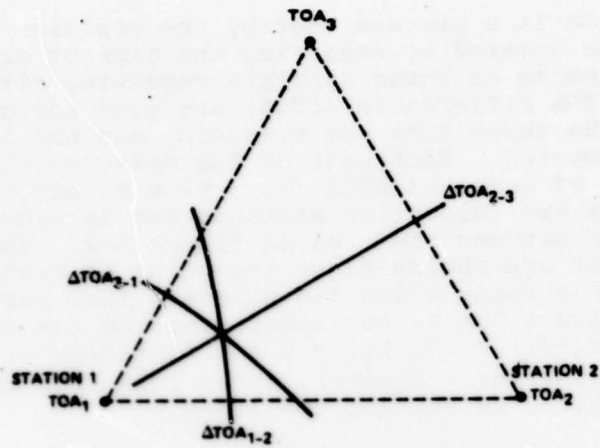


Figure A-2. Generalized TOA Position Location

- (1) Estimate or compute the standard deviation of each individual noncorrelated error contributor (S/N, etc.) to the TOA measurement.
- (2) Compute the root sum square error associated with each of the three receiving sites.
- (3) Compute and plot the root mean square position error as a function of target location.

The standard deviation of the TOA measurement ( $\sigma_{\text{TOA}}$  in (2) above) is computed as the root sum square of the following three terms:

- where:
- $\sigma_f$  = standard deviation of the TOA measurement due to non range dependent TOA errors ((1) above).
  - $\sigma_b$  = standard deviation of the TOA measurement error due to beam bending.
  - $\sigma_n$  = standard deviation in the TOA measurement due to thermal noise perturbations of the reply pulse leading edge, primarily due to range and vertical multipath fade.

Non range dependent errors consist of errors due to propagation uncertainty (lateral multipath), uncompensated equipment delays and characteristics, electromagnetic interference, and receiver site location uncertainties. This error term,  $\sigma_f$  has been calculated to be 10.2 nanoseconds. The beam bending error term,  $\sigma_b = 1.48 \times 10^{-13} R$ , where R is in feet.

The thermal noise error term,  $\sigma_n = 89.4 \sqrt{2\sqrt{S/N}}$  is plotted in Figure A-3. A composite curve of  $\sigma_{\text{TOA}}$  is shown in Figure A-4. Notice that a S/N ratio below 25 dB insignificantly contributes to the total, doubling it at 10 dB, while S/N ratios above 25 dB provide little improvement.

Unfortunately S/N prediction is complicated in the ASTC environment due to the influence of vertical multipath fade. In the airborne case, given the value of the system net gains and losses, a rapid calculation of free space path loss (which is a function of one variable, range) yields the desired result. In the ASTC case, total path loss is a function of two variables, range (R) and aircraft antenna height ( $H_2$ ), assuming a constant DAS antenna height ( $H_1$ ). The geometry is such that the aircraft will be operating on the lower side of the first lobe of the antenna and in this region path loss follows a  $1/2R^4$  instead of the free space  $1/R^2$  law.\* Analysis of vertical multipath

\*J. D. Vinatieri, "Experimental Measurements of Beacon Antenna Radiation Patterns for Surface Aircraft", MITRE Corporation, Report MTR-2780, Page 37, (26 Feb. 1974).

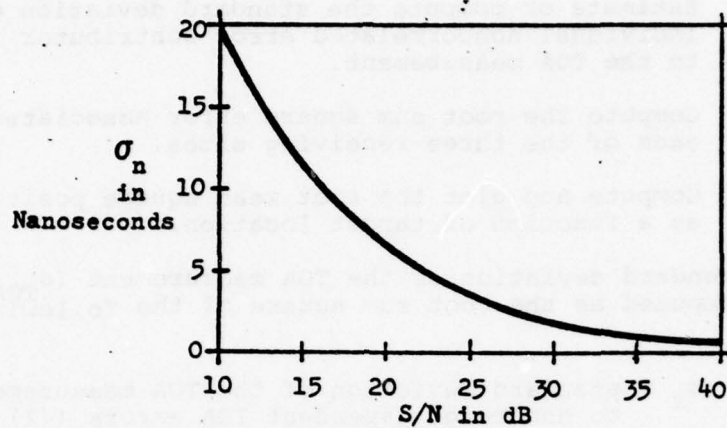


Figure A-3. Predicted Standard Deviation In TOA Due to Noise Only As a Function of S/N

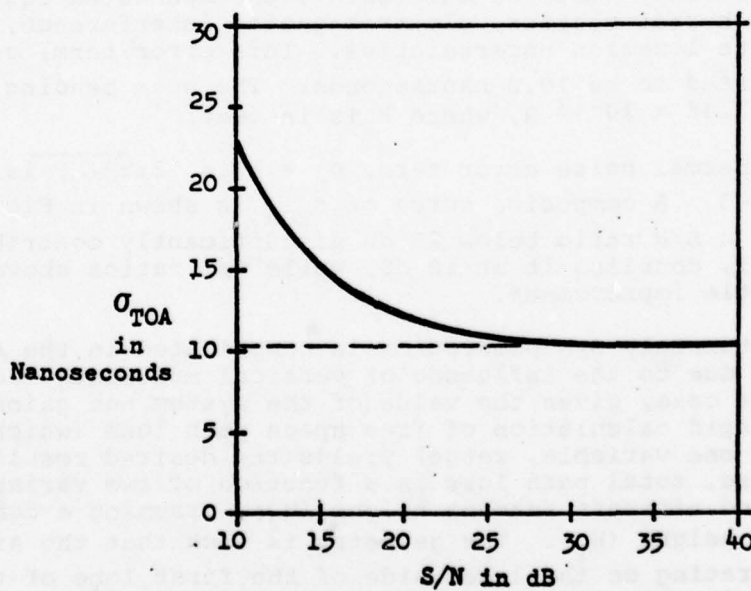


Figure A-4. Predicted Standard Deviation in TOA As a Function of S/N with Beam Bending ( $\sigma_b = 1.8$  ns) and Non Range Dependent Errors ( $\sigma_f = 10.2$  ns) Fixed

phenomena has shown the need for coverage diagrams which combine the effects of free space loss and vertical multipath fade as a single parameter plotted against range and aircraft height. Figure A-5 is an example of such a chart produced by the computer program for the case where the DAS antenna is 18 feet above the surface which is assumed to be flat except for the nominal earth curvature. It is calculated that the brassboard will have coverage down to a height of 1.823 feet at 1.5 nautical miles with a  $\sigma_{TOA} = 17.5$  nanoseconds.

Target position fix error ( $\sigma_p$ ) for one target location is then computed using the root sum square of the constituent contributions from each site:

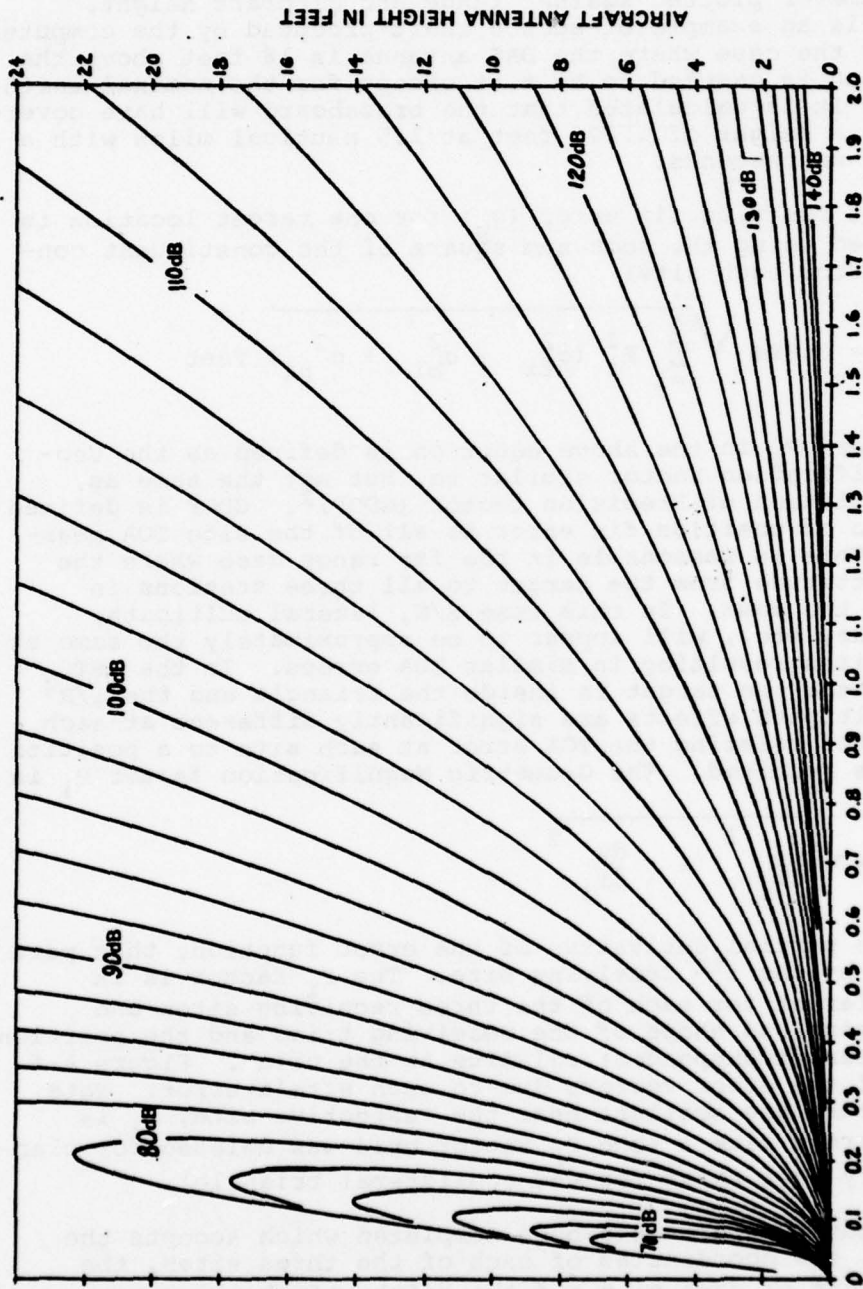
$$\sigma_p = 0.984 \sqrt{\sum_{i=1}^3 P_i^2 (\sigma_{fi}^2 + \sigma_{bi}^2 + \sigma_{ni}^2)} \text{ feet}$$

The term  $P_i$  in the above equation is defined as the Geometric Magnification Factor similar to, but not the same as, Geometric Dilution of Precision factor (GDOP)<sup>2</sup>. GDOP is defined as the ratio of position fix error to all of the site TOA measurements. This is reasonable in the far range case where the range and attitude from the target to all three stations is essentially the same. In this case S/N, lateral multipath, vertical fade, etc., will appear to be approximately the same at all three sites resulting in similar TOA errors. In the ASTC situation where the target is inside the triangle and the  $1/R^4$  loss and multipath effects are significantly different at each site, a factor relating the TOA error at each site to a position fix error is required. The Geometric Magnification factor  $P_i$  is defined:

$$P_i = \sqrt{\left(\frac{dx}{dr_i}\right)^2 + \left(\frac{dy}{dr_i}\right)^2}$$

which is the partial derivative of the error function, that part contributed by the  $i^{\text{th}}$  receiving site. The  $P_i$  factor is in general different for each of the three receiving sites and depends on size and shape of the receiving triad and the position of the emitter (transponder) relative to the triad. Figure A-6 is a plot of the error vectors due to each site's error. Note that the errors are smallest near the respective site,  $P_1$  is smallest nearest site 1 (the  $P_2$  vector grid was deleted for clarity, symmetry does exist for the equilateral triangle).

A computer program has been completed which accepts the value of  $\sigma_f$ , the coordinates of each of the three sites, the antenna heights of each site and the height of the aircraft antenna. The program then computes S/N,  $\sigma_b$ , and  $P_i$  over the region and prints out the composite error. A typical plot using



RANGE - INTERROGATOR TO AIRCRAFT IN NAUTICAL MILES  
 Figure A-5. Idealized Total Path Loss (Free Space Plus Vertical Multipath Fade)  
 Contours from an Interrogator Antenna 18 Feet Above the Surface

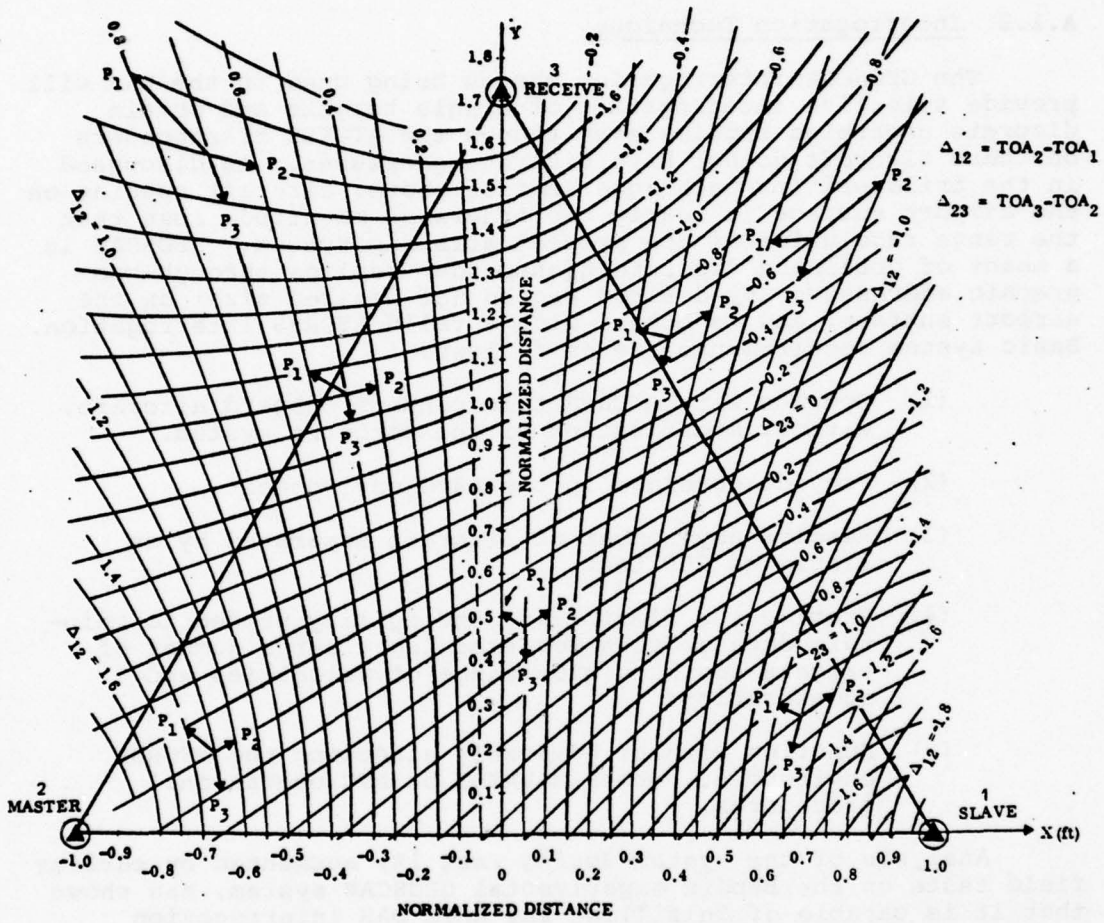


Figure A-6. Predicted TOA Error Vector Versus Position

the projected operational system parameters, a two mile baseline, site antennas at 18 feet and an aircraft antenna height of four feet (727, etc.) is shown in Figure A-7. This computer program can be used in site selections at it was at NAFEC.

#### A.1.2 Interrogation Technique

The GEOSCAN interrogation system being used in the DAS will provide selective interrogation of single targets and obtain discrete ungarbled replies even though the ATCRBS transponders on these aircraft do not have discrete addresses. As discussed in the trilateration technique section above, aircraft spacing on the airport surface is nearly two orders of magnitude less than the range resolution of the present airborne system. GEOSCAN is a means of obtaining discrete transponder replies through geographic addressing any desired region (of desired size) on the airport surface, and no other, with a valid ATCRBS interrogation. Basic system requirements are as follows:

- (1) Operate with ATCRBS transponders onboard aircraft, without modification of the airborne system.
- (2) Provide coverage in the ASTC environment.
- (3) Resolve any number of aircraft separated by as little as 200 feet.
- (4) Provide the flexibility and agility needed to maintain data updates for tracking a large number of targets having a wide range of velocities and accelerations.
- (5) Function without adversely affecting the ATCRBS environment, other NAVAIDS or ATC operational procedures.

Analysis of the system during Task 1A, augmented by earlier field tests on the Bendix experimental GEOSCAN system, has shown that it is capable of fulfilling the ASTC DAS interrogation requirements. The ASTC Approach Monitor study recently completed under this contract shows that the system may also provide an additional service necessary to the ASTC program. Due to garbling of replies of aircraft nearing touchdown, caused by aircraft closely spaced on the surface (typically at the end of runways), the ASR and ARTS III blanks the system out inside about a two mile radius. ASTC prediction of runway clearance requires knowledge of the aircraft position and velocity during this period prior to touchdown. The GEOSCAN system has characteristics which may be very well-suited to filling this void.

##### A.1.2.1 GEOSCAN Operation, Interrogation Summary

GEOSCAN imitates the operation of the ATCRBS interrogator in a controlled sequence so as to gain access to and utilize the

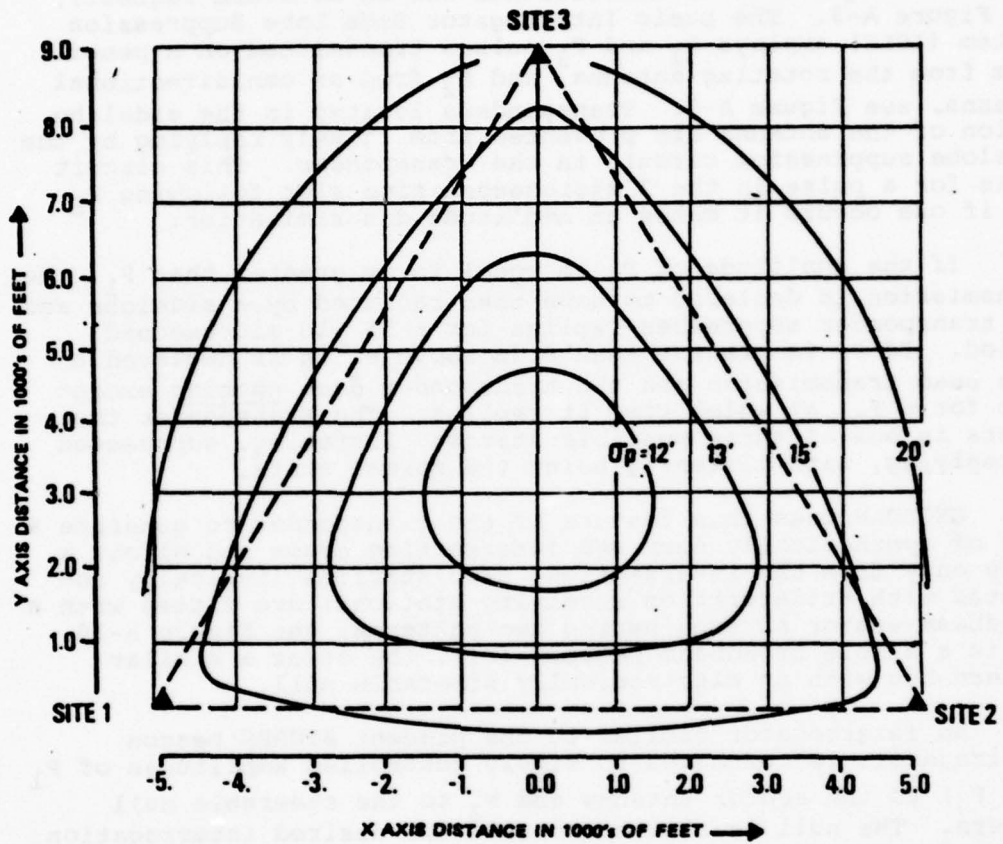


Figure A-7. Single Triad Trilateration Accuracy Contours Estimated For a Two Mile Baseline Trilateration System

ATCRBS transponder. The ATCRBS interrogation consists of three 0.8 microsecond pulses:  $P_1$ ,  $P_2$  and  $P_3$  sequentially transmitted.  $P_1$  is a reference pulse.  $P_2$  is the sidelobe suppression (SLS) pulse transmitted 2 microseconds after  $P_1$ , and the  $P_1$  to  $P_3$  spacing determines the reply mode (8 microseconds for an identification (ID) request or 21 microseconds for an altitude request), see Figure A-8. The basic Interrogator Side Lobe Suppression System (ISLS) employs  $P_1$  and  $P_3$  pulses transmitted on a pencil beam from the rotating antenna, and  $P_2$  from an omnidirectional antenna, see Figure A-9. Transponders located in the sidelobe region of the antenna are prevented from falsely replying by the sidelobe suppression circuit in the transponder. This circuit locks for a pulse in the 2 microsecond time slot following  $P_1$  and if one occurs it makes an amplitude discrimination.

If the amplitude of  $P_2$  is equal to or greater than  $P_1$ , the transmission is declared to have been radiated by a sidelobe and the transponder suppresses replies for a  $35 \pm 10$  microsecond period. If  $P_1$  is greater than 9 dB above  $P_2$  it is declared a main beam transmission and the transponder does nothing except wait for a  $P_3$ , at which time it replies. The transponder then exists in one of three possible states: listening, suppressed or replying, with listening being the normal state.

GEOSCAN uses this feature of the transponder to generate a pair of synthetically narrowed intersecting beams and elicit a reply only from the intersection. Two stations (typically collocated with trilateration receiving stations) are fitted with a broadbeam sector antenna having two patterns, see Figure A-10. One is a simple broadbeam pattern ( $P_1$ ), the other a similar pattern but with an electronically steerable null.

An interrogator similar to the present ATCRBS beacon interrogators is connected to supply controlled amplitudes of  $P_1$  (and  $P_3$ ) to the sector antenna and  $P_2$  to the steerable null pattern. The null is steered towards the desired interrogation cell and a  $P_1 - P_2$  pair is transmitted from the suppressor station, Figure A-11. Transponders inside the null will see  $P_1$  9dB greater than  $P_2$ , will be unaffected and await  $P_3$  arrival. Transponders outside the null will see  $P_2$  greater than  $P_1$  and will go into suppression for  $35 \pm 10.0$  microseconds.

Before the suppressed transponders can come out of suppression a similar pulse pair is transmitted from the interrogation station across the initial null path, Figure A-12.

Again transponders inside the null will be unaffected and will wait for a  $P_3$  referenced to this latest  $P_1$ , the second transmission having been delayed until the initial  $P_1$  clears the airport by 8 microseconds. This prevents unsuppressed transponders from falsely decoding and replying to a 8 microsecond

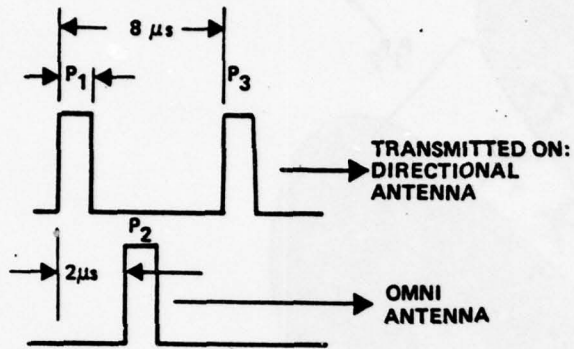


Figure A-8. ATCRBS Interrogation Characteristics

002-1017-019

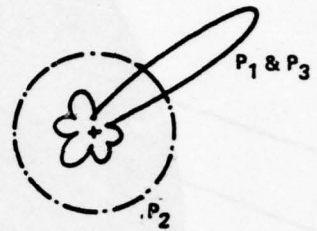


Figure A-9. ATCRBS ASR/ARSR SLS Antenna Patterns

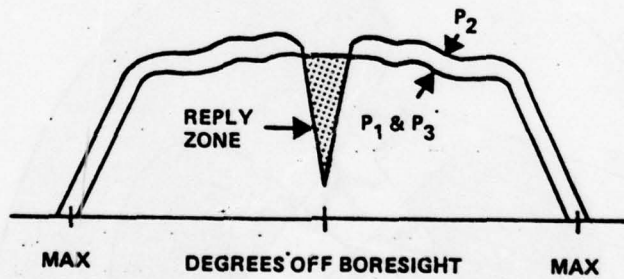


Figure A-10. Basic Geoscan Antenna Pattern

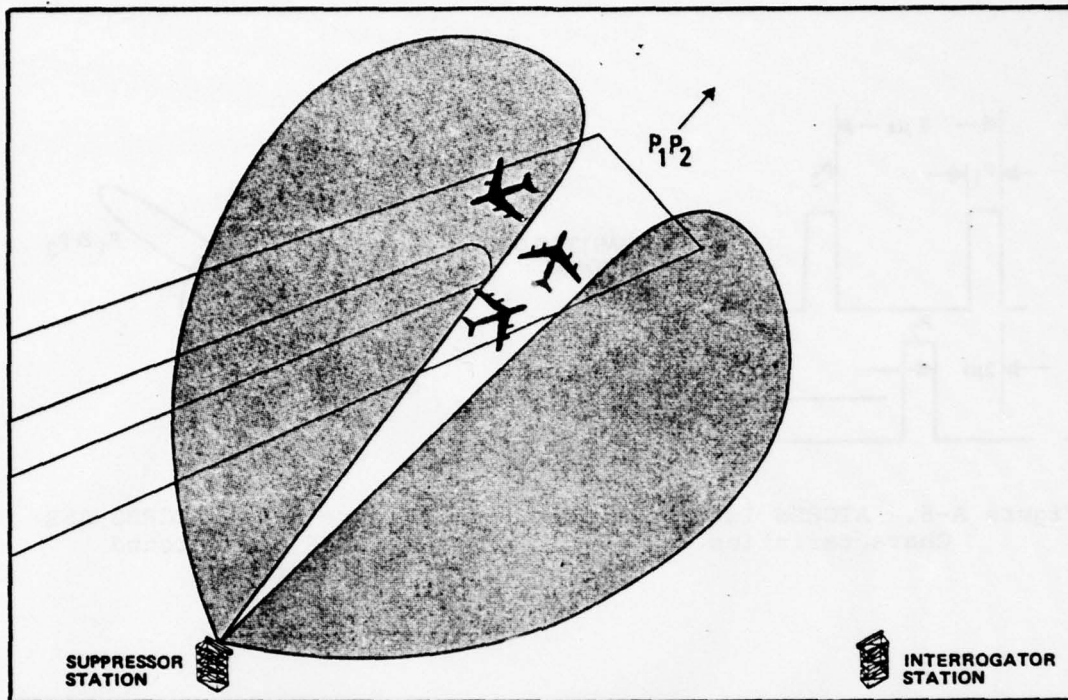


Figure A-11. Suppressor Station Transmission Showing Suppressed Regions

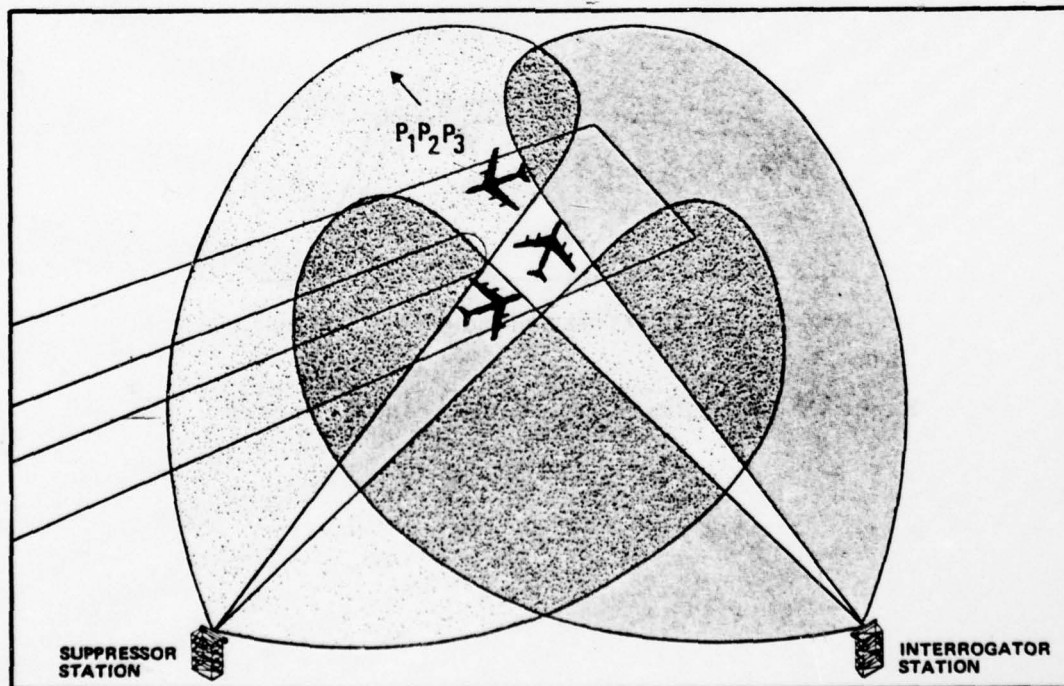


Figure A-12. Interrogator Station Transmission Showing Additional Suppressed Regions

$P_1 - P_1$  combination. Transponders outside the null will likewise be suppressed. When  $P_3$  is transmitted only transponders inside the intersection are unsuppressed and are therefore capable of replying. If the width of the nulls is reduced by increasing the amplitude of  $P_2$  in Figure A-10, the size of the intersection or "cell" can be reduced until only one aircraft and therefore one transponder can occupy the cell, yielding a single ungarbled reply. Any cell in the region may likewise be interrogated by properly steering both nulls and adjusting the null widths with the ratio of  $P_2/P_1$  to control cell size.

Two factors limit the coverage of a single GEOSCAN pair, the maximum allowable separation between stations and the interrogation cell distortion or GDOP effect. If the baseline separation is more than 9170 feet, transponders outside the three station triangle will start coming out of suppression before the second interrogation is complete, causing possible false interrogations to transponders in that region. As the angle between the two intersecting nulls diverges from 90 degrees, the cell becomes elongated as in Figure A-13. The maximum and minimum intercept angles have been nominally set at 141 and 39 degrees giving a 90 percent probability of a correct reply for aircraft separated by 150 feet.

#### A.2 BRASSBOARD DAS OPERATION

The DAS system is based on a trilateration receiving network consisting of three stations, two of which are used as GEOSCAN interrogation stations. Figure A-14 is a simplified block diagram of the Brassboard DAS showing major system blocks. The Master Station is the interface between the DAS test inputs and data outputs. Notice that the hardware blocks in the Control Group are limited to the Test Control Unit (TCU) which primarily establishes the search and timing sequences and the recorder system which stores the hyperbolic position, ID and data quality of the reply along with other information about test conditions on magnetic tape for post test processing at the TSC computer facility. The computer processing and software blocks are shown on interface C denoting that these functions simulate portions of the DAS Control Group as well as the ASTC Data Base and Display to the extent programmed in software.

Except for the TCU and the Recorder System which are specific to the brassboard, all other blocks represent modules common to the projected operational system. The Slave Station (so named because it simply follows the Master's command during the GEOSCAN sequence) and Master Station contain the same GEOSCAN interrogator and TOA receiver complement although the Slave operates as the suppressor and the Master the interrogator. The Receive Station acts only to intercept the ATCRBS reply and relay it to the TOA processor at the Master Station, as does the Slave. The reply data link is a real time system such that all three TOA readings are made at the Master Station. Two fixed

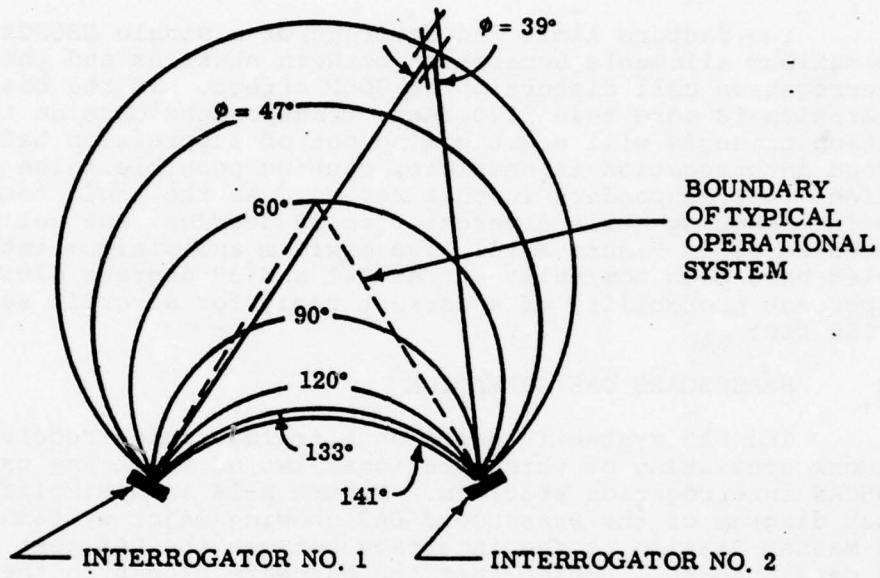


Figure A-13. Interrogator Coverage Zones

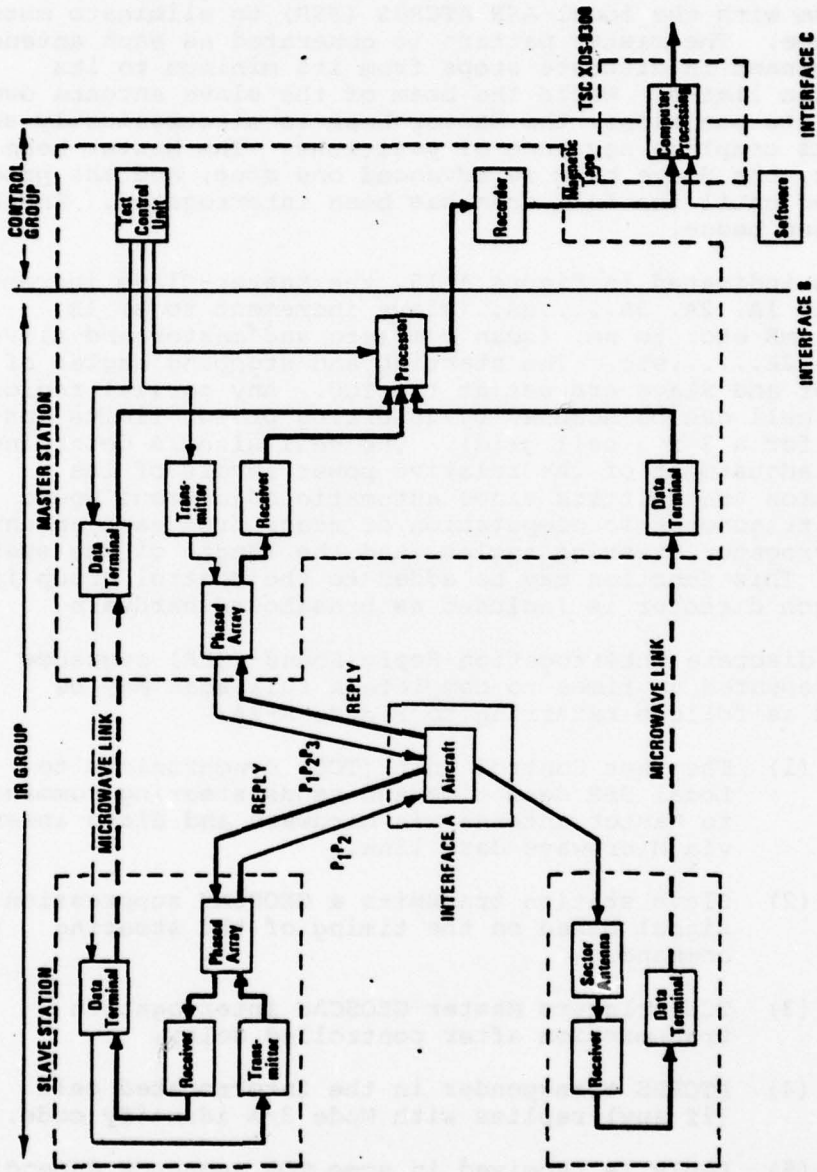


Figure A-14. Brassboard DAS Simplified Block Diagram

transponders will be used to act as reference for calibrating the system with respect to the physical map of the airport. Since real time tracking is not performed, the TCU sequences the pair of interrogation antennas through a simple raster pattern and triggers the transmission of the GEOSCAN sequence in synchronism with the local ASR ATCRBS (SSR) to eliminate mutual interference. The raster pattern is generated as each antenna beam is scanned in discrete steps from its minimum to its maximum scan limits. While the beam of the slave antenna dwells at one of its positions, the Master beam is electronically switched through its complete sequence of positions. The Master beam is then reset, the Slave beam is advanced one step, and the process is repeated until the full area has been interrogated. Another scan is then begun.

As indicated in Figure A-15, the Master-Slave increment sequence is 1A, 2A, 3A.....nA, (slave increment to B) 1B, 2B.....mB etc. to nm, (scan complete and master and slave reset) 1A, 2A.....etc. The starting and stopping angles of both Master and Slave are set at the TCU. Any partial region or single cell can be scanned by inserting proper limits (as: 7C to 10E for a 3 x 3 cell grid). The cell size is determined by manual adjustment of the relative power levels of the interrogation transmitters since automatic adjustment would require a trigonometric computation of range from each antenna, both interrogator steering angles, and the length of the system baseline. This function may be added to the control group if a track/search director is included as brassboard hardware.

A discrete Interrogation-Reply Round (IRR) sequence which is repeated nm times to complete a full scan may be summarized as follows referring to Figure A-14:

- (1) The Test Control Unit (TCU) synchronizes to Local SSR dead time and sends steering commands to Master antenna via hardware and Slave antenna via Microwave data link.
- (2) Slave station transmits a GEOSCAN suppression signal based on the timing of the steering command.
- (3) TCU triggers Master GEOSCAN interrogation transmission after controlled delay.
- (4) ATCRBS transponder in the interrogated cell (if any) replies with Mode 3/A identify code.
- (5) Reply is received in some TOA sequence depending on relative range at each of the three stations via DAS Antennas and Receivers.

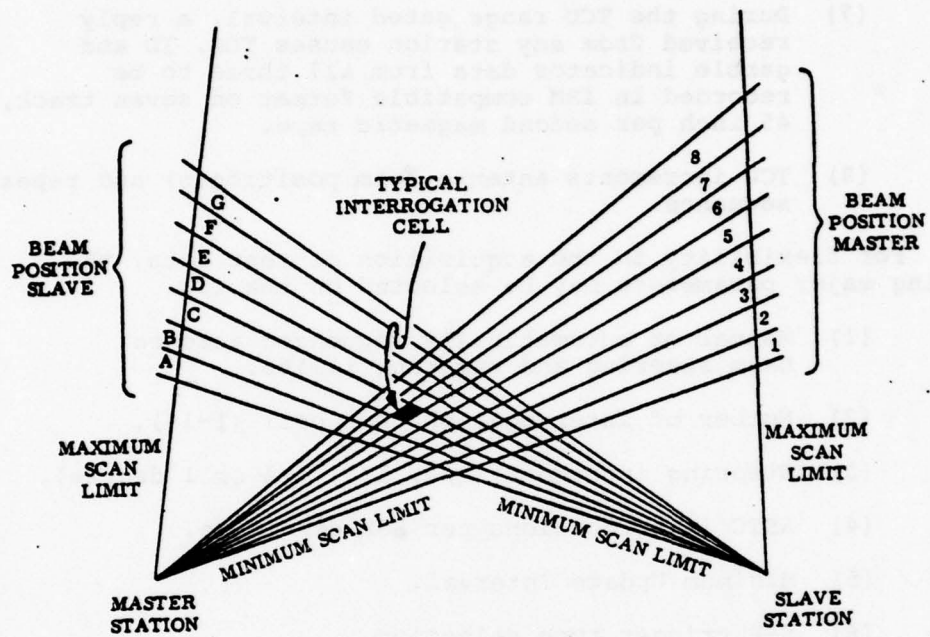


Figure A-15. System Scan Geometry

- (6) Replies received at Slaye and Receive stations are relayed to Master station Processor system via microwave Data Link in real time where TOA and ID of all three stations is measured.
- (7) During the TCU range gated interval, a reply received from any station causes TOA, ID and garble indicator data from all three to be recorded in IBM compatible format on seven track, 45 inch per second magnetic tape.
- (8) TCU increments antenna beam position(s) and repeats sequence.

For flexibility in the acquisition of test data, the following major parameters may be selected on the TCU:

- (1) Manual or automatically sequenced antenna beam steering and steering limits.
- (2) Number of interrogations per cell (1-14).
- (3) Steering increment (1/4, 1/2, 3/4 or 1 degree).
- (4) ASTC interrogations per SSR dead time.
- (5) Minimum Update Interval.
- (6) SSR trigger type selection.
- (7) Manual insertion of a data code.
- (8) Data Monitor readout of TOAs, IDs, and time-of-day (TOD).

A test run starts with actuation of the TEST RUN/STOP switch on the TCU. Following a START, two test heading words which include test data codes and pertinent switch settings are recorded after which the test sequence begins. During the test, interrogation antenna settings and the TOD (in GMT) of the SSR sync reception are recorded during the SSR dead time but only following a TOA/ID recording. Since the NAFEC and DAS systems use a common WWV time base, these data provided time synchronization and cross correlation of interrogation, tri-lateration, SSR and NAFEC Theodolite systems during post test data processing while consuming a minimum of tape.

### A.3 INSTALLATION AND PHYSICAL CHARACTERISTICS

Three office trailers each with approximately 8 by 16 feet of floor space were used to house the three station DAS during the field test. They provided the system mobility required for various sitings at NAFEC and for relocation to other airports for additional testing under pseudo operational conditions. During shipment between Bendix and NAFEC (and later to other airports), and during any extended break in field testing, all external equipment such as towers, antennas, transponders, etc., were stowed inside the trailers for security and protection.

Most of the electronics equipment is located at the master station from which the GEOSCAN interrogation system is controlled and the TOA and ID data on all three replies are measured and recorded. This equipment is accommodated in two six-foot by 19 inch rack cabinets located as shown in Figure A-16. Other features of the master station trailer are shown in the figure including the intended location of any future brassboard augmentation equipment in an additional cabinet. A 7.5 kW 1800 rpm generator supplying 115V  $\pm 3\%$  and 60 Hz  $\pm 3$  Hz, with 230 volts available if required in the future, provided an ac power budget of 1.5 kW to electronics, 2 kW for air conditioning, and 4 kW of reserve. Winter heating is provided which will maintain a 75 degree F internal temperature in a -10 degree F external ambient. The 1200 BTU/hr air conditioner can maintain a 15 degree F internal to external temperature differential with maximum internal heat load.

Generator sound and vibration isolation, easy service access, use of readily available no-lead gasoline, electric starting and a 55 gallon fuel tank providing over 60 hours of continuous operation at full load minimized the workload associated with operating a portable electric power plant. The generators used have a "vacu-flow" ventilating system which place the generator compartment under a negative pressure to ventilate the engine compartment and prevent fume seepage into the operating area.

Slave and Receive station trailers are essentially the same as the master except for smaller equipment racks and ac generators, and the deletion of air conditioning in the receive station. Forced air ventilation is provided and both generators (6.5 kW and 4 kW, respectively) are sized for air conditioning and heat load grows through equipment augmentation.

#### A.3.1 Equipment Location and Site Layout

DAS operation can be conducted independent of airport electric power and landline communication to allow maximum flexibility in selecting site layouts. Except for tower guy anchoring, site preparation is essentially nil. The selection of a particular site requires a compromise between the optimum geographic configuration and the constraints of the airport physical environment. For reasons of economy, a basic objective

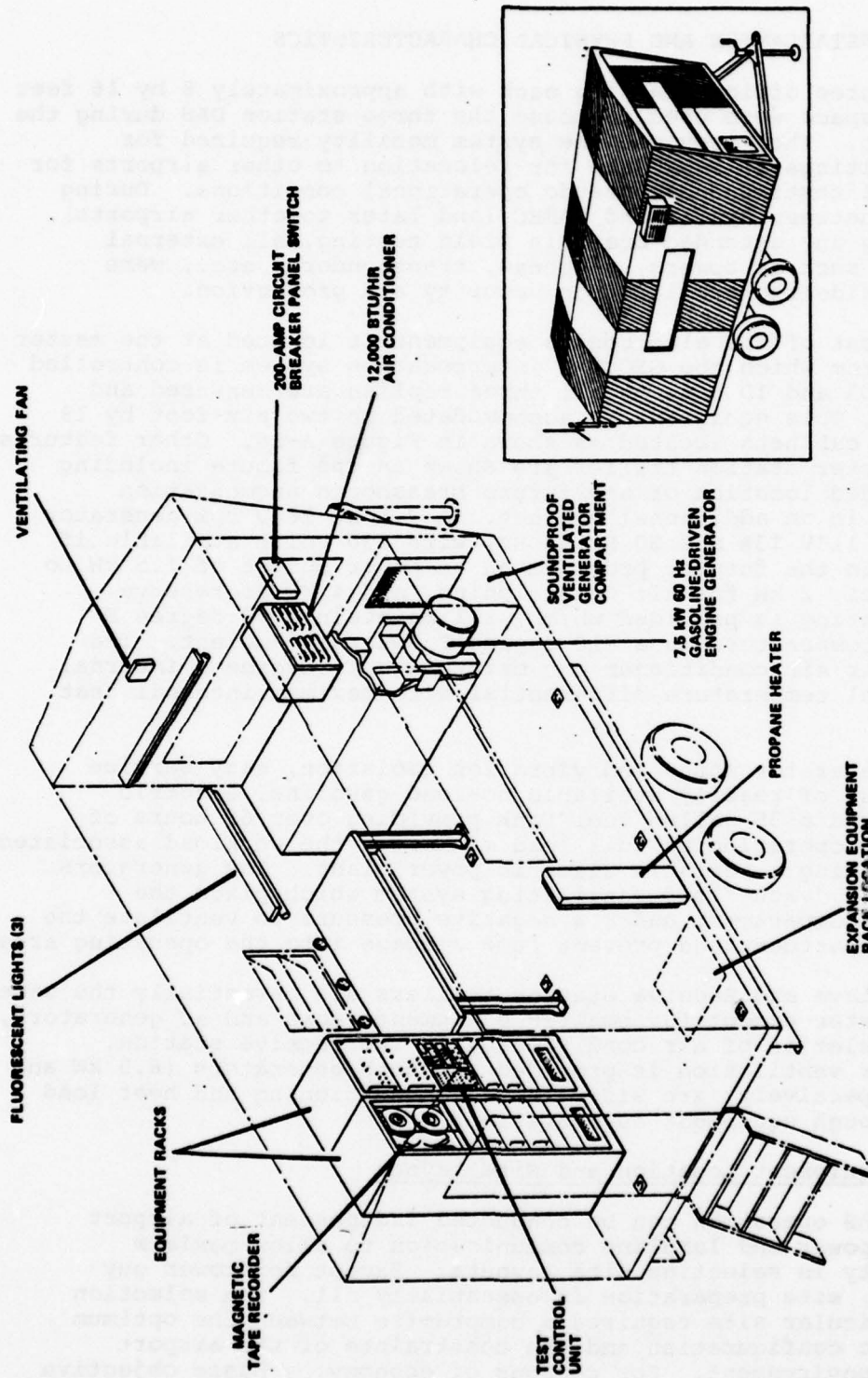


Figure A-16. Master Station Trailer Details

is to obtain as much coverage as possible with a minimum number of sites. Interstation separation is based on electrical performance. Maximum coverage is obtained when the TOA stations are located at the vertices of the largest practicable equilateral triangle. Two of these TOA stations can serve as GEOSCAN interrogators with some loss of coverage along their common baseline resulting from the limit on interrogation cell distortion, see Figure A-13.

The brassboard system layout which maximizes coverage with a 1.5 nautical mile baseline (equal to the maximum allowable separation between a pair of GEOSCAN interrogators) is shown in Figure A-17. The small arc near each station is the minimum range limitation of 600 feet.

Actual airport runway/taxiway configurations, available real estate and existing buildings or other structures will require consideration when making the layout. In addition to the siting of the three DAS stations, the master station must be able to receive sufficient signal strength from the local ASR (ASR-4 at NAFEC) to maintain reliable SSR synchronization. Two fixed transponders at carefully surveyed locations are used to calibrate the TOA position calculations with respect to the airport map. They must provide reliable line of site coverage to the three TOA stations. Test data on position and ID accuracy were acquired in various static and moving test situations for both a single target and a pair of targets using surface vehicles and aircraft equipped with beacon transponders. Typical brassboard DAS deployment and siting is shown schematically in Figure A-18 and A-19, respectively.

#### A.3.2 Antenna Deployment

The brassboard DAS contains a total of 14 primary antennas plus various antennas on test vehicles required to perform and support the field tests. The 14 main antennas are as follows:

- (1) DAS Antennas: Two Phased Array Interrogation Antennas, one at the Master Station and one at the Slave Station. One Sector Omni Receiving Antenna at the Receive Station.
- (2) Data Link Antennas: Four Parabolic Dish Antennas, two at the Master Station and one each at both the Slave and Receive Stations.
- (3) Communications Antennas: Three VHF Antennas, one at each station.
- (4) SSR Sync Receiving Antenna: One Standard Gain Horn at the Master Station.

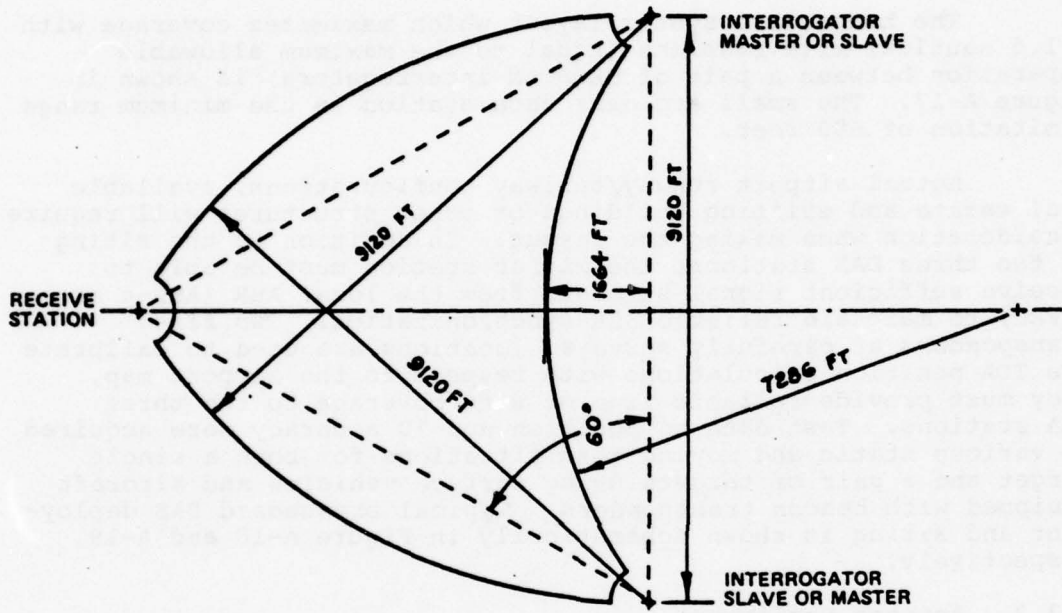


Figure A-17. Brassboard DAS Layout for Maximum Coverage

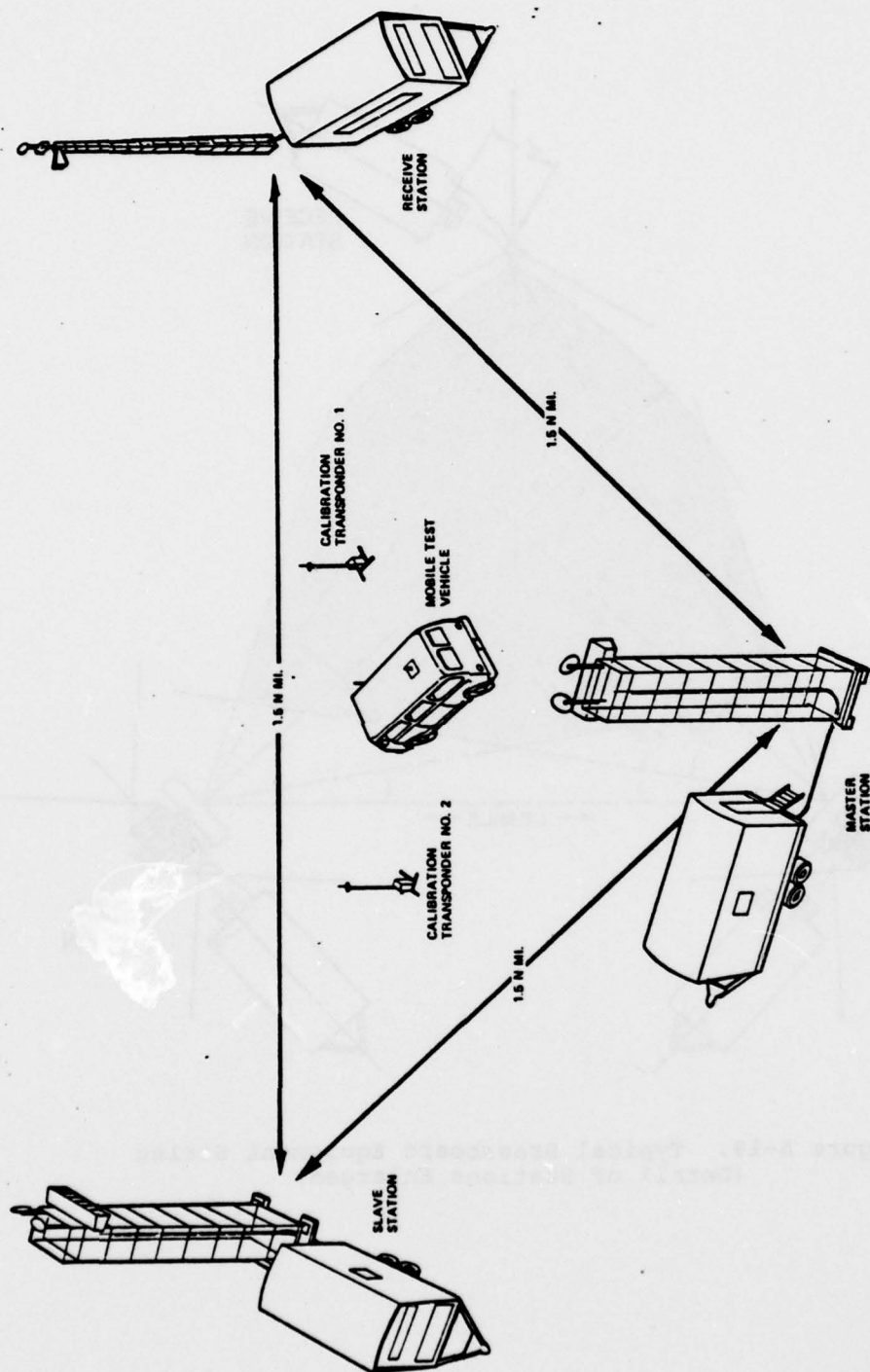


Figure A-18. Brassboard DAS Equipment Deployment

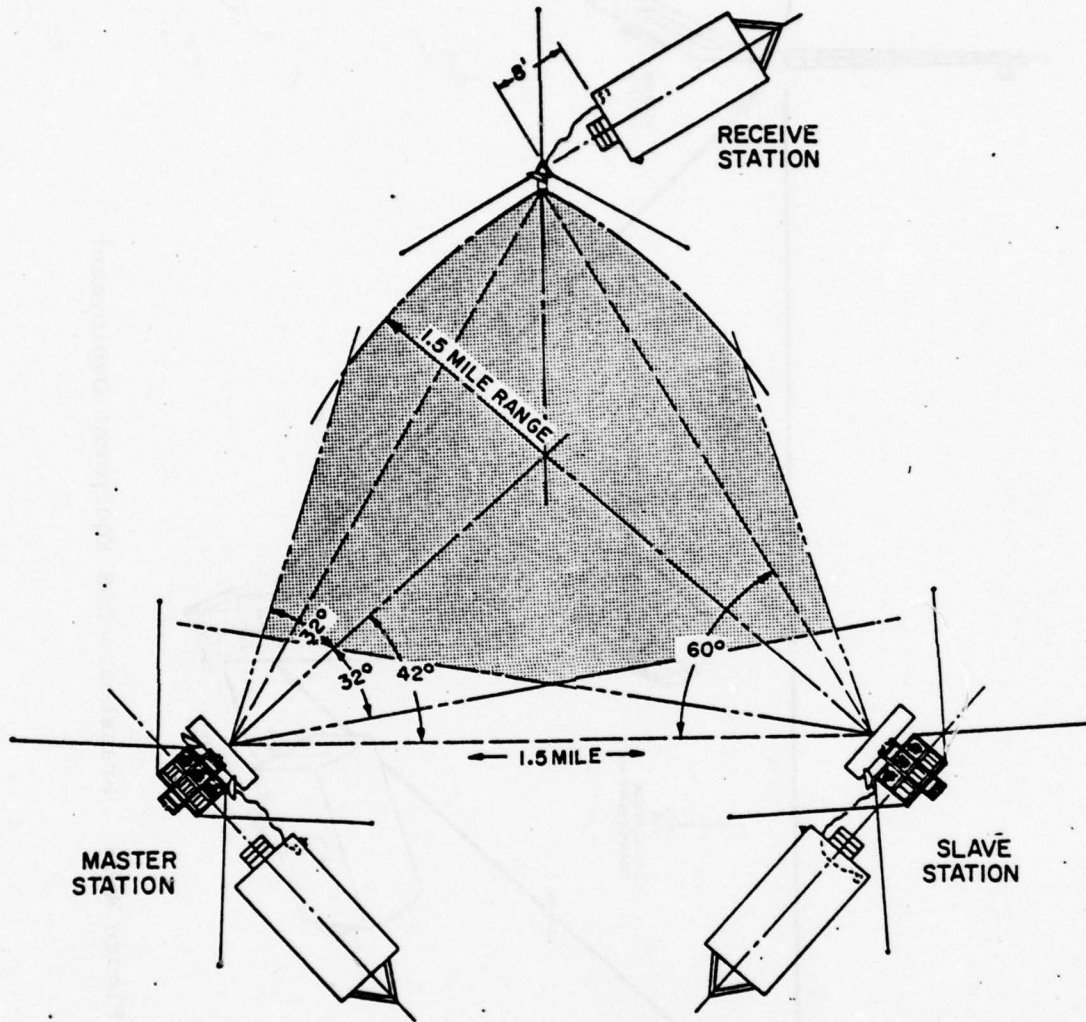


Figure A-19. Typical Brassboard Equipment Siting  
(Detail of Stations Enlarged)

- (5) WWV Receiving Antenna: One long wire capacitive antenna with matching network at the Master Station.
- (6) Calibration Transponders: Two standard aircraft 1/4 wavelength monopoles above a ground plane, one at each transponder with a height above ground of six feet.

Phased array interrogation antennas at the Master and Slave Stations were the only ones requiring critical boresight alignment during installation. For coverage into the 600 foot minimum range, minimum angle off the baseline the boresight angle must be set at  $35.75 \pm 3.75$  degrees. To obtain coverage outside the triad for evaluating GDOP, the boresight angles can be increased to 60 degrees or more.

Boresight was established approximately using optical sighting. A reference point along the correct boresight was first located with surveying instruments. The antenna was then mechanically boresighted to the reference using an optical telescope mounted on the antenna. The telescope was calibrated to electrical boresight during factory antenna range tests. Then the instrumented transponder at the reference point was used to true in the electrical boresight within one degree or less. System accuracy is based on the TOA measurements, not the accuracy of the interrogation angles.

The Receiving Station DAS antenna coverage matches the  $P_1$  receiving element in the phased array. The 3 dB beamwidth is 140 degrees so that boresighting is completely non critical.

The Data Link antennas were mounted at the top of the towers, approximately 26 feet above the surface. This height will clear all ground vehicles and most aircraft so as to minimize blockage of the line-of-sight path. Antenna alignment consisted of adjusting both transmit and receive antennas for maximum received signal strength. Metering AGC voltage in the receiver simplified this procedure.

Communications antennas were mounted on the side of the station trailers to insure line of sight voice communications between stations.

Calibration transponders antennas required no special deployment except for establishing the location for calibration purposes. The NAFEC theodolite and surveyed bench marks were used for establishing coordinates.

Antennas on the test vehicles were clip-on antennas for the ATCRBS transponder and VHF tower communications. Calibration transponders used standard aircraft monopoles mounted above a small ground plane at a height of six feet.

Two different tower designs are required to accommodate the two types of GEOSCAN antennas used in the brassboard DAS. Both interrogation stations (Master and Slave) use an electronically steerable phased array antenna which weighs approximately 480 pounds is 12 feet long, 2.5 feet high and 3 feet deep, including steering electronics. The Receive Station tower requirements are substantially less due to the smaller weight to be supported and less-critical stability requirement of the data link antenna.

The brassboard DAS electronics described above are shown in Figures A-20, A-21, and A-22 for the Master, Slave, and Receive Stations, respectively.

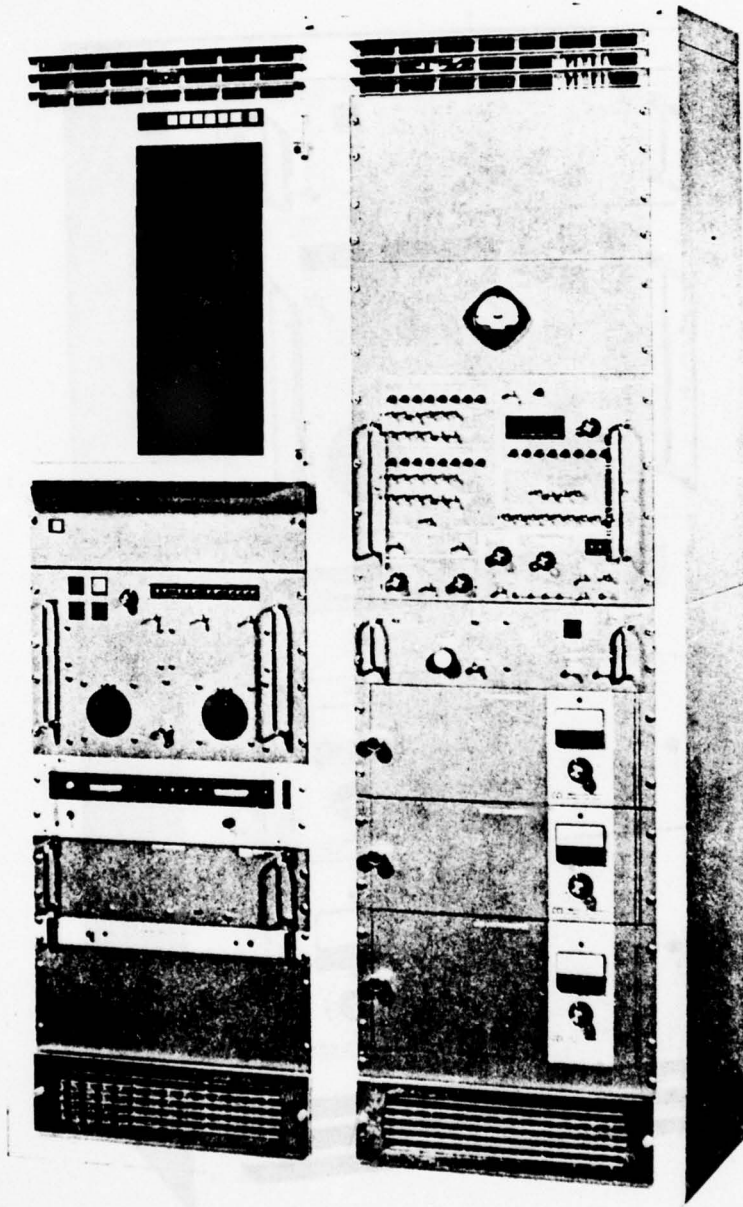


Figure A-20. Master Station Electronics Equipment

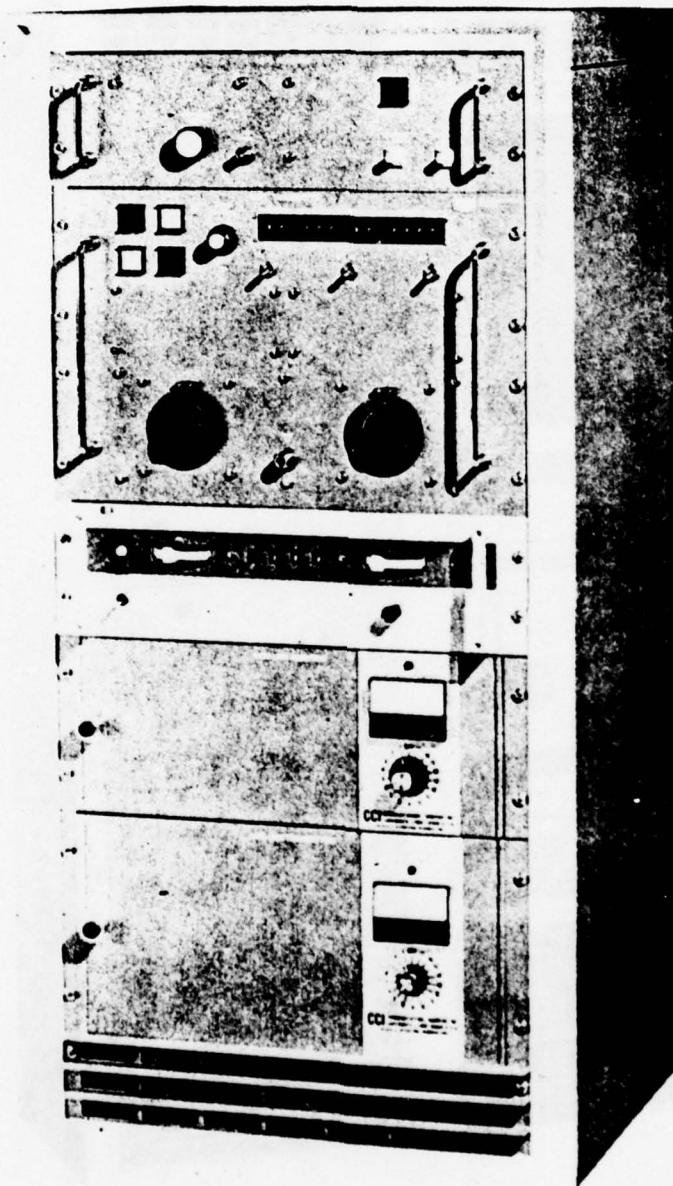


Figure A-21. Slave Station Electronics Equipment

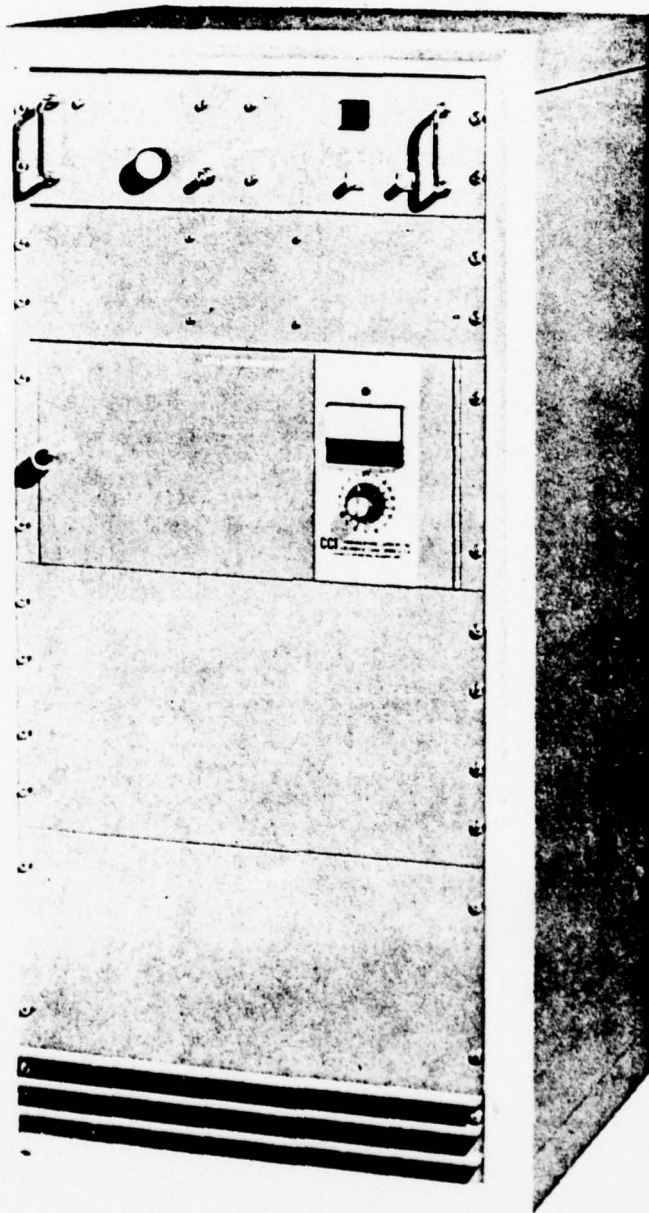


Figure A-22. Receive Station Electronics Equipment

## APPENDIX B

### BRASSBOARD DAS PERFORMANCE CHARACTERISTICS

#### B.1 SUBSYSTEM PERFORMANCE

##### B.1.1 Antennas

Only three antennas are directly involved in DAS technology, the two phased array antennas and the receive station sector antenna. These two antenna types will be discussed in this subsection. All other antennas supporting operation of the brassboard DAS and the test program will be discussed along with their respective subsystems.

##### B.1.1.1 Phased Array Antenna

###### Performance Summary

Operating Frequency	1030.0 MHz + 3.0 MHz (array) 1027 to 1100 MHz (sector)
Polarization	Vertical
Peak Input Power	4 kW
Average Input Power	40 watts
Elevation Beamwidth	32 degrees (-3 dB)
Azimuth Beamwidth	120 degrees
Null width - 16 active elements	4.53 degrees at -6 dB 0.47 degrees at -25 dB
6 active elements	12.1 degrees at -6 dB 1.25 degrees at -25 dB
Sidelobes	-25 dB
Steering Range	64 degrees
Steering Increments	Down to 0.25 degrees
Steering Accuracy	$\pm$ 0.15 degrees
Ripple on Sector Pattern	$\pm$ 2 dB
Number of Active Array Elements	16/6 selectable
Total Number of Antenna Elements	24
Time to Steer -32 degrees to +32 degrees	15 microseconds (one step)

Phase Shifters	6 Bit, PIN Diode Type
Array Elements Spacing	1/2 wavelength
VSWR, Input	1.5:1 maximum

#### Technical Description

The Phased Array antenna accommodates the antenna requirements of both GEOSCAN interrogator and trilateration subsystems which are part of the Master and Slave stations. To accomplish this it must produce two separate antenna patterns:

- (1) A broadbeam sector pattern required to transmit the GEOSCAN  $P_1$  and  $P_3$  pulses on 1030 MHz and receive the transponder replies on 1090 MHz.
- (2) A similar sector pattern having a narrow steerable null in the azimuth plane. The  $P_2$  pulse is transmitted on this pattern as required to generate the GEOSCAN nonsuppression beam.

The first pattern is a simple single element pattern which has a 120 degree azimuth beamwidth allowing transmission and reception over the complete field of interest, Figure B-1. The second type of pattern is effectively that of the single element but with a steerable null generated by a linear phased array. The full aperture null width can be made 2.67 times wider by means of the 6 element partial aperture.

While it has been shown that an array of this type has the ability to generate a high gain pencil beam with a central null and variable gain with respect to the sector portion, only the broad pattern was implemented. This was done to investigate the worst case multipath reception problems resulting from use of a broad pattern as well as holding development costs within contract funding.

To provide these performance characteristics the phased array antenna subsystem consists of the following major components:

- (1) Radiating aperture
- (2) RF Phase Shifters
- (3) RF Power Distribution Network
- (4) Phase Shifter Drivers and Monitors
- (5) Beam Steering Computer

The radiating aperture is a linear array of 24 identical elements in the azimuth plane. The elements are 1/4 wavelength vertically polarized electric monopoles exciting a trough antenna. In the elevation plane the antenna is a flared horn,

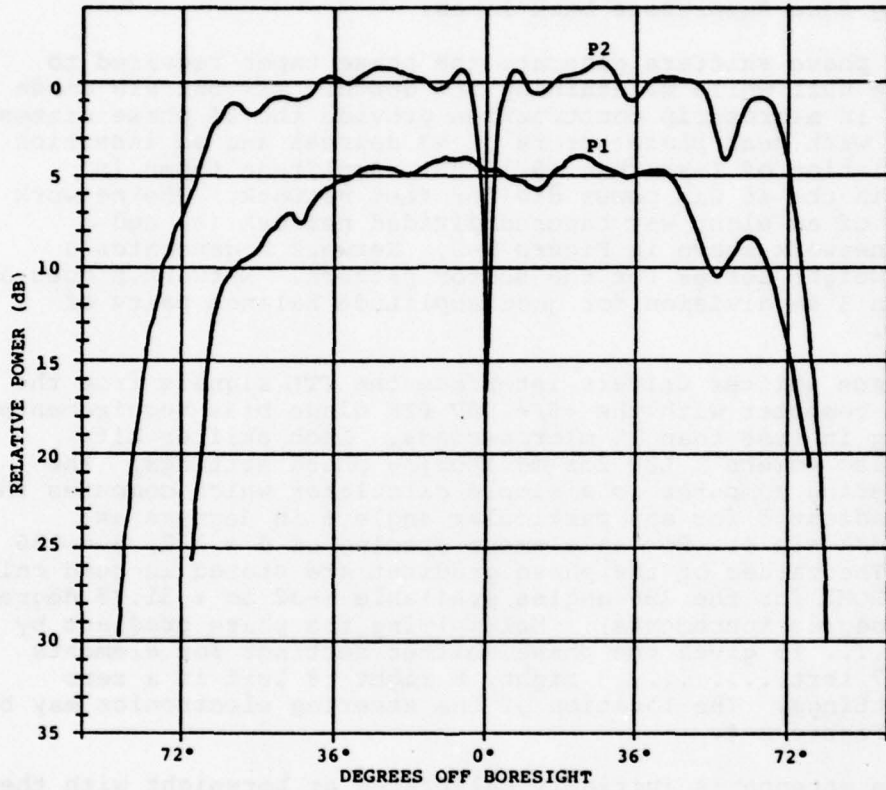


Figure B-1. Measured Brassboard DAS Antenna Patterns  
 (Note: Null at approximately 54°  
 generated by antenna range, not an  
 antenna characteristic)

see Figure B-3. A single element (9L) forms the  $P_1$  sector pattern and is independent of the other subsystem components. The 22 array elements are equally spaced at  $1/2$  wavelength and are symmetrically located about the array centerline. 16 elements are active and used to generate the  $P_2$  pattern. The reduced aperture uses the center six elements. The remaining elements are terminated in a matched load to minimize end-effects. A  $1/4$  wavelength choke along top and bottom of the radiating face suppresses back lobes.

RF phase shifters generate the phase taper required to steer the null while maintaining its depth. Six bit PIN diode shifters in microstrip construction provide the 64 phase states required with peak phase errors of  $+3$  degrees and an insertion loss variation of less than  $+0.15$  dB. Amplitude taper is derived in the 16 way power divider feed network. The network consists of an eight way tapered divided network (A) and a divider network shown in Figure B-2. Network A generates a Fourier weight series for the sector pattern. Network B does a precision 3 dB division for good amplitude balance pairs of elements.

Phase shifter drivers interface the TTL signals from the steering computer with the  $+5/-150V$  PIN diode bias requirements, switching in less than 15 microseconds. Each shifter bit driver also powers a LED for monitoring phase settings. The beam steering computer is a simple calculator which computes the phase gradient  $\delta$  for any particular angle  $\phi$  in degrees as:  
 $\delta = 360 d/\lambda \sin \phi$ . For an element spacing of  $d = \lambda/2$ ,  $\phi = 180 \sin \phi$ . The values of the phase gradient are stored in read only memory (ROM) for the 256 angles available ( $-32$  to  $+31.75$  degrees in 0.25 degree increments). Multiplying the phase gradient by 0, 1, 2,..... 15 gives the phase shifter settings for elements 8 left, 7 left,....., 7 right, 8 right (8 left is a zero phase settings. The location of the steering electronics may be seen in Figure B-4.

The antenna is initially calibrated at boresight with the calibration adders. Each element is adjusted to the proper phase by adding a number to its zero setting which will produce a zero phase on the left half of the array and 180 degrees phase on the right half. This "calibration" automatically superimposes the null pattern on the steering pattern which is generated for each angle. Antenna tests will include a determination of the steering accuracy at each angle. Due to truncation and phase shifter errors, some angles will not meet the requirements for "contiguous null patterns". To bring these steering angles into the desired positions, two types of phase corrections can be utilized. One type sets the same nominal bias phase on every phase shifter. The actual bias existing at each shifter due to random errors can "slightly reposition the null. The second type of correction applies one bit of phase to shifter 8L or 8R. Combinations of both types of corrections can also be used.

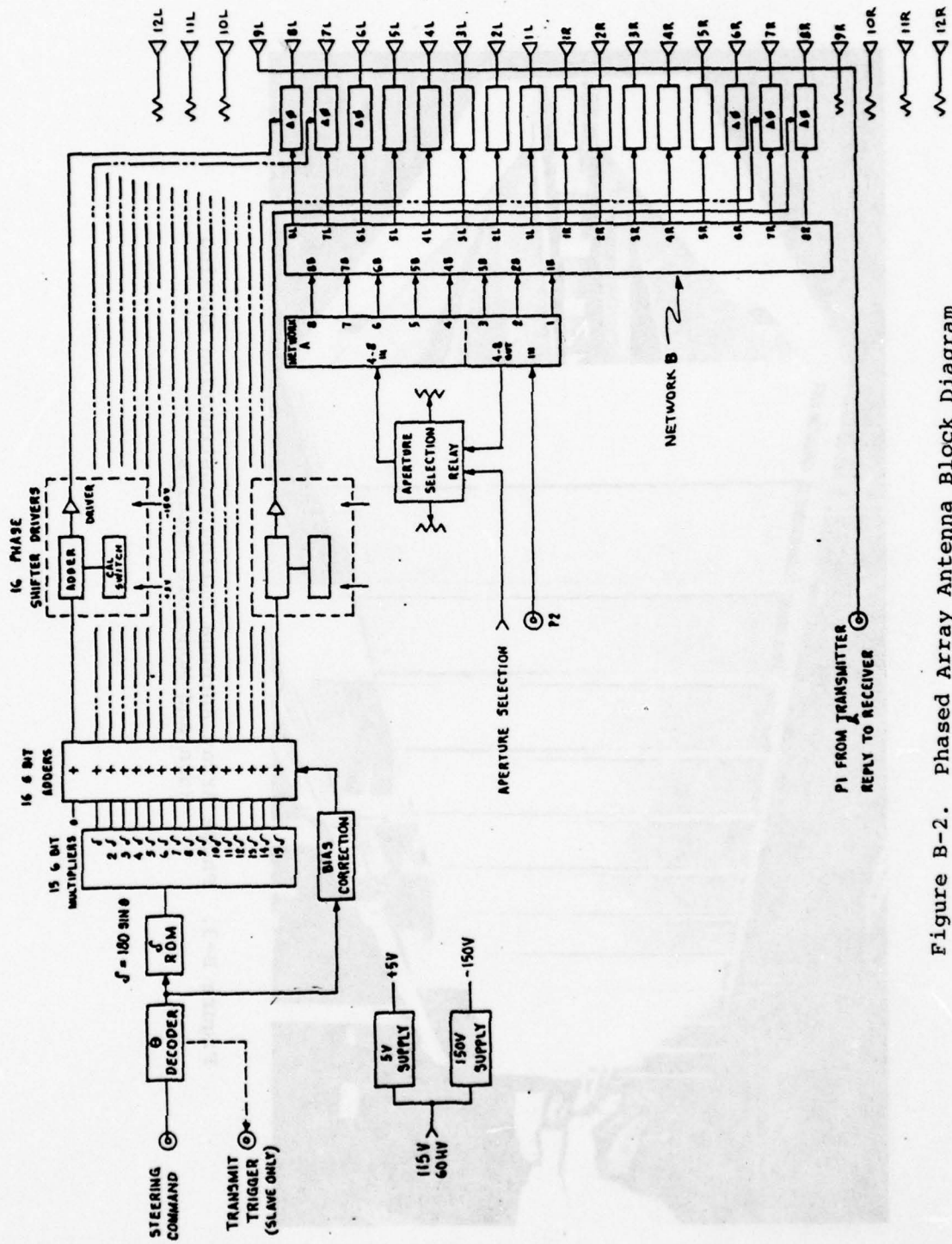


Figure B-2. Phased Array Antenna Block Diagram

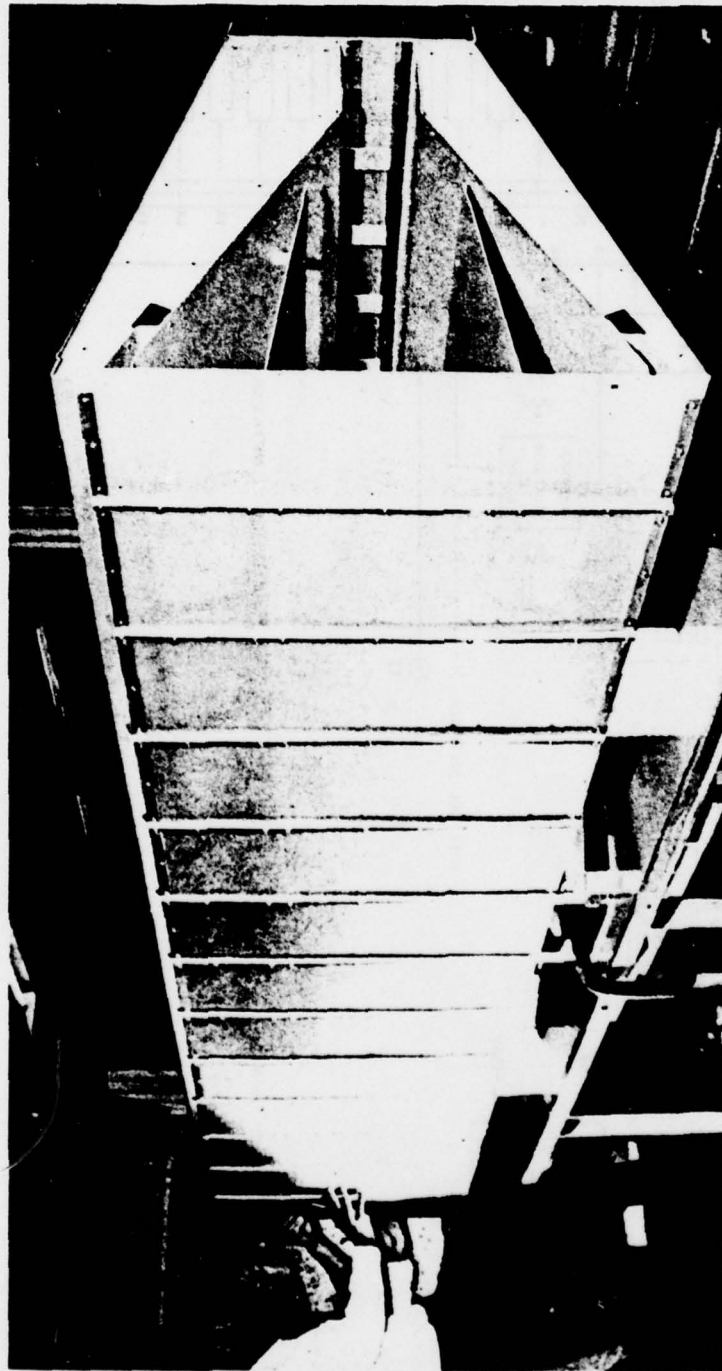


Figure B-3. Phase Array Antenna During Construction Showing  
Horn and Monopole Details



Figure B-4. Phased Array Antenna During Range Testing

Measured phase shifter errors were used in computing the correction to apply to each element via the bias phase adders.

The output of the final adder at each element is gated into the phase shifter drivers for only about 50 microseconds around transmission time, reducing power consumption.

#### B.1.1.2 Sector Receiving Antenna

##### Performance Summary

Operating Frequency	1090 MHz $\pm$ 10 MHz
Polarization	Vertical
Elevation Beamwidth	32
Azimuth Beamwidth	120 degrees
Sidelobes	-25 dB
VSWR	1.5:1 maximum

##### Technical Description

This antenna will simulate the receive element of the phased array antenna. Elevation and azimuth patterns will be matched so as to equalize performance at all three receiving sites. The antenna was fabricated using a dipole array above a ground plane. Three stacked dipoles with a tapered illumination closely matches the horn array's vertical pattern.

#### B.1.2 Interrogator and Suppressor

The interrogator and suppressor subsystems are identical transmitter modules. Controls are provided to allow selection of the GEOSCAN interrogation  $P_1$ ,  $P_2$  and  $P_3$ , or the suppressor transmission using  $P_1$ ,  $P_2$  only. The Master station normally acts as the interrogator with  $P_3$  inserted by a transmitter module front panel switch. At the Slave, the  $P_3$  is deleted. Control of the relative  $P_1$  to  $P_2$  power ratio and the absolute power of  $P_1$  is manually adjustable at the transmitter.

##### Performance Summary

Frequency	1030 $\pm$ 0.2 MHz, crystal controlled
Transmitter Power	
Output $P_2$ broad only	2750 watts peak, 13.8 watts avg.
$P_2$ narrow*	1830 watts peak, 9.2 watts avg.
$P_2$ broad*	920 watts peak, 4.6 watts avg.
$P_1$ ( $P_3$ )	312 watts peak, 3.2 watts avg.

P <sub>1</sub> to P <sub>3</sub> ratio	+1/2 dB
Control over Common (P <sub>1</sub> , P <sub>2</sub> , P <sub>3</sub> ) output	30 dB
Control over P <sub>2</sub> with respect to P <sub>1</sub>	17 dB minimum
Load VSWR	1.5:1 maximum
Modulation Pulsewidth	0.80 +0.03 microseconds, adjustable in 50 nanosecond increments
Pulse Spacing P <sub>1</sub> to P <sub>2</sub>	2.0 +0.05 microseconds, adjustable in 0.1 microseconds increments
P <sub>1</sub> to P <sub>3</sub>	8.0 +0.05 microseconds, adjust- able in 0.1 microsecond incre- ments
Pulse Sequence Selection	P <sub>1</sub> - one per trigger P <sub>2</sub> - one per P <sub>1</sub> , selectable ON/OFF P <sub>3</sub> - one per P <sub>1</sub> , selectable ON/OFF

#### Technical Description

Each transmitter module consists of an RF/Modulator drawer on a 12 inch high EIA 19 inch panel and a high voltage power supply on a 5.25 inch high EIA 19 inch panel. All RF circuits are contained in an EMI shielded enclosure with line filtering. The drawer slides out and tilts for ease of maintenance. All controls normally used are located on the front panel. Calibration controls are located internally to control maladjustment during field tests. This can be seen in Figure B-5.

Under contract to the FAA, Bendix developed and is currently supplying the latest ATC beacon interrogator, the ATCBI-5. The transmitter components of the system are capable of developing 5 kW peak and 50 watts average power output. This exceeds the DAS transmitter requirements of 2.75 kW peak and 17 watts average. It was decided to substitute the BI-5 exciter and power amplifier for the GE tuned oscillator-power amplifier modules originally proposed. The BI-5 has a crystal controlled source power amplifier modules originally proposed. The BI-5 has a crystal controlled source which deletes the need for frequent frequency calibration in the field.

The exciter is all solid-state and contains a crystal controlled source and amplifiers developing 15 watts peak power output at 1030 MHz. The exciter will be used, as in the BI-5, to supply the 1030 MHz CW local oscillator signal to the receiver subsystem. The power amplifier string will be reduced from four to three stages, as the dual output stages feeding

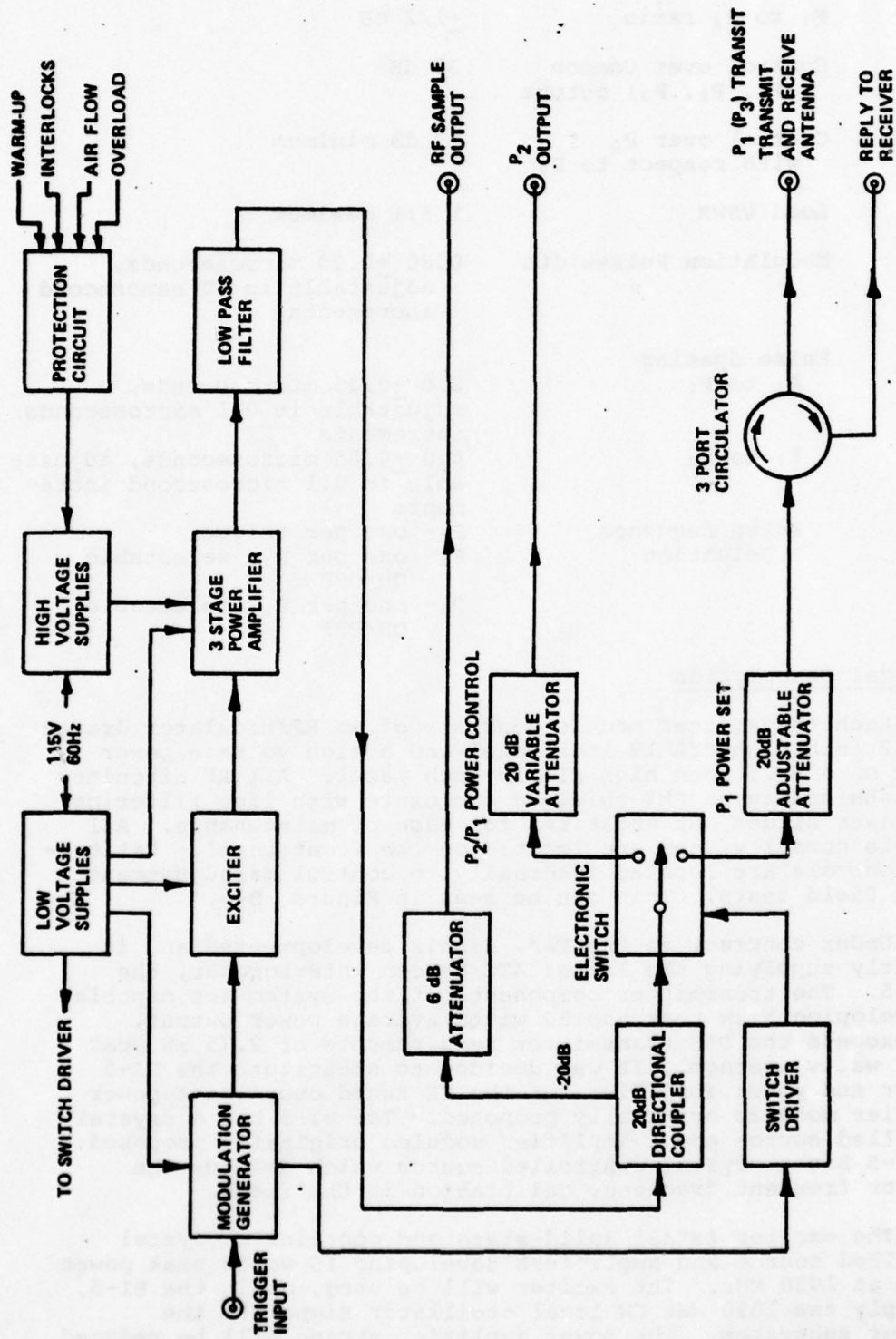


Figure B-5. Transmitter Module Block Diagram

the ISLS system can be reduced to a single output. The high voltage supply can be reduced from 4 kV develop peak power output required. A Hewlett-Packard 6525A 0-4 kV dc regulated power supply having a 100% reserve power capacity with current limiting was selected for this test system.

All other RF components are standard catalog items which did not require additional development. HV interlocks are installed in the transmitter to switch off the high voltage and discharge the storage capacitor for personnel protection. Complete overload, HV turn-on, and air flow interlock protection is also provided.

The transmitter operation is simple and straightforward except perhaps for the unusual outputs required by the phased array steerable null antenna. As shown in Figure B-5, the transmit trigger developed in the Test Control Unit is applied to the modulation generator circuit.  $P_1$  is immediately generated and applied to the exciter as a TTL signal. In the exciter, the CW 1030 MHz source is modulated in the first two Class A amplifier stages, then amplified in two Class C stages developing a 20 watt peak output. The three stage triode power amplifier (PA) uses 8533 ceramic-metal tubes has an effective gain of 44 dB at 4 kV. Amplifier gain is reduced to a net loss as the anode supply approaches zero.

Amplifier output is filtered, sampled (for checking power and pulse width out of amplifier) and split into three signals. During  $P_1$  or  $P_3$  transmission, the electronic switch routes the pulse through the  $P_1$  power set attenuator and circulator out  $P_1$  rear panel output connector. This connects to the Phased Array center element. The reply coming back to the antenna is routed to the receiver by the circulator.

At  $P_2$  transmission time the electronic switch routes the power first through the  $P_2/P_1$  variable attenuator controlling  $P_2$  power output.

### B.1.3 Receiver

The brassboard DAS Receiver Subsystem contains all the RF and quantizing circuitry except for the antenna and duplexer necessary to detect the incoming reply and generate a TOA "time tick". A total of three identical Receiver modules are used, one at each station. At the Master and Slave stations the phased array provides the antenna, and the duplexer is a circulator in the transmitter module. The receive station the sector horn antenna is connected directly to the receiver. The local oscillator is provided by the transmitter exciter except at the Receive station where a separate exciter oscillator is required.

On each receiver two outputs are provided. TOA and ID quantized video, which interface with either the data link or TCU as required. The actual TOA measurement is performed in the

processor portion of the TCU, where a 100 MHz clock is sampled three TOAs are measured at the same place with the same clock, simplifying accuracy checking. ID video is decoded on the ATCRBS 1.45 microseconds data pulse interval time base and recorded on tape. The 12 bit ID code pulses are recorded directly as is the SPI pulse. A single bit garble indication is used to indicate a pulse in the invalid position or in the two slots between F2 and the SPI pulse.

#### Performance Summary

##### RECEIVER

Operating Frequency	1090 <u>±</u> 3 MHz
RF Bandwidth	20 MHz
Receiver Noise Figure	10 dB maximum
Log Dynamic Range	70 dB minimum
Manual RF Gain Control	0-60 dB, 10 dB steps
Maximum Safe Input 1090 MHz	200 mW CW, 15 W peak 10 W CW, 300 W peak

##### QUANTIZER

Quantizer Circuit	Peak Amplitude Estimator Type, Separate TOA and ID
Threshold Jitter and	1.25 nanoseconds (one sigma)
TOA Variation over 70 dB Dynamic Range	1.2 nanoseconds (one sigma)
Propagation Delay Variation	4.0 nanoseconds (one sigma estimate)
Multipath Effect, Two Equal Amplitude Signals - All Delays	7.5 nanoseconds (one sigma estimate)

#### Technical Description

The receiver module is a straightforward single frequency superhetrodyne log IF receiver with separate video quantizers for TOA and ID. The RF portion of the receiver will be constructed using commercially available components, eliminating circuit development. Figure B-6 is a block diagram of the receiver.

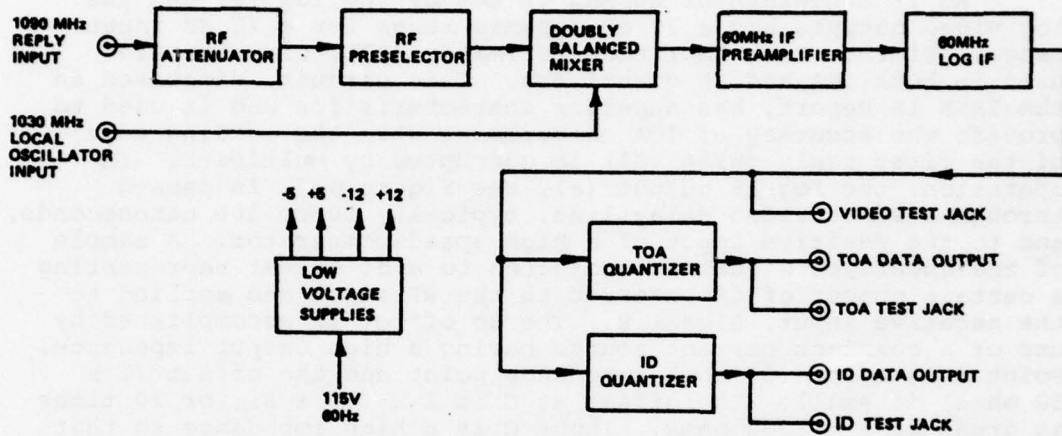


Figure B-6. Receiver Block Diagram

The incoming signal level at 1090 MHz is set with the RF attenuator. Out of band signals are rejected in the 5 pole preselector, and the filtered signal is applied to the doubly balanced diode mixer. The 1030 MHz L.O. signal developed in the transmitter exciter produces a 60 MHz IF at the input to the 2.5 dB noise figure linear IF preamplifier. Gain provided by the preamplifier raises the input signal level to the log threshold at the log IF amplifier input and masks the poor log IF amplifier noise figure.

An IF bandwidth of 20 MHz is set by the log IF, and the log video outputs has a 20 dB dynamic range for a 70 dB input range. Similar Peak Amplitude Estimator (PAE) circuits are used in both TOA and ID quantizers. This circuit, discussed in the TASK 1A Report, has superior characteristics and is used to provide the accuracy of TOA measurement when the leading edge of the first reply pulse (F1) is corrupted by multipath. In operation, the log IF output (a), see Figure B-7, is passed through a short video delay line, typically 50 to 100 nanoseconds, and to the positive input of a high speed comparator. A sample of the undelayed signal is subjected to a dc offset representing a certain number of dB referred to the RF input and applied to the negative input, signal B. The dc offset is accomplished by use of a constant current source having a high output impedance. Point A is a low (50 ohm) impedance point and the offset ( $I \times 50$  ohms) is small. The offset at C is  $I \times (50 + R)$ , or 20 times as great if  $R = 1000$  ohms. Input C is a high impedance so that the voltage at C is described by  $C = A - IR$ .

The output signal A is a linear voltage function of the RF input in dB. Therefore, a constant offset in A at C represents a constant offset in dB. If this offset were set to a typical value of 6 dB and a signal introduced at A, timing waveforms for A, B, C and D, shown in Figure B-8, would result.

Different values of delay and offset were selected to optimize the performance of each circuit with 6 dB for TOA and 3 dB for ID being used during the NAFEC test program.

#### B.1.4 Communications

An operational ASTC DAS will require a means of data transmission between the remotely located GEOSCAN/Trilateration stations and the central ASTC Data Base-Displays. The brass-board DAS program requires site mobility and field test operation independent of airport power and land line communications. Intersite communication must then be maintained using a radio intercommunication system.

A high speed microwave data link is used to communicate GEOSCAN interrogation commands from the Master station to the Slave station. Transponder replies received at each of the Slave and Receive stations will be relayed to the Master station via microwave data link. The data link subsystem

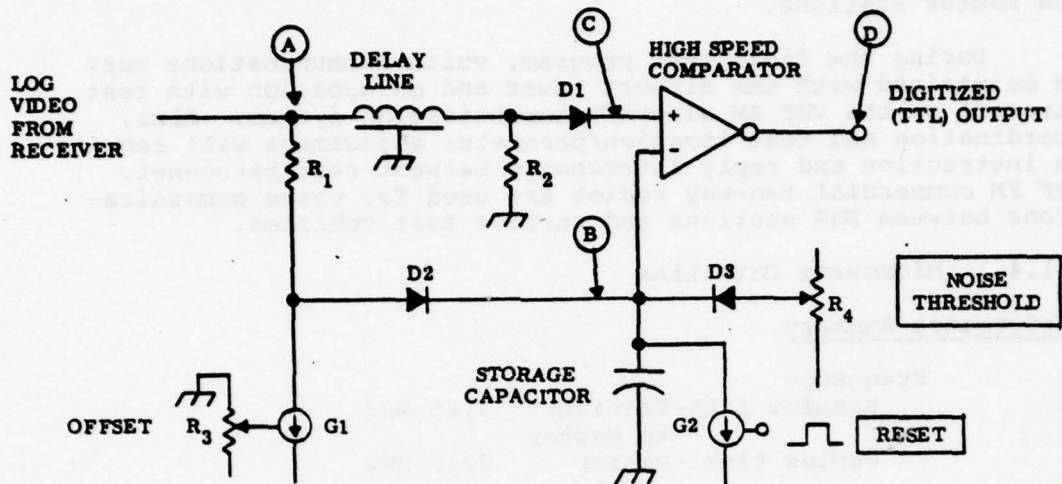


Figure B-7. Basic PAE Circuit

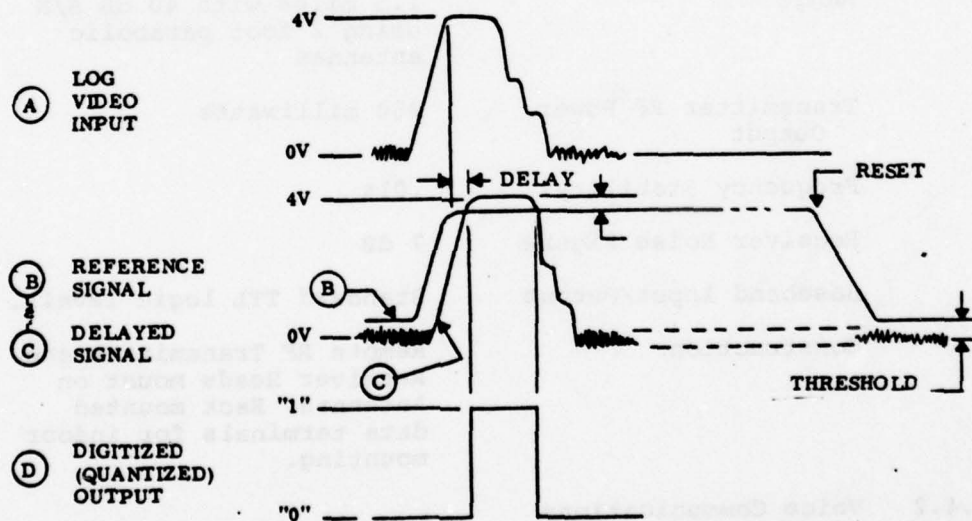


Figure B-8. PAE Circuit Timing Waveforms

consists of a two-way or duplex link between Master and Slave stations and a separate one-way or simplex link between Receive and Master Stations.

During the field test program, voice communications must be maintained with the airport tower and on occasion with test aircraft on the VHF AM aircraft communication system. Also, coordination and test location/parameter adjustment will require an instruction and reply interchange between test personnel. VHF FM commercial two-way radios are used for voice communications between DAS stations and surface test vehicles.

#### B.1.4.1 Microwave Data Link

##### Performance Summary

Frequency	
Simplex Link-Receiver	7185 MHz
to Master	
Duplex Link -Master	7240 MHz
to Slave	
-Slave to	7135 MHz
Master	
Frequency Response	1 Hz to 10 MHz
Deviation	+2 MHz
Range	1.5 miles with 40 dB S/N using 2 foot parabolic antennas
Transmitter RF Power Output	250 milliwatts
Frequency Stability	.01%
Receiver Noise Figure	7 dB
Baseband Input/Output	Standard TTL logic levels.
Construction	Remote RF Transmitter and Receiver Heads mount on Antennas, Rack mounted data terminals for indoor mounting.

#### B.1.4.2 Voice Communications

##### VHF FM Interstation Communications System

This system consists of the following equipments:

- (1) Four portable FM Transceivers operating on 165.1725 MHz with +5 KHz deviation.

- (2) Two base station adapters for use at Master and Slave stations, including remote microphone, battery charger and antennas for mounting to trailer mast.
- (3) Two mobile station adapters for use with vehicle clip-on antennas.

#### VHF AM Aircraft Transceivers

Four systems, one with self contained units having built in antenna and battery pack were provided GFP to the program. Also, a 118 to 135.95 MHz 3-8 watt unit, with 50 KHz spacing allowing communication with aircraft on special assigned frequencies, was provided GFP.

#### B.1.5 Calibration Transponder and Auxiliary Equipment

This subsection covers all those equipments not directly involved in the DAS or communications subsystems but required to support or perform the field test program. Specifically these equipments include:

- (1) Calibration Transponders
- (2) Instrumented Transponder
- (3) Test Equipment, Laboratory type

##### B.1.5.1 Calibration Transponder

Two of these equipments can be used during field tests to act as calibration beacons. These beacons are located at surveyed points within the search region and will reply with a specific code when interrogated. During post test data processing the software program will first calculate the xy position of these two beacons in the TOA system coordinates. The position of the two beacons will be known in both true (surveyed) airport and TOA (measured) coordinate systems. The software program will adjust the TOA coordinates to correct the beacons to their true airport coordinate values. This technique effectively removes translation and rotation bias errors and adjusts the magnification factor for map registration. The velocity of light need not be known. It will be solved for, though not directly, when the magnification factor is derived.

#### Performance Summary

Beacon Transponder	Bendix TR661
Antenna Type	1/4 wavelength vertical monopole above a ground plane
Antenna Height	6 feet, nominal

Power Source	12 volt, 35 amp-hour wet cell battery
Normal Operating Time Between Changes	16 hours continuous
Environmental Protection	Operates in -30 +55° C ambient, in rain tight case.

#### Technical Description

Transponders are standard off-the-shelf aircraft type units; therefore, no electrical design is required. Batteries are used for remote power. They can be recharged on a rotating basis. The transponder is mounted in a weatherproof container. The battery is mounted in the open to allow fumes to vent without attacking the transponder. A six foot mast supports the antenna which is an omnidirectional vertical monopole above a small ground plane. The calibration transponders may be seen in Figure B-9.

#### B.1.5.2 Instrumented Transponder

A standard ATCRBS transponder was instrumented to measure interrogation efficiency and derive interference statistics. During early tests, it was used as a standard to "map" interrogation areas and to measure the effects of multipath on reply efficiency. The transponder was calibrated to conform to nominal standardized transponder performance values as stipulated in the U.S. National Standard for ATCRBS.

The detected log video is applied to a sync decoding circuit for detection of the local ASR/ATCBI interrogations. From these signals timing gates are generated, just as the ASTC Master site, so that the local ATCBI, the ASTC, and remote ATCBI interrogations can be individually identified with time of occurrence, to permit interrogation rate statistics to be measured.

#### Performance Summary

Transponder Specification	Nominal values for TSO'd units
Sample Function	Continuous/single period
Sample Period	1000/100 ASR triggers
Displays	(1) ASTC interrogation count (2) ASTC suppression count (3) Non ASTC interrogation count (4) Non ASTC suppression count

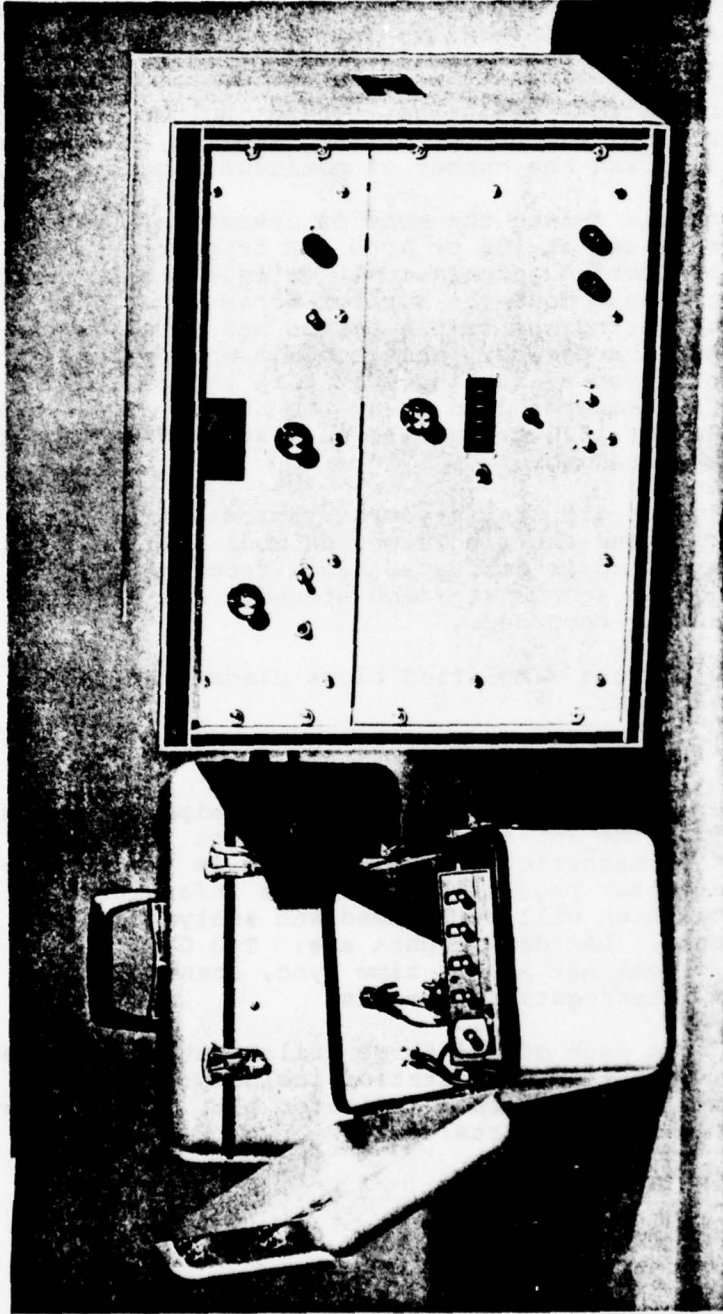


Figure B-9. Calibration Transponders (Left) and Instrumented Transponder (Right)

## Technical Description

The instrumented transponder/monitor utilizes a standard omnidirectional antenna. Internally generated transmitter triggers and suppression gate signals are applied to special counters and other logic circuits which accumulate and display the various interrogation statistics. These include the number of ASTC interrogations, the number of ASTC replies, the number of non-ASTC replies, and the number of nonlocal suppressions.

Several controls select the mode of operation. The sample period can be set at 100 or 1000 ASR trigger periods. The monitor can be operated continuously or in a single sample mode. In the continuous mode the monitor accumulates the various statistics during one sample period and displays the results during the next period. This mode is appropriate for "mapping" an area or for evaluating multipath effects. As the test vehicle progresses around an area, the number of successful interrogations for 1000 tries will be displayed and updated about once each half second.

To obtain and record statistics of various parameters the longer sample period and the single period mode will be used. When a pushbutton switch is activated, data from one 10,000 cycle sample period is accumulated and stored. The displays is then read and manually recorded.

Figure B-10 shows a simplified block diagram of the instrumented transponder.

### B.1.6 Recorder

The Recorder subsystem consists of the equipment necessary to collect data from the TCU and record this data in an IBM compatible format on magnetic tape. This data is the primary output of the field test program and contains information on DAS inputs/outputs which will be reduced and analyzed on the TSC XDS9300 computer. DAS data inputs are: TCU Data Code Control settings, local ASR ATCRBS time sync, standard time (GMT) and GEOSCAN interrogation commands.

Reply data from each of the three trilateration receivers is the DAS output, Data from each station includes: measured TOA, decoded ID and a reply garble indicator bit. The subsystem consists of three component parts:

- (1) Data Buffer
- (2) Tape Formatter
- (3) Magnetic Tape Deck

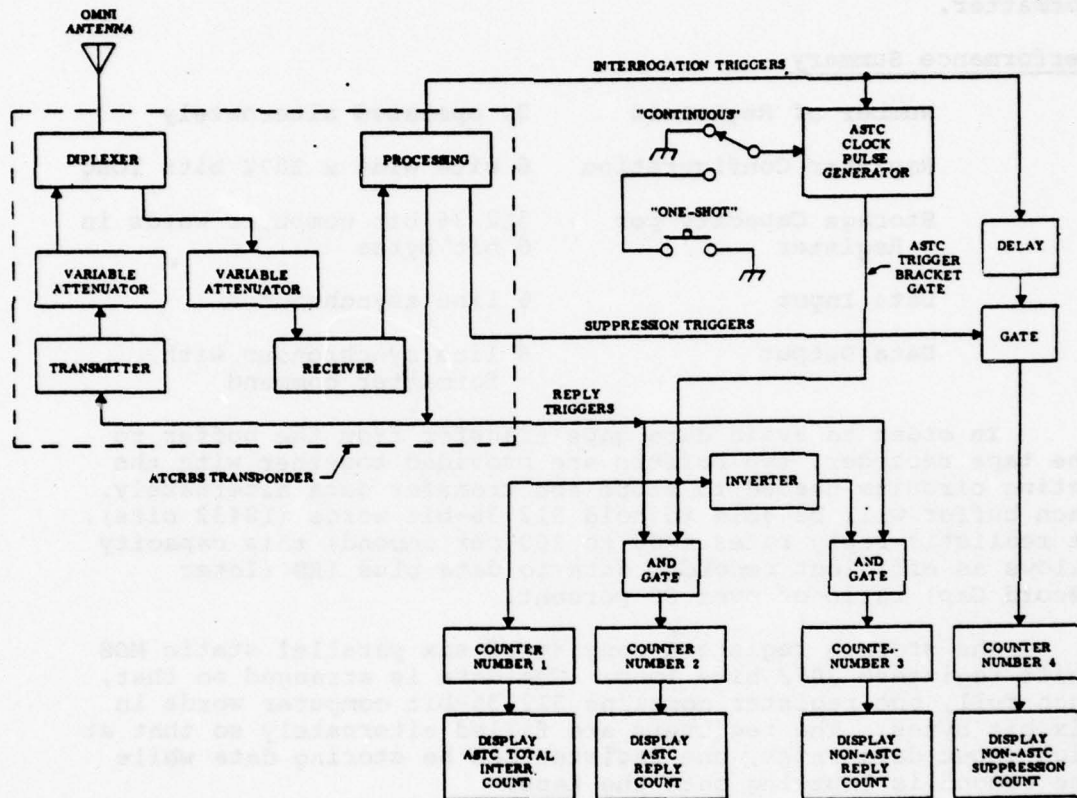


Figure B-10. Instrumented Transponder Simplified Block Diagram

#### B.1.6.1 Data Buffer

This unit is located in the TCU and accumulates data as it is being generated by the DAS and stores it until half the buffer register is full. At that time, data begins filling the other half of the buffer register and the full buffer is read into the formatter.

#### Performance Summary

Number of Registers	2, operated alternately
Register Configuration	6 bits wide x 3072 bits long
Storage Capacity per Register	512 36 bit computer words in 6 bit bytes
Data Input	6 line asynchronous
Data Output	6 line synchronous with formatter command

In order to avoid data gaps transfer from the buffer to the tape recorder, two buffers are provided together with the gating circuits needed to store and transfer data alternately. Each buffer will be able to hold 512 36-bit words (18432 bits). At realistic reply rates (400 to 800 per second) this capacity allows an efficient recorded data to data plus IRB (Inter Record Gap) ratio of over 80 percent.

The storage registers consist of six parallel static MOS shift registers 3072 bits long. The data is arranged so that, when full, one register contains 512 36-bit computer words in six bit bytes. The registers are filled alternately so that at high input data rates, one register can be storing data while the second is emptying onto the tape.

Each time data is to be recorded (heading data at the beginning of a test, TOA/ID data for each reception, and periodic time data), the multiplexer feeds data bytes into the buffer under control of the Data Word Control circuitry in the TCU. The number of bytes stored in the buffer is accumulated in a counter. When the counter fills at 3072 bytes, the buffer flags the control circuitry to switch subsequent data into the second buffer and initiates a record cycle. The data is recorded by byte with parity added, via the formatter. As soon as the record is finished (i.e., the buffer is empty), the IRF is made on the tape, and recording halts until the other buffer is full, at which time the switching and recording cycle repeats. Since the recording rate is 36 K bits/second, all 18,432 bits in the buffer plus 3,072 parity bits can be transferred to the tape in about 600 ms.

If, at the time the IRG is recorded, the "test run" switch is "off", a file mark is recorded by the formatter and

the test tape terminated.

#### B.1.6.2 Formatter

This is a standard commercial unit used as a companion to the magnetic recorder. It functions to accept 36 bit computer word data in six bit bytes, add parity to each 6 bit byte and read out the 7 bit word to the magnetic tape recorder. In addition to adding parity, the formatter generates the IRG and File Mark data per IBM format.

##### Performance Summary

Type	IBM compatible, write only
Packing Density	800 bits per inch
Tape Speed	45 inches per second
Channels	Seven
Interrecord gap	0.75 inches
Parity	Selectable: even or odd
Size	19 inch dia rack x 3.5 inches high
Weight	25 pounds
Power	100 watts, 115 VAC $\pm 10\%$ , 48 to 63 Hz

#### B.1.6.3 Tape Deck

A 45 inch per second (ips); 800 bits per inch, seven track IBM format compatible tape transport is used. Standard commercial equipment can be used in the Master station controlled environment. Servo amplifier drives on these machines eliminate any problem associated with line frequency variation of the portable power plant. A seven bit system was selected to be compatible with TSC data processing equipment.

##### Performance Summary

Tape Speed	45 inches per second
Tape Speed Variation	+3% instantaneous <u>+1%</u> average
Stop Time	8.33 milliseconds
Start Time	16.67 milliseconds
Rewind Speed	200 inches per second

Number of Tracks	Seven
Packing Density	800 bits per inch
Recording Format	IBM compatible
Reels	10.5 inch diameter maximum, IBM Hub
Tape	IBM P/N 457892 or equivalent
Power	300 watts maximum 115 VAC $\pm 10\%$ , 48-63 Hz
Electronics	Standard 930-7400 with TTL interfaces
Physical Size	24 inches high 19 inches EIA rack
Weight	80 pounds

#### Technical Description

The Bright Industries Model 2700 is used. This machine provides:

- (1) Dynamic braking and programmed restart - braking provided by the reel drive motors, not mechanical brakes. Reels stop smoothly without spilling tape, even if the power should fail.
- (2) Electronic write de-skew - Precise bit alignment is assured by channel-by-channel write de-skew. This system assures that tapes can be written in such a way as to be read without error on the XDS 9300 tape decks at TSC.
- (3) IBM guide spacing - Precise IBM guide spacing complements the electronic write de-skewing in assuring that IBM equipment can be used to read tapes generated with this machine.

#### B.1.7 Data Processing

The software developed was used to process test program data at key points as visualized in the data flow diagram of Figure B-9. The following major software packages were developed for various important portions of the data reduction.

- (1) a data simulator package to generate sample simulated DAS output tapes for initial testing of

data processing programs and procedures.

- (2) a quick look package to check for proper functioning of DAS by rapid selective processing of individual test tapes.
- (3) a post-test data analysis package for statistical evaluation of system performance, based on analysis of multiple tapes and multiple data sources, producing merged output tapes.
- (4) a graphics package using merged output tapes from the data analysis package to produce off-line plots and histograms and simulated - real time moving displays.

The following sections give more detailed descriptions of each of the software packages, its interfaces, and its current status.

#### B.1.7.1 Data Simulator

The Data Simulator Program produces, as output, simulated DAS tapes containing information similar to the expected real data and in formats identical to those currently specified. As input, one may specify the locations of the master, slave, and receive stations in three dimensions, the master and slave nominal orientations, and all information set for the actual system on the Test Control Panel. The program simulates SSR frame time stepping, the beam-direction cycling procedure of the master and slave antennas, and the ASTC trigger signals during the ASR dead time. This information is then compared with another set of data driving a target traffic generator that moves simulated aircraft in synchronism with the SSR time clock. The traffic generator can handle as many targets as specified by increasing array dimensions to the limit of available storage. Equations of motion are defined by the parameters of a third-degree series in time. Alternately, one of the targets may have its motion specified by interpolating between points on a magnetic tape at which position and velocity are specified. We have in fact been using a NAFEC-supplied sample phototheodolite tape for this purpose. Thus, the Data Simulator can be used to generate sample DAS output tapes that may be used along with the sample phototheodolite tape to test out Data Analysis modules designed for tests in which the NAFEC phototheodolites would be used.

For every target, depending on master and slave beam orientations, the probabilities that the ASTC triggers will be suppressed are calculated; and a random number determines whether simulated target reply words are to be written.

#### B.1.7.2 Quick-Look Package

As illustrated in the data flow diagram of Figure B-11, the Quick-Look Package is designed to expedite verification of a particular test before the next working day in accordance with the proposal. The computer used was the TSC XDS-9300 that was to be available on a dedicated (exclusive) basis. Thus, the Quick-Look Programs are designed to permit maximum operator intervention through the interrupt buttons, sense switches, and system typewriter.

The basic operations of the Quick-Look Package include reading of the DAS test tapes using double buffering, compiling statistics on data validity (parity errors, etc.) decoding and identifying data words, compiling basic statistics on data content (garble, invalid ID, ID mismatch, missing ID, etc.), computing fixes when possible, with indication of distance from center of current interrogation cell, checking on master and slave beam cycling, etc.

At the operator's option from the computer console, intermediate printouts of the processing can be obtained. Physical records and/or data words can be dumped in octal. Wild points can be checked, to be smoothed or suppressed as desired. Statistical means, variances, etc., may be accumulated as desired for any desired choice of variables of interest, e.g., position coordinates of unknown fixed targets or position discrepancies of known fixed targets.

For moving targets, instantaneous speeds, accelerations, etc., can be calculated. These can then be averaged over short time periods, either operator-specified or controlled by program sensing of change of state (e.g., acceleration rising above a threshold in case of nominally constant speed targets).

The key requirement for the Quick-Look Package is flexibility. Just enough of each type of data need be processed to indicate the success or lack thereof in data gathering for a particular test run, so that other tests may also be verified.

#### B.1.7.3 Post-Test Data Analysis Package

The post-Test Data Analysis Package incorporates all of the analysis options of the Quick-Look Program, but with less emphasis on flexible, quick response and the detection of unusable test data. Rather, it is oriented towards comprehensive processing of all the data of a given test run, using all relevant analysis procedures available, not just selected computations over limited portions of a test run for purposes of verification.

There will be different program modules for different major types of tests. For example, in the case of a known, non-moving target the calibration of the constant TOA delays for

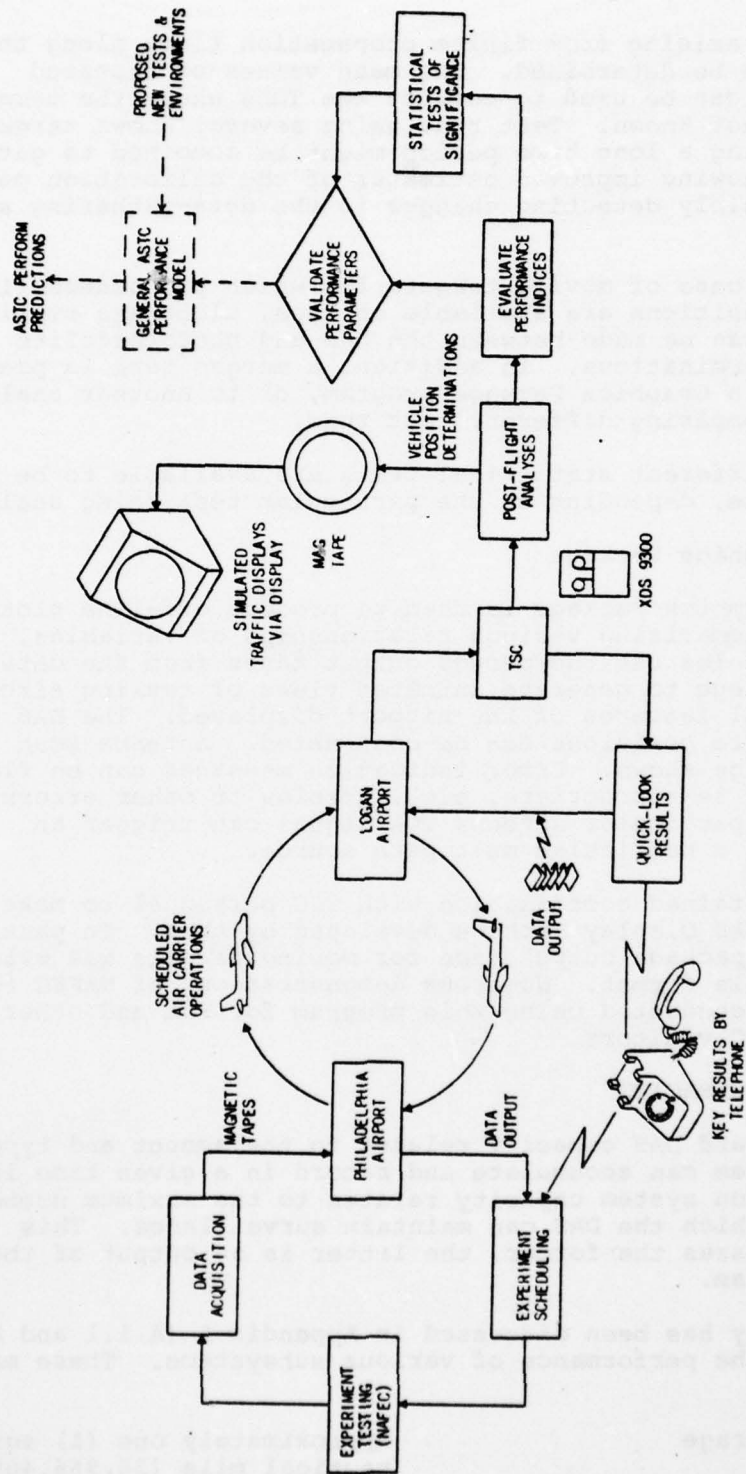


Figure B-11. Data Flow Concept

each station arising from finite propagation times along the data link can be determined. The mean values of repeated measurements can be used to correct the TOAs where the target location is not known. Test runs using several known targets and/or covering a long time period might be combined to gather statistics showing improved estimates of the calibration parameters or possibly detecting changes in the data-gathering system with time.

In the case of moving targets for which phototheodolite-determined positions are available on tape, elaborate statistical comparisons can be made between the DAS and phototheodolite position determinations. In addition, a merged tape is prepared for input to a Graphics Package program, or to another analysis module for comparing different test runs.

Many different statistical tests are available to be used as appropriate, depending on the particular test being analyzed.

#### B.1.7.4 Graphics Package

The Graphics Package is used to produce off-line plots and histograms summarizing various relationships of variables. In addition, modules use the merged output tapes from the data analysis package to generate animated views of taxiing aircraft, with principal features of the airport displayed. The DAS and phototheodolite positions can be contrasted. Antenna scan patterns can be shown. Error indication messages can be flashed on the screen as appropriate, e.g., garbles or other errors with respect to a particular antenna TOA signal can trigger an indication of a particular multipath source.

We maintained coordination with TSC personnel to make use of the ASTC DAS Display Package developed by them. In particular, the analysis package output tape for moving targets was written in a compatible format. Numerous demonstrations of NAFEC test results were conducted using this program for FAA and other interested TSC visitors.

#### B.2 SYSTEM CAPACITY

Brassboard DAS capacity relates to the amount and type of data the system can accumulate and record in a given time interval. Operation system capacity relates to the maximum number of aircraft on which the DAS can maintain surveillance. This section discusses the former, the latter is an output of the overall program.

Capacity has been discussed in Appendix A (A.1.1 and A.1.2.1) in terms of the performance of various subsystems. These may be summarized:

Coverage

Approximately one (1) square  
nautical mile (36,966,400

	square feet) depending on interrogator relative angles.
ASTC Update Rate per Target	Variable between 1 per 10 seconds and 10 per second.
Maximum Reply Recording Rate per Receiver	4800 per second.
Tape Running Time	32 minutes at 4800 replies/second 6 hours at 800 replies/second
Maximum Number Targets	Unlimited except by coverage and target separation (150 feet) requirement.
Update Rate	Determined by interrogation rate and number of cells per scan. Full scan with 1° increments at an interrogation rate of 380/second requires 10.44 seconds. Update on entire 9000 foot runway using 380 interrogations/second is 8 times per second.

### B.3 DATA ACQUISITION

The Data Acquisition Subsystem will function properly if the target information is generated with sufficient dependability to assure reliable target tracking. This information consists of three major components:

- (1) Target Interrogated - Necessary to elicit a reply.
- (2) Target Detected - Enables position determination from the detected reply.
- (3) Target Identified - Permits target position updating for multiple targets.

A fourth possible event, the false target report, must be dependably infrequent so as to preclude confusing false target clutter. We are interested therefore in establishing a measure of the probabilities of interrogation, detection, identification and false report.

#### B.3.1 Probability of Interrogation Prediction

A successfully interrogation depends on the time/space coincidence of the target transponder antenna and the crossover area of the two nonsuppressed (GEOSCAN) regions and the receipt of the P<sub>1</sub> and P<sub>2</sub> pulses during their broadcast. The three prime interrogation modes are: Search, Acquisition, and Tracking. Search is blind interrogation of specific designated areas,

looking for targets not being tracked. Once a search interrogation generates a reply, the Acquisition mode is entered. Here a directed search in the area of reply acquires enough additional data (speed and direction) to establish a track.

Finally, a target under track is interrogated by successive interrogation of the predicted location cell and adjacent cells until a reply is obtained. Thus the probability of interrogation depends on the possibility of a target moving out of a cell between interrogations or of gaps or gray areas in the contiguous cell coverage. The chosen track and search scanning techniques involve overlaps in adjacent beams and therefore in adjacent cell positions. Thus a margin is provided for errors in the positions of both target and beam. We can express these relationship in terms of the standard deviations of the beam pointing and position error (or position change during interrogation) as well as the null beamwidth, the steering increment (i.e. beam overlap) target acceleration, interrogation period, the measurement prediction time interval, which could be different from the interrogation period, the range, and the GDOP factor (Geometric Dilution of Precision due to acuteness of intersection angle of beams or loci). From these constraints it can be shown that the system design parameters provide an overlap margin sufficient to result in a 90% probability of interrogation when beam pointing and position prediction errors are as large as two standard deviations. That is, the system margin allows for 95% of all errors in each of the crossing scan directions giving a 90% joint probability of successful interrogation.

### B.3.2 Probability of Detection Prediction

The likelihood of successful reception of a triad of TOA measurements, independent of successful ID determination, depends on the combined likelihood of successful nonsuppression from one station and successful interrogation from the other. As mentioned in paragraph B.3.1 above, the cell overlap is adjusted to give 95% probable successful interrogation and nonsuppression at all points. Thus with a minimum of 100 feet aircraft separation and with beam steering increments generating sufficient overlap to accommodate that separation, the probability of a reply is 90%.

The likelihood of successful detection of the transponder reply at the three receiver sites, ignoring the ID and garble question, is virtually 90% for the following reasons: The propagation to two of the TOA sites is along a path reciprocal to path of the interrogation and suppression pulses. Thus if those pulses were received, the response will with a very high likelihood be received. The third path to the TOA receiver is subject to unpredictable variations in signal strength estimated to be no more than 75 dB maximum for the proposed TOA receiver at minimum height above ground. The peak amplitude estimator circuit in the receiver is expected to operate over a 60 to 80 dB dynamic range with little deterioration. Also the expected dynamic range can be substantially reduced by limiting antenna locations so that the minimum target range exceeds the 100 feet

assumed above. Finally situations of blockage by permanent structures and terrain may be accommodated by additional receiver stations. Thus one may conclude that the probability of detection will not be significantly different from the probability of reply, that is, 90% per update.

### B.3.3 Probability of Identification Prediction

Proper identification depends on the ability to decode the mode 3/A aircraft reply correctly which in turn depends on receiving an ungarbled reply at one or more TOA stations. Therefore, the Probability of Identification is approximately = 1 - Probability of Garble. The requirement on the number of valid ID's required to identify the target is not fixed but is related to target density. However, the probability of an ungarbled reply at one, two or three stations can be calculated using an assumed model.

There are three components of garble:

- (1) Garble due to fruit (replies received which are not in response to a valid interrogation from this system, i.e., unsynchronized or random replies generated by a variety of means).
- (2) Garble due to multipath.
- (3) Garble due to multiple responses.

These three probabilities were calculated by MITRE\* using a model having the following properties:

Assume 200 aircraft, transponder equipped, in line of sight of all receivers and 50 interrogators in line of sight of each of these aircraft. If each interrogation is assumed to have a 5 second scan period and a hit rate of 14 hits per transponder per scan, each transponder will at most generate  $(50 \times 14)/5 = 140$  reply sequences per second.

Also, assume that a transponder has replied to an interrogation and that this reply sequence must be detected at several receivers such that no garbling of any of the 13 I.D. bit locations occurs due to destructive interference. Using the Poisson probability law, the probability of the number of garbled replies due to overlap can be calculated per unit time.

The results of the MITRE analysis are as follows:

- (1) Probability of garble due to fruit = .049
- (2) Probability of garble due to multipath = .0622

\*J. D. Vinatieri, "Feasibility Analysis of an ATCRBS Based Surface Trilateration Surveillance System, "MITRE, Report FAA-RD-73-75, (June 1973)

- (3) Probability of garble due to multiple replies =  
.329

This last probability, garble due to an undesired transponder response is based on all 200 aircraft being in a position to be incorrectly interrogated. However, the probability of an unwarranted reply from an aircraft less than 150 feet from the one intended is only 0.1, and there are assumed to be at most 20 of the 200 total aircraft so spaced. The overall probability of a second reply is then 0.01 which results in a probability of garble equal to 0.0033.

These three garble probability components can be combined into a single factor on a root-sum-square basis to determine the probability of garble considering all sources, Pg.

$$P_g = 0.074$$

Thus, it is anticipated that on the average 7.4% of all interrogations result in a garbled I.D. code at each receiver. This probability is the average over a long interval of time where aircraft densities and locations are variable. The short term probability of garble may be higher or lower depending on the aircraft density and location with respect to the interrogation sector and airport and receiver geometry.

Using the binomial theorem, the probabilities of obtaining an ungarbled reply at the triad of TOA stations can be calculated. Thus the probability of obtaining:

Three out of three ungarbled I.D. Codes = .794

Two out of three ungarbled I.D. Codes = .984

One out of three ungarbled I.D. Codes = .999

#### B.3.4 Probability of False Reports Prediction

The probability of false reports insofar as it affects garbling was evaluated above. Of additional interest is the impact on those aircraft which may be clustered in a high density region such as a departure queue. The probability of a false report depends on the interrogation resolution. The probability of a correct reply  $P_{CR}$  is the probability that aircraft number 1 replies and that aircraft number 2 does not. Thus,  $P_{CR} = P_{R1} \times (1 - P_{R2})$ .

On the assumption that actual interfering aircraft will be randomly distributed relative to the interrogation cell center, measure of the average resolvability of the system is presented in Figure B-12 for various beam intersection angles. This figure graphs the average probability of receiving a reply only from an aircraft transponder located close to the center of the interrogation cell and not from another transponder located at distance R from the first. The interfering aircraft is positioned

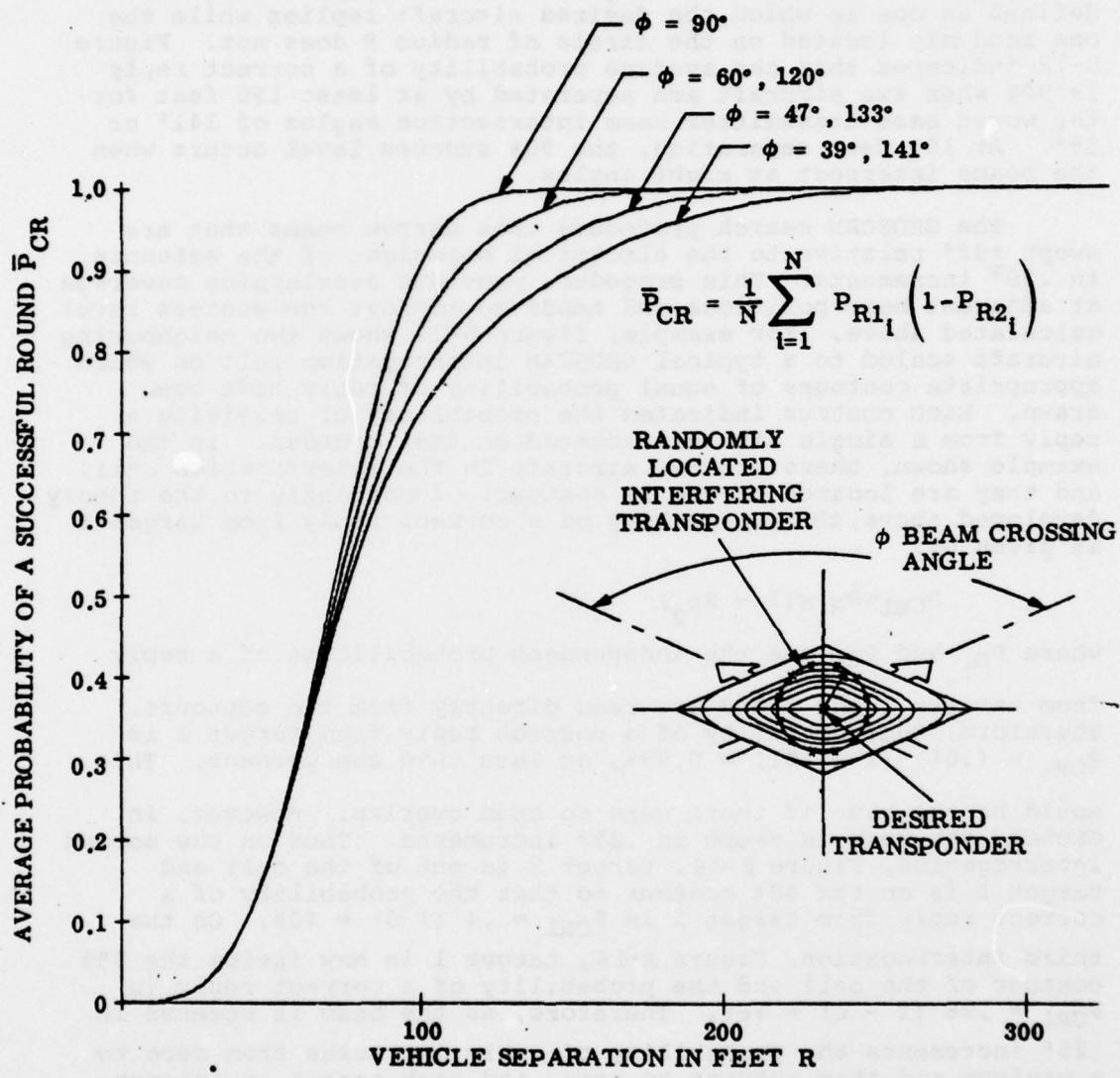


Figure B-12. Interrogator Resolution

randomly on a circle of radius R and the average probability of a successful round is graphed as a function of the distance R for different beam intersection angles  $\phi$ . A successful round is defined as one in which the desired aircraft replies while the one randomly located on the circle of radius R does not. Figure B-12 indicates that the average probability of a correct reply is 90% when two aircraft are separated by at least 150 feet for the worst case transmitter beam intersection angles of 141° or 39°. At 100 feet separation, the 90% success level occurs when the beams intersect at right angles.

The GEOSCAN search procedure uses narrow beams that are swept +32° relative to the electrical boresight of the antennas in .25° increments. This procedure provides overlapping coverage at adjacent beam positions and tends to improve the success level calculated above. For example, figure B-13 shows two neighboring aircraft scaled to a typical GEOSCAN interrogation cell on which appropriate contours of equal probability of reply have been drawn. Each contour indicates the probability of receiving a reply from a single aircraft located on that contour. In the example shown, there are two aircraft in the interrogation cell, and they are located on the 1% contour. Accordingly to the theory developed above, the probability of a correct reply from target 1 is given by:

$$P_{CR1} = P_{R1} \times (1 - P_{R2})$$

where  $P_{R1}$  and  $P_{R2}$  are the independent probabilities of a reply from targets 1 and 2 and are read directly from the contours. Therefore, the probability of a correct reply from target 1 is  $P_{CR1} = (.01) (1 - .01) = 0.99\%$ , or less than one percent. This

would be the case if there were no beam overlap. However, in GEOSCAN the beam is swept in .25° increments. Thus on the second interrogation, Figure B-14, target 2 is out of the cell and target 1 is on the 40% contour so that the probability of a correct reply from target 1 is  $P_{CR1} = .4 (1-0) = 40\%$ . On the third interrogation, Figure B-15, target 1 is now inside the 95% contour of the cell and the probability of a correct reply is  $P_{CR1} = .96 (1 - 0) = 96\%$ . Therefore, as the beam is steered in .25° increments the probability of reply increases from zero to a maximum and then returns to zero, and each target is interrogated at least four times as the beam sweeps by.

The same situation holds for targets along the other axis. It should also be mentioned that this scheme applies only for the GEOSCAN search mode. In the track mode position and velocity are predictable so that the target will always be situated at or near the center of the cell where there is a high probability of a correct reply and little chance that a neighboring aircraft will be interrogated.

The above discussion applies to perpendicular beams and a

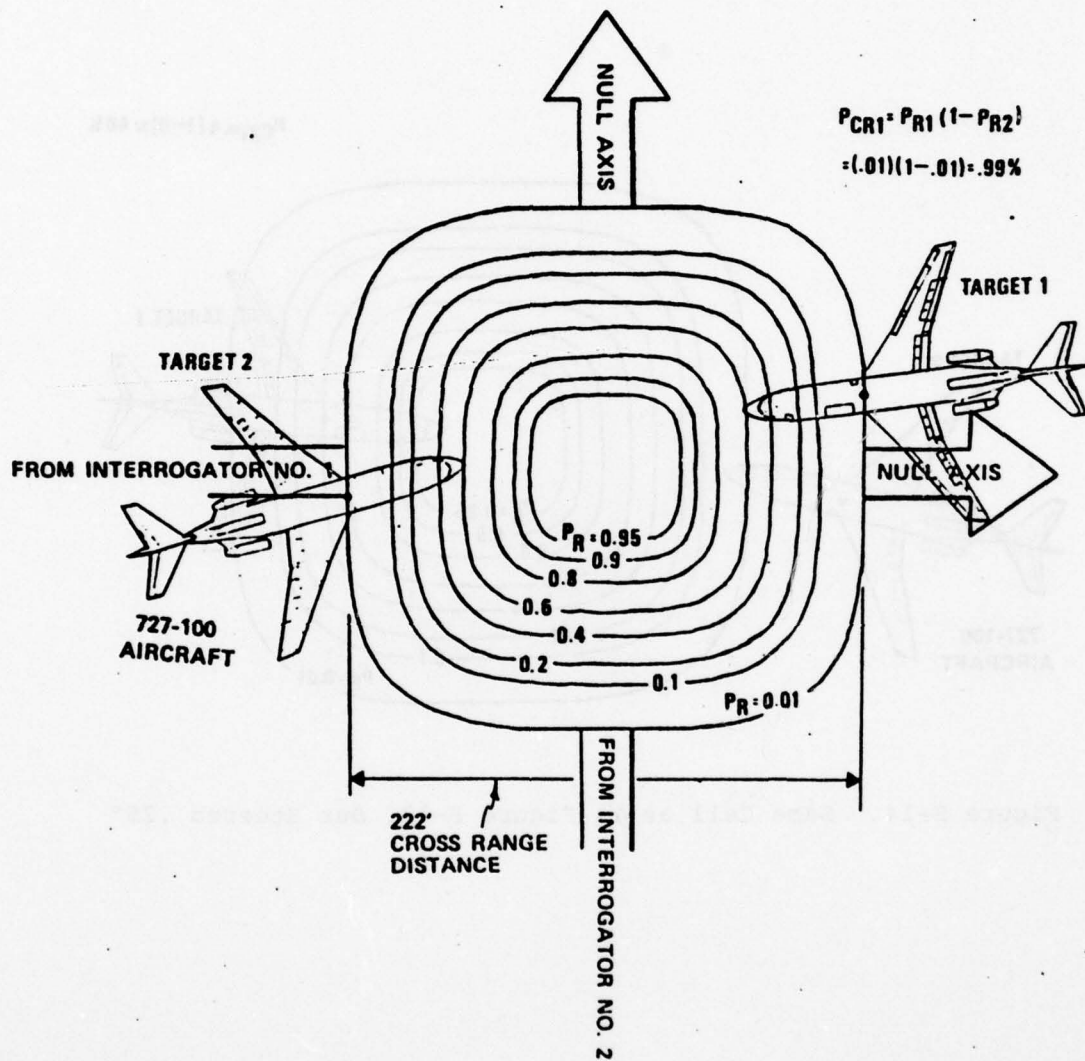


Figure B-13. Geoscan Cell Coverage of Two Close Proximity Aircraft

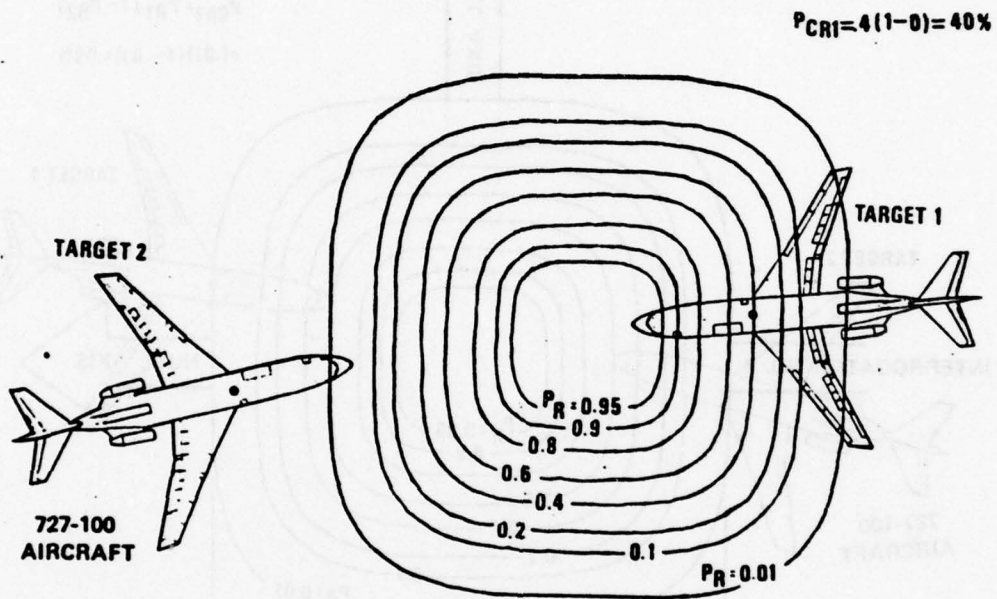


Figure B-14. Same Cell as in Figure B-13, But Steered  $.25^\circ$

...the same cell as in Figure B-14, but steered .25° ...

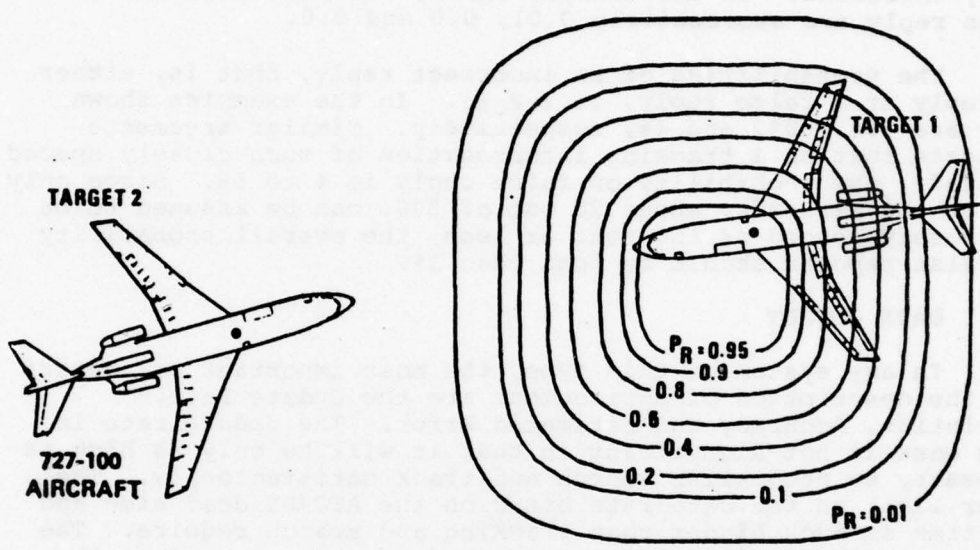


Figure B-15. Same Cell as in Figure B-14, but Steered .25°

...the same cell as in Figure B-14, but steered .25° ...

rectangular cell. If the beam intersection angle differs from  $90^\circ$ , the cell becomes diamond-shaped but the same discussion applies. That is, by incrementing the beam  $.25^\circ$  the probability of a correct reply increases as the beam center approaches the targets.

The probabilities of a false reply in the above scanning example decrease during the scan as the probability of a correct reply increases. In the example shown, the probabilities of a false reply are successively 0.01, 0.0 and 0.0.

The probabilities of an incorrect reply, that is, either no reply or a false reply, is  $1 - P_{CR1}$ . In the examples shown they are 99%, 60%, and 4%, respectively. Similar arguments indicate that on a tracking interrogation of such closely spaced aircraft, the probability of false reply is 4 to 5%. Since only 10% of the aircraft, about 20 out of 200, can be assumed to be so closely spaced as 150 feet or less, the overall probability of false reports should be less than 1%.

#### B.4 DATA OUTPUT

In any system of this type, the most important parameters for the description of data output are the Update Rate, Resolution, Accuracy and Estimated Error. The update rate in this case is not significant in that it will be only as high as necessary to accomplish search and track satisfactorily. The upper limit on the data rate based on the ATCRBS dead time and IRR time is much higher than tracking and search require. The lowest possible update rate is desired in order to reduce the likelihood of interference with other transponders.

##### B.4.1 Resolution Prediction

Resolution being the property of the system to distinguish between adjacent transponders has two possible limitations: the resolution based on cell size for interrogation and the resolution based on the accuracy of position determination. Since the later aspect is really a matter of ungarbled identification, it will be deferred to a later section and only cell resolution will be treated here. The probability of an ungarbled reply was discussed in section B.3.

The ASTC Cell is defined as the region occupied by the intersection of the two GEOSCAN beams where nonsuppression and interrogation take place. The definition and performance specifications for GEOSCAN are based on the system specifications established for the transponder in the U.S. National Standard for ATCRBS. It is the task of the DAS to establish cells of proper size and location about the airport surface.

The brassboard scanning technique uses a simple raster scan. The size of each cell is controlled by manually adjustment of the  $P_2/P_1$  ratio and also by aperture selection using electro-

mechanical relays on the antenna at both the Master and Slave stations. This adjustment procedure is not arbitrary but is based on the range of the target being interrogated. Due to the fact that each nonsuppression region or "track" across the airport surface is on an arc determined by the  $P_2/P_1$  ratio and the antenna aperture size, the width of this "track" increases with increasing range, as depicted in Figure B-16.

If a nominal 150' track width were desired between ranges of 600 and 12,000 feet,  $\theta$  would have to vary from  $14.25^\circ$  at 600 feet to  $.72^\circ$  at 12,000 feet. Obviously a continuous angle change as a function of range might be desirable if the track width were accurately predicted by the track angle,  $\theta$ . Unfortunately, the sidelobe suppression (SLS) circuit in the transponder which makes the suppression/nonsuppression decision based upon the amplitude relationship of  $P_2$  to  $P_1$  has a 9 dB tolerance or gray zone where operation is unpredictable. In the case where  $P_2 < P_1 - 9$  dB, nonsuppression is required. The actual track width is then described by the lower and upper limits for any particular transmitted ratio of  $P_2/P_1$ . This may be seen in Figure B-17, where  $\theta$  maximum is determined by the points  $P_1 = P_2$  and  $\theta$  minimum is determined by the points  $P_1 = P_2 + 9$  dB. A  $\theta$  nominal is defined at  $P_2 = P_1 - 4.5$  dB.

The track width may then be projected based on acceptable limits, maximum and minimum, which vary as a function of range, transponder SLS suppression ratio, DAS antenna null width curve (based on aperture), and the transmitted  $P_2/P_1$  signal in space ratio. The values used for this analysis are: maximum track width = 225 feet; minimum track width = 50 feet. A number of different  $\theta$  maximum angles, as determined by the  $P_2/P_1$  ratio in space, are required. While an infinite number are possible with an infinite variable  $P_2/P_1$  attenuator, the minimum number required and the settings for each is of prime importance.

Figure B-18 shows the number of segments and the track widths from 1.5 nmi (9120 feet) down to 500 feet. Note that the width scale is expanded for clarity. For the brassboard, seven steps are required using both 16 and 6 element antenna apertures.

The operational system requirements would be the same out through 1.5 nmi (9120 feet) with additional segment parameters as shown in Table B-3. It is important to note that as the minimum range is increased the number of sequences decrease rapidly. An operational system covering ranges 1000 feet to 2 nmi should only require six segments.

Segment G overlaps segment F to allow the useful cell area to be reasonably sized. Segment E could be obtained with the 16 element aperture but at a low ( $<3$  dB) transmitted  $P_2/P_1$  ratio. This performance is based on an interrogation antenna design using 0.5 wavelength element spacing. The segment parameters are listed in Table B-1. Table B-2 lists angles and  $P_2/P_1$  ratios for each segment.

AD-A057 933

BENDIX CORP BALTIMORE MD COMMUNICATIONS DIV  
DESIGN, FABRICATION, AND TESTING OF A BRASSBOARD MODEL ATCRBS B--ETC(U)  
JUN 78 A L BROCKWAY, J B KUHL, P J WOODALL DOT-TSC-769

F/G 17/7

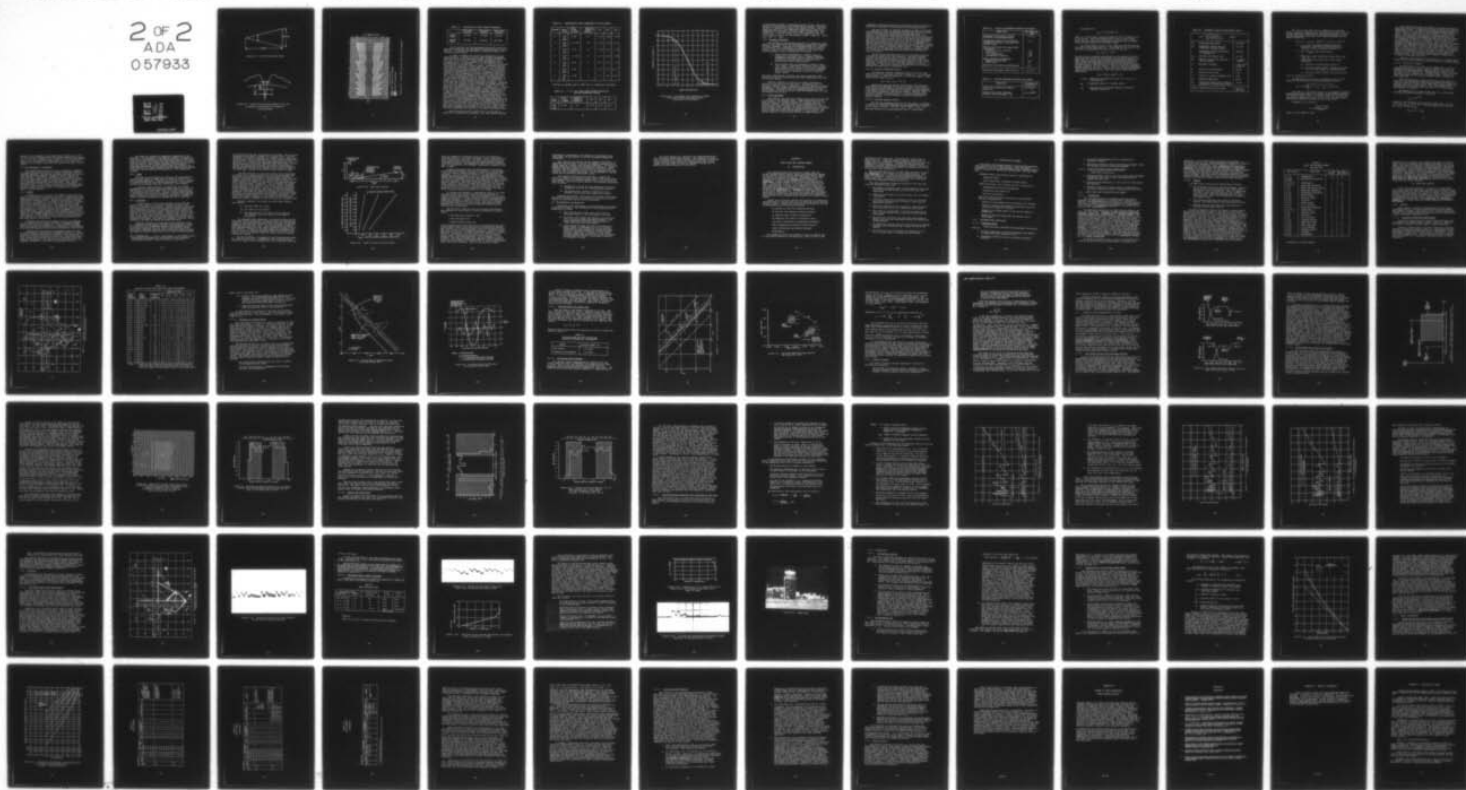
UNCLASSIFIED

BENDIX-489A09A

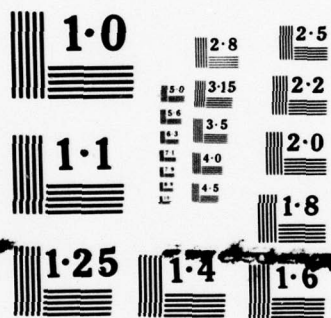
FAA-RD-78-63

NL

2 OF 2  
ADA  
057933



END  
DATE  
FILMED  
10-78  
DDC



NATIONAL BUREAU OF STANDARDS  
MICROCOPY RESOLUTION TEST CHART

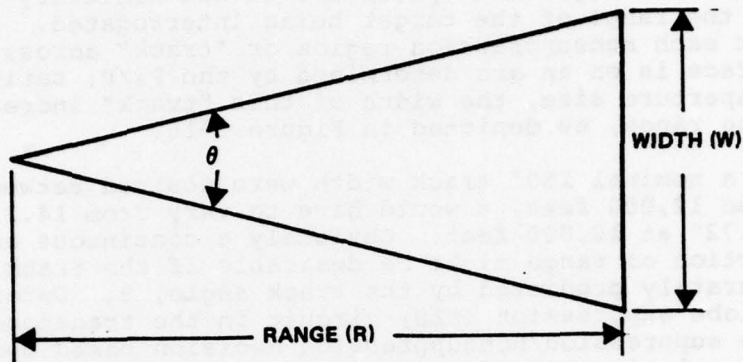


Figure B-16. Track Width Versus Range

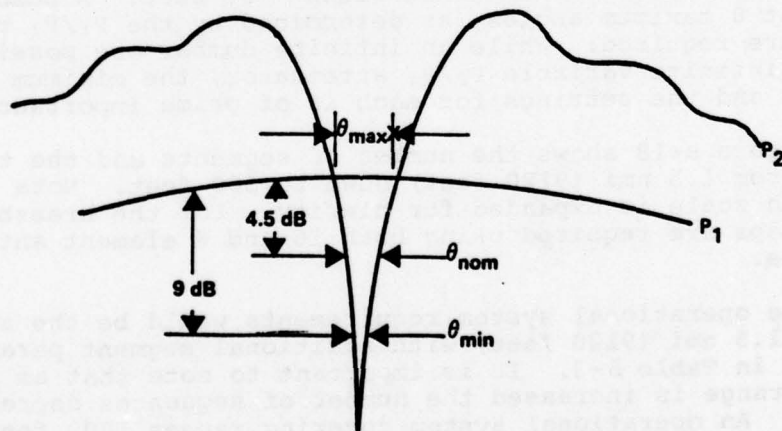


Figure B-17. Angular Relationships between the  $P_2$  and  $P_1$  Patterns as Determined by Transponder SLS Performance

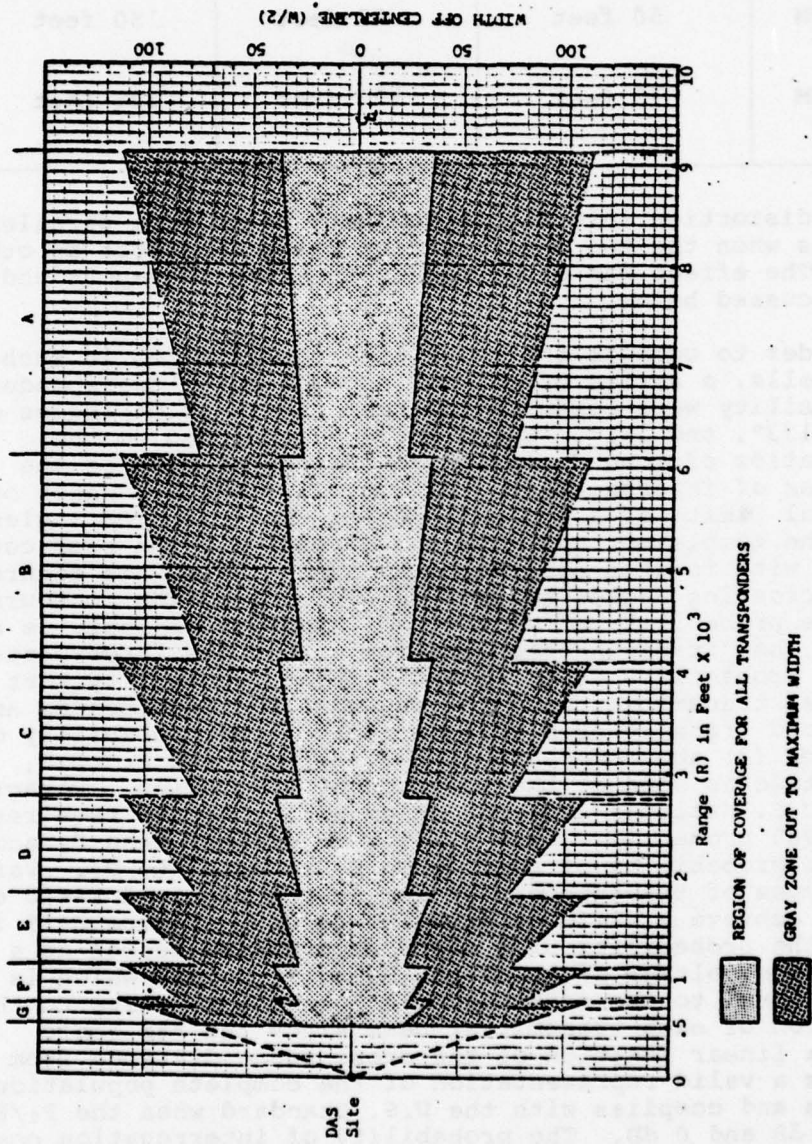


Figure B-18. Track Width and Cell Size Control Segments

TABLE B-1. INTERROGATION TRACK SEGMENT PARAMETERS

	TRACK WIDTH MINIMUM	TRACK WIDTH NOMINAL	TRACK WIDTH MAXIMUM
MINIMUM RANGE	50 feet	87 feet	150 feet
MAXIMUM RANGE	75 feet	130 feet	225 feet

Cell distortion into the approximate shape of a parallelogram results when the two interrogation beams intersect at other than 90°. The effect was described in the Task 1A report and further discussed below.

In order to compute the resolution capabilities in such distorted cells, a series of contour maps of equal transponder reply probability were computed for beam intersection angles of 90°, 120°, 133°, and 141°. These angles correspond to the following ratios of long dimension to cross dimension of the parallelogram of intersection: 2, 2.0, 2.5, and 3.0 which bound the practical limits of a typical system. Intersection angles which are the complement of those above result in the same contour shapes with rotated parallelogram axes. Thus, the figures illustrate crossing angles between 30° and 141°. The contours indicate the probability of eliciting a transponder reply as a function of that transponder's location within the interrogated cell. This probability depends on the joint probability that (1) the first transmitter does not suppress the transponder and (2) the second transmitter elicits a reply. The probability of either (1) or (2) above depends on the ratio of the  $P_2$  to  $P_1$  pulse amplitude as seen at the transponder's location. Paragraph 2.7 of the U.S. National Aviation Standard for ATRBS requires a reply with 90% probability when  $P_1$  is 9 dB greater than  $P_2$  and less than 1% probability of reply when  $P_1$  is equal to  $P_2$ . Various makes and types of transponders differ in the required ratio of  $P_1$  to  $P_2$  to achieve a valid suppression decode. Figure B-19 is a graph of the probability of a valid suppression decode as a function of the voltage ratio of the  $P_2$  to  $P_1$  pulse, which is in turn proportional to the transponder's location relative to the null direction of each transmitter beam since the far field voltage is a linear function of the cross range distance from the null. It is a valid representation of the complete population of transponders and complies with the U.S. Standard when the  $P_2/P_1$  ratio is -9 dB and 0 dB. The probability of interrogation contours were derived from the curve of Figure B-12. These contours were used to compute the probability of a single correct reply when two transponders are located in the same interrogation cell.

The two scaled aircraft overlaid on a contour map in Figure B-13 illustrate the technique. The first vehicle labeled

TABLE B-2. INTERROGATION TRACK PARAMETERS FOR EACH SEGMENT

SEGMENT	RANGE (feet)	P2/P1 (Signal in Space)	Aperture (Number of Elements)	Min.	Nom.	Max.
A	9120 to 6080	16 dB	16	0.47°	0.82°	1.41°
B	6080 to 4078	11.5 dB	16	0.76°	1.35°	2.12°
C	4078 to 2728	9 dB	16	1.05°	1.8°	3.16°
D	2728 to 1790	5.5 dB	16	1.6°	2.75°	4.72°
E	1790 to 1060	10 dB	6	2.7°	4.3°	7.2°
F	1060 to 680 <sup>a</sup>	6 dB	6	4.2°	6.6°	12.1°
G	735 <sup>a</sup> to 500	3 dB	6	5.7°	9.8°	17.4°

<sup>a</sup> Overlap at minimum range to make the cell dimensions reasonable.

TABLE B-3. 1.5 to 2 nmi TRACK WIDTH SEGMENT PROJECTION  
FOR THE OPERATIONAL SYSTEM

Range (feet)	P2/P1 (Signal in Space)	Aperture (Number of Elements)	Min.	Nom.	Max.
12160 to 8185	16 dB	22	0.35°	0.62°	1.06°

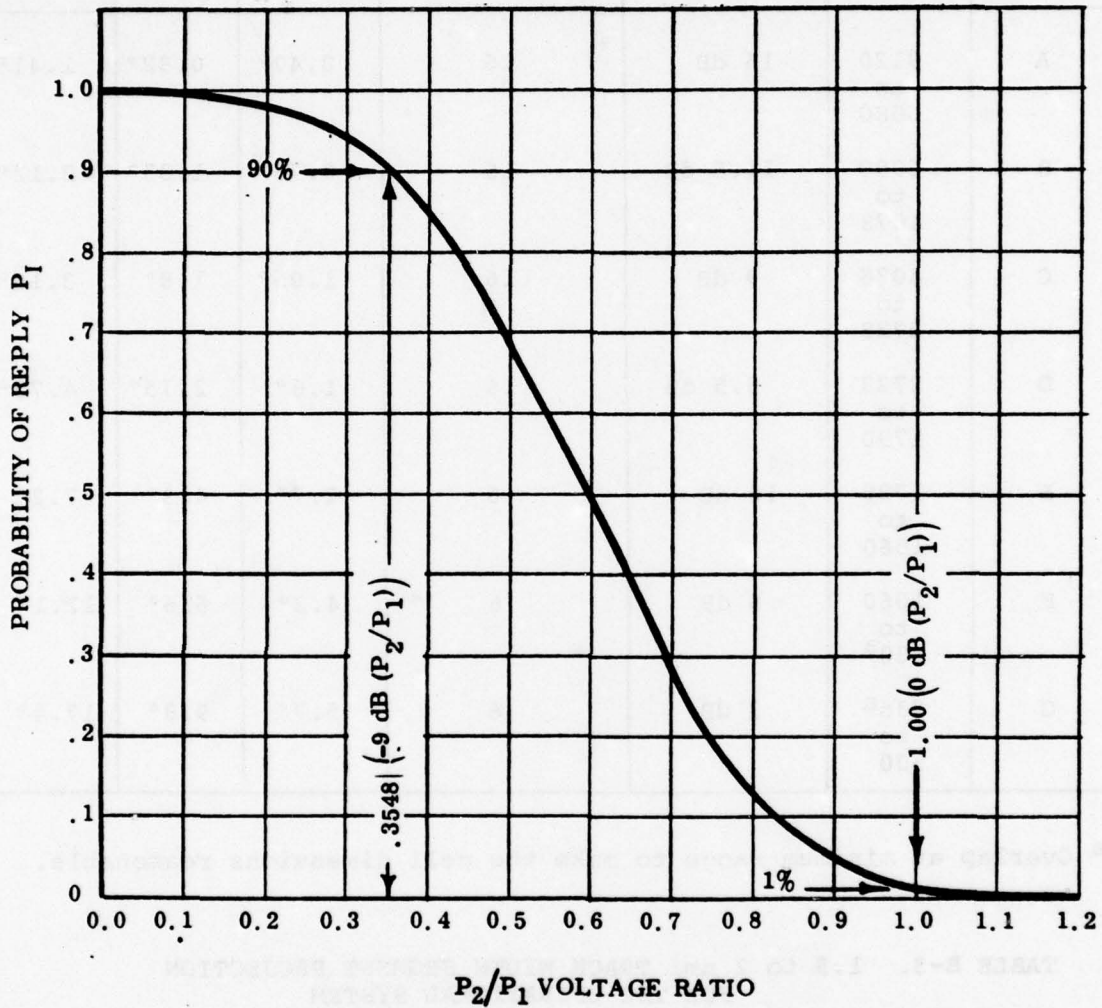


Figure B-19. Transponder Valid Suppression Decode Probability (Normal Distribution about Referenced Points Assumed)

"interrogated aircraft" is positioned so that it has a 95% probability of replying while the second vehicle labeled "interfering aircraft" is positioned to have a 10% chance of reply. The two-sigma resolution of a two dimensional distribution occurs with a probability of resolution (a correct reply) of about 88%. The probability of a correct reply  $P_{CR}$  is the probability that aircraft number 1 replies and that aircraft number 2 does not. Thus,  $P_{CR} = P_{R1} \times (1 - P_{R2})$ .

#### B.4.2 Accuracy Prediction

The accuracy of the measured position of a responding transponder is not affected by the interrogation system once a response has been triggered. Since position determinations are a matter of solving for the intersection of hyperbolic lines of position based on time of arrival differences ( $\Delta TOA$ ) of the reply, the accuracy depends on the following sets of factors:

- (1) Those factors independent of location such as: propagation uncertainty due to lateral multipath, uncomensated equipment delays, receiver and signal processing, radio frequency interference, and receiver site survey uncertainties.
- (2) Those factors which are dependent on vehicle location, namely: propagation uncertainty due to atmospheric beam bending, signal to noise ratio dependent uncertainties in the receiver and signal processor, and the so-called Geometric Dilution of Precision (GDOP) factor.

As in the interrogation situation this factor amplifies uncertainties in position determination when the intersecting loci are not at right angles.

Analytic treatment in Section B.4.3 below indicates an accuracy on the order of 20 feet total. Experiments were run using six different vehicle locations in an area subject to lateral multipath, from buildings, ASR/SSR interrogations and interfering transponders. The results show the standard deviation at the worst of the six points to be +17.6 feet and maximum error for any one reading to be 30 feet.

#### B.4.3 Error Estimates

This section lists the error sources which affect the position fix accuracy of the GEOSCAN system. These estimated errors are used to predict the accuracy contours for a typical two mile trilateration system. Aircraft position is determined from the relative time of arrival (TOA) of a pulse as measured at three or more receiver sites. Ideally, the three receiving sites are located at the corners of an equilateral triangle with the aircraft confined to positions within the boundaries of this triangle. The precise position of each surface vehicle is computed from two

independent differences between the three time of arrival measurements and a knowledge of the location of the receiving sites.

Position accuracy is affected by errors in each of the three TOA measurements, with the receiver furthest away from the interrogated vehicle generally contributing the greatest error. In general, the TOA errors associated with each site result in a different contribution to the overall position error of the vehicle. The total mean square position error is the sum of the mean square position error resulting from each site TOA error taken separately. RMS position accuracy varies from about 12' to 16' depending on vehicle location within the triad of receivers. These error values are a typical two mile baseline system and include all known sources of error as listed in the error budget tables. A complete error contour map of the idealized two mile system is included, Figure A-7, shows the estimated RMS position errors as a function of vehicle location.

The TOA errors associated with each of the three receiving sites can be grouped into two categories. The first category includes all error sources that are not a function of vehicle location and the second category includes those TOA errors which depend on the location of the transponder relative to the receiving sites. Tables B-4 and B-5 list each category of errors respectively. The errors listed are the RMS error in TOA measurement and are specified in nanoseconds (ns).

#### B.4.3.1 Location Independent Errors

The composite location independent error is the root sum square value of the components listed in Table B-4. It is defined by the symbol  $\sigma_{fi}$  where the subscript  $i$  is the site number. From Table B-4 the value of  $\sigma_f$  is:

$$\sigma_{f1} = \sigma_{f2} = \sigma_{f3} = 10.2 \text{ ns}$$

These errors are the same for each of the three receiving sites and are not dependent on aircraft location. Some of the error sources listed, such as lateral multipath, may be dependent on aircraft location and different for each of the three sites for a few discrete regions of the airport surface. However, these errors are neither a deterministic nor a continuous function of aircraft location, and are therefore treated as independent of vehicle location.

#### B.4.3.2 Location Dependent Errors

The location dependent errors are of two kinds as indicated in Table B-5. These are different for each receiving site depending on vehicle location. The first type of error is  $\sigma_{B_i}$ , the RMS beam bending error associated with the  $i^{\text{th}}$  receive site.

TABLE B-4. LOCATION INDEPENDENT RECEIVER SITE ERRORS

ERROR TYPE	RMS ERROR PER SITE
Propagation Uncertainty Lateral Multipath (see paragraph below)	7.5 ns
Propagation Delays Within Equipment Uncompensated Delays (variation over dynamic range)	4.0
Receiver and Signal Processing Characteristics	
Threshold Jitter and Drift	1.25
Clock Drift	.80
Clock Quantization	2.90
Log Amplifier Linearity	1.20
Radio Frequency Interference	
Galactic and Man Made	2.0
ATCRBS Fruit	3.8
Receiver Site Location Uncertainties	0.8
Total Root Sum Square (RSS) Error $\sigma_f$	10.2 ns

TABLE B-5. LOCATION DEPENDENT RECEIVER SITE ERRORS

ERROR TYPE	RMS ERROR PER SITE (ns)
Propagation Uncertainty Bending Delay ( $\sigma_B$ )	1.8 (R/R <sub>0</sub> )
Receiver and Signal Processor Signal-to-Noise Dependent ( $\sigma_N$ )	89.4/ $\sqrt{2S/N}$

From Table B-5:

$$\sigma_{B_i} = 1.8 (R_i/R_o) \text{ ns,}$$

where  $R_i$  is the distance from the vehicle to the  $i^{\text{th}}$  receiver and  $R_o$  is 2 miles. This beam bending error is due to path length variations that result from atmospheric anomalies and is assumed to be a linear function of total path length.

The second type of error is that resulting from the received S/N ratio at each receiving wite. From Table B-5 the value of the receiver noise dependent TOA error at the  $i^{\text{th}}$  site is:

$$N_i = 89.4 / \sqrt{2 \text{ S/N}}$$

The S/N ratio is inversely proportional to the square of the distance from the vehicle to the receiver site and proportional to a fade factor due to vertical multipath as indicated in Table B-6. These values represent typical performance characteristics of an entire class of transponders and the operational projections of the ASTC program. The S/N ratio in turn is a function of distance between receiving site and vehicle. There are two range dependent factors effecting S/N ratio. The first is the simple range squared space loss and the second is a fade loss due to ground spectral reflections.

$$\text{S/N} = (\text{S/N})_o (R_o/R)^2 \times F_F$$

$(\text{S/N})_o$  = reference free space S/N ratio at  $R = R_o$ ,  $F_F = 1$   
(see Table B-6)

$R_o$  = reference range of 2 nautical miles

$F_F$  = fade factor due to ground spectral reflection  
(vertical multipath)

TABLE B-6. REFERENCE SIGNAL TO NOISE RATIO (S/N)<sub>o</sub>

$S/N = \frac{P_T L^2 G_T G_R A_S}{(4\pi)^2 R_o^2 K T_o B F}$		where:
P <sub>T</sub>	transponder peak power	125 watts
G <sub>T</sub>	transponder antenna gain (0° elevation, average azimuth)	-2.0 dB
-	transponder transmit wavelength at frequency of	1090 MHz
G <sub>R</sub>	receiver site antenna gain	16.0 dB
R <sub>o</sub>	reference range from receiving site to vehicle	2 nautical miles
K	Boltzman's constant	1.38 x 10 <sup>-13</sup> joules/°K
B	receiver noise bandwidth	12 MHz
F	receiver noise factor	3 dB
L	receiver to antenna plumbing loss	3 dB
T <sub>o</sub>	standard temperature	290° K
A <sub>S</sub>	attenuation factor due to vehicle shielding in azimuth plane (max.)	-15 dB
(S/N) <sub>o</sub>	computed from equation above	24,547.1 (43.9 dB)

The value of the fade factor  $F_F$  depends on transponder height, receiving antenna height, distance between these antennas and the reflection coefficient of the airport surface. At the low grazing angles encountered the following approximation was used to compute  $F_F$ .

$$F_F = [1 + \rho \cos (\phi + 180^\circ)]^2 + [\rho \sin (\phi + 180^\circ)]^2$$

$\rho = (1 - 0.1\beta)$ , the average magnitude of the reflection coefficient of earth, asphalt or concrete at very low grazing angles  $\beta < 5^\circ$ .

$\beta = \tan^{-1} \frac{h_1 + h_2}{R}$ , the grazing angle

$\phi = \frac{2h_1 h_2}{R} \frac{360}{\lambda}$ , phase difference between direct and ground reflected signal due to path length difference

$h_1$  = receiving antenna height, about 18'

$h_2$  = aircraft antenna height, nominally selected as 4' for the example illustrated herein

$R$  = distance between vehicle and receiver site

#### B.4.3.3 Position Fix Error

The RMS position fix error is computed as the root sum square of the constituent contributions from each site:

$$\sigma_P = 0.984 \sqrt{\sum_{i=1}^3 P_i^2 (\sigma_{f_i}^2 + \sigma_{B_i}^2 + \sigma_{N_i}^2)} \text{ feet}$$

The term  $P_i$  in the above equation is the important Geometric Magnification factor which is a result of the Geometric Dilution of Precision factor (GDOP). The Bendix Factor  $P_i$  is defined as the ratio of position fix error to one of the site TOA measurement errors, holding the other two site errors fixed.

Therefore,  $P_i$  is given by

$$P_i = \frac{\sqrt{(\Delta X)^2 + (\Delta Y)^2}}{c(\Delta t)}$$

where  $c$  is the speed of light.

This definition differs from GDOP in the sense that GDOP is defined as the ratio of position fix error to all of the sites TOA measurement errors. In this sense the Bendix Geometric Magnification factor is a GDOP effect. The importance of the term  $P_i$  is that it relates a TOA error at the  $i^{\text{th}}$  site to a position fix error. This quantity is determined by differentiation of the position fix equations with respect to TOA at each of three sites. The dimensions of position fix and TOA are both in feet or both in nanoseconds so that  $P_i$  is a numeric. The  $P_i$  factor is in general different for each of the three receiving sites and depends on relative transponder location on the airport surface. For example if an aircraft is close to one of the three receiver sites that  $P_i$  factor for that site is on the order of 0.6. This means that a 10 ns TOA error at that receiving site results in a position error of 6 nanoseconds  $\times$  0.984 = 5.9 feet. On the other hand, a TOA of 10 ns at one of the two remote receiving sites will typically result in a position error of about 9.8 feet due to a  $P_i$  factor on the order of unity.

Vehicles lying outside of the boundaries of a triangle whose corners are the three receiving sites will result in larger factors.

#### B.4.3.4 Position Fix Example

The RMS position fix error  $\sigma_p$  was computer for a two mile baseline equilateral triangle receiver configuration using the parameters and budgeted errors indicated above. Figure A-7 is the result of this computation. The RMS position error is printed for each 500 foot interval on a rectangular grid. Contours of equal error show the relationship between vehicle location and error magnitude.

Using the equations in Table B-5 and the values shown in Table B-6, the S/N equation shows signal strength falls below the 12 dB S/N threshold at about 20,500 feet which is well beyond the required range of the ASTC system. The 12 dB threshold was selected for a false alarm rate less than  $50 \times 10^{-6}$  per second, and developed as follows.

The probability of a false alarm, that is, a noise signal exceeding the signal threshold, is given by

$$P_{fa} = e^{-10^{T/10}}$$

where T is the threshold in dB relative to RMS noise. If T is 12 dB then  $P_{fa}$  is  $1.31 \times 10^{-7}$ . Now the number of false alarms per trail is given by  $N_{fa}$

$$N_{fa} = B \times \tau \times P_{fa}$$

where B is the bandwidth of the signal and is equal to  $12 \times 10^6$  Hz, and  $\tau$  is the receiving period of one ASTC period and is equal to  $25 \times 10^{-6}$  sec. Therefore  $N_{fa}$  is equal to  $3.9 \times 10^{-5}$  per second. Thus a 12 dB threshold will insure about  $3.9 \times 10^{-5}$  false TOA readings due to thermal noise per each receiver per each 1 second trial.

## B.5 ELECTROMAGNETIC INTERFERENCE

The interference environment is not exclusively relegated to interference possibilities on the Beacon frequencies (1030 to 1090 MHz) employed. The ASTC-DAS equipment must also live with a wide spectrum of frequencies assigned to various NAVAIDS and other services. The system, considered as both a source and a victim of interference, faces the identical problems of any beacon interrogator with regard to spurious emissions. However, no new or special problems have been identified. Some special advantages exist in that siting criteria can be developed to be applied to each particular airport installation, and the geometry can be arranged so as to minimize the likelihood of adverse effects on other NAVAIDS.

### B.5.1 ATCRBS

Interference to or from the local ATCRBS is precluded even though the same channel assignments are used. Compatibility with ATCRBS is provided by confining operation to the dead time during each ATCRBS interpulse period. Returns from beyond 60 nautical miles are of no interest to the ATCRBS so the receiver is blanked during their expected return time, hence the term "dead time". Such returns are infrequent and of low signal energy so their effect is not of much importance on the ASTC-DAS. Buffer margins are provided by a guard time between ASTC interrogations and the next ATCRBS pulse. Synchronization with the ATCRBS is assured by making the interrogation sequence of the ASTC-DAS depend on the reception of an ATCRBS pulse delayed by the 60 nautical mile range return period. If the ATCRBS pulse is missed no interrogations take place so the likelihood of a spurious unsynchronized ASTC-DAS interrogation is very small.

Frequency sharing with the ATCRBS brings to the ASTC-DAS all the interference protection relative to neighboring ATCRBS systems which the local ATCRBS has. Since neighboring ATCRBS sites are assigned PRF sequences that minimize such interference, these same PRF sequences bring similar advantages to the ASTC-DAS.

Interference from airborne transponders inside the range of the ASTC-DAS but interrogated by neighboring sites is a garble generating problem which must be considered. The discussion in Section B.3.3 above evaluates the effects of a very heavy dose of such interference, generated by 50 other interrogators and 200 airborne transponders. The probability of obtaining two or more ungarbled ID codes on three tries is estimated to be 98.4%.

The effect of interfering suppressions generated by the ASTC-DAS on the performance of neighboring ATCRBS is minimized by restricting interrogations to the minimum required for search and track and by restricting power and high angle radiation to minimum practical levels. This problem has been studied by TSC and preliminary findings are that no major problems are anticipated.\* Increased interrogator antenna vertical aperture to reduce high angle radiation is a major tradeoff item for combating such effects if further testing indicates the possibility of an operational problem.

#### B.5.2 TACAN

The same out-of-band spurious radiation and susceptibility criteria which apply to ATCRBS apply to TACAN by virtue of the same frequency selection. These criteria are selected to minimize or eliminate TACAN and other NAVAID interference. As mentioned earlier no new problems have been identified in this regard.

In general, TACAN channels are paired with ILS and VOR frequencies to provide the common-use VORTAC system, in which the DME function of the TACAN serves also to provide a DME function in conjunction with civil VOR's. However, certain TACAN channels in the vicinity of 1030 and 1090 MHz have no paired VOR frequency. These channels have limited utilization, especially in CONUS, in order to minimize interference to ATCRBS and thus to ASTC-DAS.

#### B.5.3 Multipath

A unique aspect of the general geometry of the ASTC DAS system is that vertical and lateral multipath effects on the system are separable and different. Vertical multipath associated with reflections from the ground represents extremely short path length differences because of relatively low antenna heights at each end of all transmission paths. Therefore its effect on TOA accuracy is limited to the effects of signal fades. Lateral multipath, on the other hand, with more significant path delays, produces timing errors whose significance depends on receiver signal processing techniques. The results of extensive multipath studies relating to the ASTC DAS design are summarized below.

Vertical multipath is a phenomenon which manifests itself as a modulation of the antenna vertical coverage pattern, caused by a portion of the transmitted energy being reflected off the ground and interfering with the direct (line-of-sight) signal. This effect, sometimes referred to as ground plane effect, causes the familiar vertical lobing structure in radar coverage diagrams.

\*M. J. Moroney and H. J. Glynn, "Measurements of the ATCRBS Surface Interrogation Environments at Chicago O'Hare and Los Angeles International Airports (AD-A-31 147/2WT)", (July 1976).

As an aircraft flies thru this pattern at altitude, loss of target frequently occurs when it passes thru a pattern null. Vertical multipath in the ASTC environment is a special case of this situation in which only the lower portion of the vertical pattern need be considered. Analysis has shown that essentially null free operation can be obtained for reasonable ASTC geometries. However, during operations at or below the first lobe of the antenna pattern, as constrained by system and aircraft antenna heights, the system path loss may vary inversely with the fourth power of the range  $\frac{14}{R}$ , instead of the normal inverse square law  $\frac{12}{R}$ .

Vertical multipath is a far field effect which arises when a portion of the energy transmitted by an antenna impinges upon the ground and is reflected back into space having suffered a change in amplitude and in phase. This reflected signal will then modulate (by vector summation) the direct signal everywhere in space; however, the effect is most serious only when both signals are of the same order of magnitude. One can measure the effect of multipath by using a receiver to trace out lines of constant signal strength in the vertical plane. The familiar multilobed antenna patterns will result. The theory of vertical multipath is well developed and the quantitative results can be accurately predicted. The number of lobes and the angles at which the peaks and nulls occur are predominantly determined by the height of the interrogator antenna relative to the operating wavelength. The pattern is somewhat dependent on the actual ground reflection coefficient which is complex in nature and will be discussed later.

Generally speaking, the higher the interrogator antenna above ground

- (1) The more lobes will exist
- (2) The lobes will be narrower
- (3) The lobe peak and null angles will get smaller, and therefore the first lobe will be closer to the ground.

For reasonable ASTC geometries, the aircraft antenna should never pass through interrogator antenna pattern nulls because the constraint can be applied that the minimum range for the aircraft antenna is such that the aircraft is not at an angle at which the interrogator pattern has a null. This is assured by excluding from coverages ranges less than those depicted as R peak in Figure B-20 and B-21. In order to fix these ranges the confirmation of value of H1 was an important empirical output of the NAFEC field testing which can be further optimized during testing at planned operational airports.

The two components of propagation loss, fade and space loss, are functions of H1 and R. Propagation loss is reduced at any range as H1 and/or H2 are increased up to the first peak since the

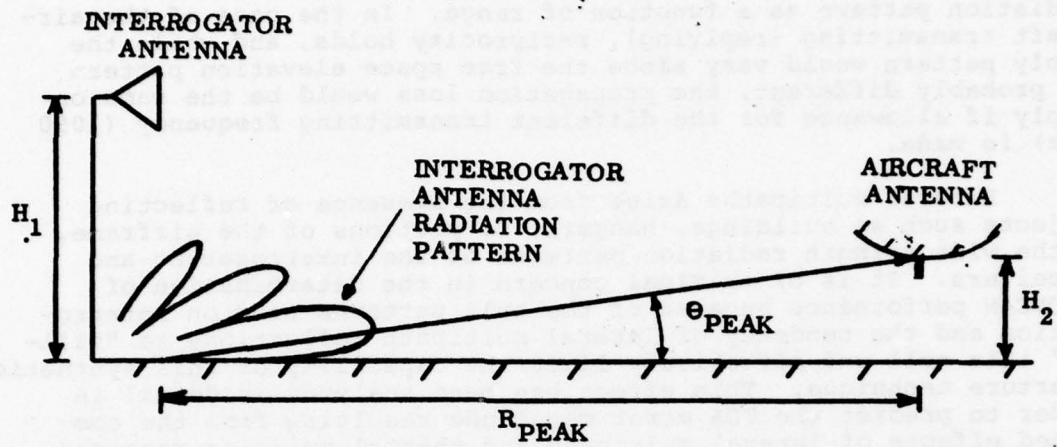


Figure B-20. Peak Angle Defined

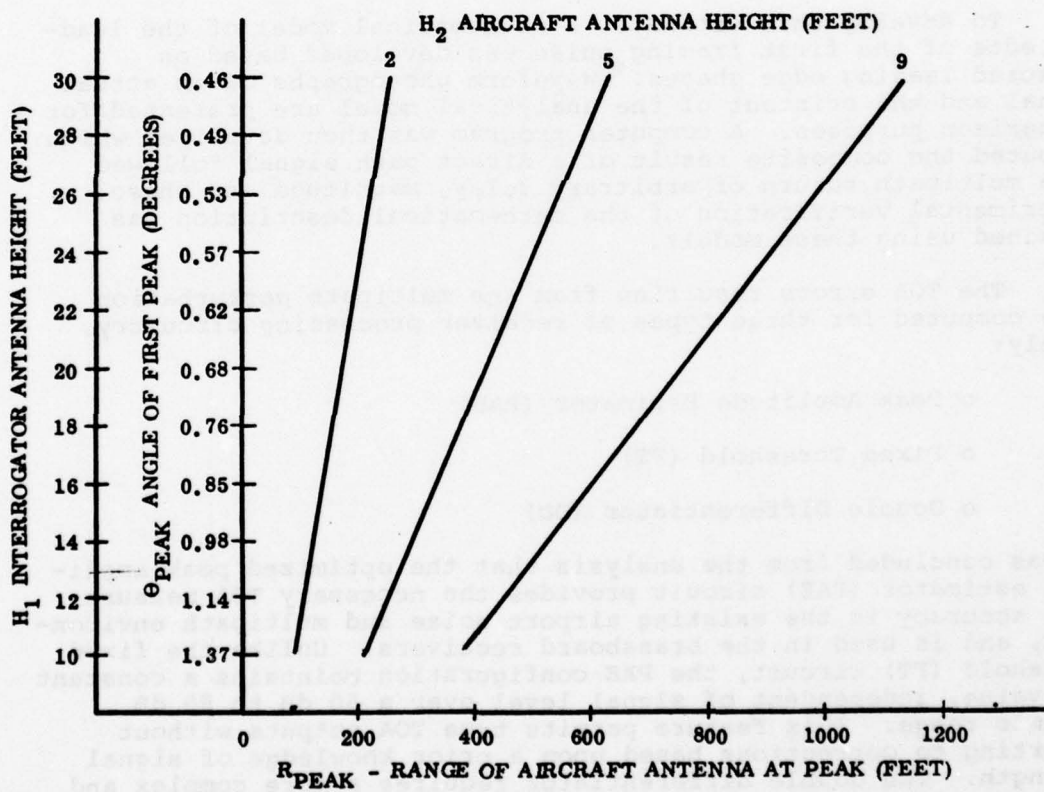


Figure B-21. Range at Which First Peak Occurs

fade loss component correlates directly with the transmitter radiation pattern as a function of range. In the case of the aircraft transmitting (replying), reciprocity holds, and while the reply pattern would vary since the free space elevation pattern is probably different, the propagation loss would be the same on reply if allowance for the different transmitting frequency (1090 MHz) is made.

Lateral multipaths arise from the presence of reflecting objects such as buildings, hangars, or portions of the airframe, in the wide azimuth radiation patterns of the interrogators and receivers. It is of critical concern in the determination of GEOSCAN performance because of the null patterns used on interrogation and the tendency of lateral multipath reflections to "fill-in" this null and effectively limit the capability of this synthetic aperture technique. This effect has been analyzed in detail in order to predict the TOA error magnitude resulting from the combined effects of lateral multipath and thermal noise as measured by the trilateration receiver. The peak multipath error was estimated to be 7.5 ns for a reflection coefficient magnitude of unity, to which thermal noise adds 4.2 ns (1 sigma).

To develop this estimate, a mathematical model of the leading edge of the first framing pulse was developed based on measured leading edge shapes. Waveform photographs of an actual signal and the printout of the analytical model are presented for comparison purposes. A computer program was then developed which computed the composite result of a direct path signal followed by a multipath return of arbitrary delay, magnitude and phase. Experimental verification of the mathematical description was obtained using these models.

The TOA errors resulting from the multipath perturbation were computed for three types of receiver processing circuitry, namely:

- o Peak Amplitude Estimator (PAE)
- o Fixed Threshold (FT)
- o Double Differentiator (DD)

It was concluded from the analysis that the optimized peak amplitude estimator (PAE) circuit provides the necessary TOA measurement accuracy in the existing airport noise and multipath environment, and is used in the brassboard receivers. Unlike the fixed threshold (FT) circuit, the PAE configuration maintains a constant TOA value, independent of signal level over a 60 dB to 80 dB dynamic range. This feature permits true TOA outputs without resorting to corrections based upon a prior knowledge of signal strength. The double differentiator requires a more complex and costly receiver system, and the potential for improved performance should that prove necessary. While it may provide a slight

improvement in performance, the unknowns of transponder reply pulse shape and performance in low S/N situations offsets its advantages.

As a check on the validity of the computer simulations, an experiment was performed in the lab to generate electronically a signal composed of direct and multipath components. The waveform shapes agree very closely with the computer simulation. These multipath perturbed signals were then fed to the PAE and the FT circuits. The indicated TOA values were then compared with those resulting from an undistorted signal. The differences in the TOA values are the multipath induced TOA errors.

The computer program was then modified to compute TOA errors as a function of reflected signal delay (with unity reflection coefficient) for different combinations of circuit delay and bias voltage. From this printout matrix, the following conclusions could be drawn:

- (1) Maximum error values for each combination of circuit parameters occur for the 0 degree phase condition.
- (2) The maximum error values are smallest for the shortest circuit delay and largest bias voltage.

Although the smallest circuit delay and largest bias produce the minimum multipath error, the effects of noise were also considered in optimizing the TOA circuit parameters.

#### B.6 ENVIRONMENTAL CONSIDERATIONS

The effect of the environment on DAS performance was treated in the Task 1A Report. The conclusions of this analysis may be summarized as follows:

- (1) Rain, falling snow, sleet, etc., will have no measurable effect on the performance of the DAS.
- (2) Multipath, both lateral and vertical, are accounted for in the error budget and system analysis. The errors introduced are within the projected one sigma operational ASTC requirements.
- (3) Line-of-sight blockage will have a variable detrimental effect on performance in that it reduces interrogation round reliability in marginal cases; reduces or prevents coverage of discrete areas by denying a signal path to targets in those areas. In severe cases these effects can only be eliminated through judicious siting of interrogation stations and redundant coverage.

All three effects will continue to be investigated during field testing at operational airports. More complete confirmation of predictions of system accuracy were confirmed as predicted during the NAFEC field totals and siting criteria and a better insight into the extent of need for redundant coverage will be among the ultimate outputs of this program.

## APPENDIX C

### NAFEC FIELD TEST PROGRAM SUMMARY

#### C.1 INTRODUCTION

The brassboard model Data Acquisition System (DAS) for Airport Surface Traffic Control (ASTC) was installed and tested at the National Aviation Facilities Experimental Center (NAFEC) per Task 2B of Contract DOT-TSC-769. The purpose of the test series was to establish the FEASIBILITY and operational POTENTIAL of a sensor system based on the Air Traffic Control Radar Beacon System (ATCRBS) as the surveillance technique for ASTC. As described in detail in the Test Program Plan for the ASTC Brassboard DAS, the tests were designed to validate the analytical performance predictions of Task 1A and to empirically establish the FEASIBILITY and POTENTIAL performance capability of the beacon based approach. In addition these tests provide a broad base of information from which operational ASTC DAS performance specifications can be developed to effectively complement other portions of the Upgraded Third Generation Air Traffic Control System.

Exhibit One of Contract DOT-TSC-769 specifies the operational characteristics of the DAS which must be evaluated during the Test Program at NAFEC. Exhibit One also defines the mission of the DAS as the meeting of the following objectives:

"To measure how well the subsystem performs;  
To see that the subsystem functions properly  
to support airport surface surveillance;  
To ascertain the effects of multipath, fruit  
and other interference on subsystem performance;  
and To determine the extent to which line-of-  
sight interference may degrade subsystem  
performance."

The brassboard design requirements as given in Exhibit One of the contract pertain to the functional areas and also to DAS

performance within each area. The functional areas listed in Exhibit One are: Subsystem capacity, density, probability of target detection, probability of detecting identity, accuracy, and probability of false reports. The ASTC DAS test program was designed to evaluate operational feasibility through a series of tests which evaluate specific performance parameters which relate to functional area performance.

The principle objective of the ASTC Test Program is to prove the FEASIBILITY of the concept of using ATCRBS for ASTC. This was accomplished by; 1) field testing the Brassboard DAS at NAFEC; 2) obtaining a data base of performance by recording DAS input/output data; 3) analyzing this data off-line to evaluate how well the performance objectives were met.

This test program was conducted according to the test plan using the following guide lines:

- 1) The number of specific tests and the number of test runs will be the minimum needed to achieve all other test objectives.
- 2) Test will be designed to provide results that are readily interpreted.
- 3) Individual tests will be designed so that the recorded data can be post-processed to provide a wide range of performance results.
- 4) Tests will provide the data required to generate performance specifications for an operational ASTC system.
- 5) The tests will be designed to provide an indication of basic design changes which could significantly improve performance.
- 6) The tests will establish the broad data base needed to develop the logic and algorithms required for operational system software.
- 7) The tests will provide inputs for the solution of problems resulting from interfacing ASTC systems with other ATC systems.
- 8) All field test will be designed and conducted so as to have a minimum impact on neighboring ATC systems.

## C.2 OVERVIEW TEST PROGRAM

The overall test program consists of three phases performed under Tasks 2A and 2B of the contract. These test phases correspond to the test system development from equipment assembly through installation, application and analysis. The test steps are:

Equipment tests, from Contract Task 2A, consisting of:

Laboratory Tests

Local Field Tests (conducted at Bendix Plant)

NAFEC Field Tests, from Contract Task 2B, consisting of:

Installation and Initial Calibration,

Engineering Field Tests and

Test Data Acquisition

Field Test Data Processing and Analysis, also Contract Task 2B, consisting of:

Reduction of DAS Taped Data with printout for analysis

Merging of DAS and Phototheodolite Reference Data with printout and graphs for analysis,

Evaluation of ATRCBS Impact on DAS and DAS Impact on ATRCBS, and

Merging of DAS and ATRCBS Data and analysis into a Final Report

### C.2.1 EQUIPMENT TEST DESCRIPTION

#### C.2.1.1 Laboratory Tests

Task 2A: These test were conducted during equipment fabrication,

- 1) Incoming Inspection on Purchased Assemblies and Modules (IF Amplifier, Power Supplies, etc.).
- 2) Engineering Checklist Tests on each Major Subsystem Interface

- 3) Performance Measurements prior to Installation in Equipment Trailers.
- 4) Engineering Checklist Tests on each Station (Master, Slave and Receive) along with Auxiliary Equipment.

#### C.2.1.2 Local Field Tests (Bendix Towson Plant)

These tests consisted of:

- 1) Hardware checkout test of the three station DAS and ATCRBS transponder using coaxial cable interconnections to simulate RF path loss.
- 2) Generation and processing of a test tape to verify proper DAS operation.
- 3) Radiation tests over limited range at low power as a preliminary operations check, no quantitative data taken.

#### C.2.2 NAFEC FIELD TEST INTRODUCTION AND SUMMARY

##### C.2.2.1 Introduction

The overriding purpose of the NAFEC field tests was to determine the feasibility of the ATCRBS based trilateration approach (including the GEOSCAN technique) for obtaining surveillance data on surface based targets equipped with transponders, and to evaluate the operational potential of the concept for an eventual ASTC implementation.

In considering feasibility and operational potential, the seven critical issues - accuracy, surface coverage, resolution, multipath, update rate, interference, and vehicle effects - had to be evaluated during the field tests. Specific tests in each area would simplify analysis. Unfortunately most of the critical issues are interrelated. Thus, most of the individual tests involved many of these issues and, therefore, most of the issues could not be explicitly evaluated by individual tests. Rather, conclusions about - or insight into - the critical issues could, in general, only be inferred from the test data and subsequent analysis. For example, during a single test that involved the movement of a test vehicle over 3,140 feet at varying speeds in 70 seconds, all of the critical issues except resolution were involved in an interactive manner. Thus, although the issue of accuracy was clearly established by this test, conclusions about all other issues except resolution could be meaningful inferred but not clearly established.

Of the seven critical issues, clearly interpretable quantitative results could only be established for accuracy and

resolution. As for interference (with other ATC systems - in particular ARTS and NAS), the establishment of quantitative measures was essentially impossible since no meaningful effects (i.e., interference) were observed. Thus, feasibility and operational potential were clearly established for the issues of accuracy, resolution, and interference. In the following paragraphs, comments on the other critical issues are largely drawn from inference. This particularly applies to surface coverage, multipath, and vehicle effects. Had these issues presented any meaningful problem during the NAFEC field tests, it is a certainty that the excellent accuracy and resolution results would not have been achieved.

#### C.2.2.2 Summary

The NAFEC field testing can be categorized as follows:

1. The collection of data on tape for subsequent reduction by the TSC XDS 9300 Computer Facility. Most of the testing fell into this category. Table C-1 summarizes the tests in this category that were run at NAFEC. A total of 30 DAS tapes, incorporating over 348 files, were generated. Each file included from 20 seconds to 30 minutes of data.
2. Oscilloscope photographs were taken of individual replies. Multipath effects were evaluated from these.
3. ARTS and NAS data reduction tapes were employed to determine interference effects.

The data contained on most of the tapes to be processed by the TSC XDS 9300 computer could be analyzed to provide direct quantitative measures of several of the critical issues and meaningful insight into others. Since the analysis process is tedious and frequently involves iteration - with human interpretation of the results in the loop - it was completely impractical to fully complete a test with adequate analysis before deciding that additional testing of the same type was need to adequately evaluate one of the critical issues. Thus, it was concluded that any cost-effective full testing program would have to involved a very substantial "overkill" in terms of the amount of data taken. The simple logistics of setting up the equipment, scheduling NAFEC support facilities (e.g., the phototheodolite), scheduling the TSC computer, etc., demanded that whatever data might be needed be taken as quickly as possible. Since the data taking was an "overkill" and since the several tapes that have been partially or wholly reduced and analyzed have sufficed to adequately establish feasibility and operational potential with regard to the critical issues involved, most of the data can be considered

TABLE C-1  
NAFEC TEST PROGRAM SUMMARY  
AUG-NOV 1975

TEST DATA	TEST TYPE	NO. DAS TAPES	NO. TAPE DATA FILES
18 AUG	INTERFERENCE	1*	10
22 AUG - 25 SEPT	ENGINEERING EVALUATION	7*	-
29-30 SEPT	INTERFERENCE	3	68
30 SEPT	BENCH MARK REFERENCE	1	4
1 OCT	BENCH MARK/MOVING TARGET	1	15
7 OCT	BENCH MARK REFERENCE	1	8
10 OCT	ENGINEERING EVALUATION	2*	3
16 OCT	MOVING TARGET	1	18
19 OCT	MULTIPLE TARGET	1	34
21 OCT	MULTIPATH	1*	2
22 OCT	MOVING TARGET	1	18
23 OCT	L-O-S BLOCKAGE	1	18
24 OCT	BENCH MARK REFERENCE	1	31
29-30 OCT	INTERFERENCE	1	39
3 NOV	MULTIPLE TARGET	1	27
4 NOV	MULTIPATH	1*	9
6 NOV	L-O-S BLOCKAGE	2	53
7 NOV	APPROACH MONITOR	2	7
11 NOV	MULTIPATH TARGET	1	32
12 NOV	SMALL AREA SCAN	1	27
13 NOV	L-O-S BLOCKAGE	1	6
13 NOV	APPROACH MONITOR	2	13
14 NOV	MULTIPATH	1*	7
18 NOV	INTERFERENCE	5	58

\*SUPPORTED BY LOG BOOK RECORDS

redundant and its reduction and analysis would shed little additional light on conclusions that already seem obvious. For this reason, only about five percent of the data has been reduced and incorporated into the analytical results described in the following paragraphs. While "overkill" in taking the data was most reasonable, any extensive additional data reduction and analysis would definitely appear to be an unreasonable - and rather costly - "overkill". Perhaps the real measure of the success of the NAFEC field tests has been the rather clear conclusions concerning feasibility and operational potential, in consideration of the seven critical issues, that were possible after only five percent of the data was fully evaluated.

### C.3 NAFEC TEST RESULTS

In the following paragraphs, the results of those NAFEC field tests, that have been fully analyzed, are presented as they relate specifically to the seven critical issues. As will be made obvious in the discussion, the issues are largely interrelated and the same tests are therefore referred to in many of the paragraphs. In the presentation of the results, emphasis has been placed on interpretation as pertains to the feasibility and operational potential of an ATRBS based ASTC system employing trilateration and GEOSCAN.

#### C.3.1 ACCURACY

The accuracy of estimating target position, from single transponder replies, has been investigated by extensive measurements made at a number of bench marks, by a rigorous analysis of the data from a moving target test, and from the data taken during a static two-target (resolution) test.

##### C.3.1.1 Accuracy of Bench Mark Measurements

During the overall period of testing many bench marks were established on the NAFEC airport surface. Table C-2 summarizes the errors of position estimates made at these bench marks.

Figure C-1 shows a map of the NAFEC airport with predicted constant contours from analysis (Task 1A). The position of each bench mark is shown with the value of  $\sigma_p$  in parenthesis. A few bench marks are shown with no indication of the error. No data was taken at these points. They are shown on the figure because they are referred to, in connection with other tests, in later paragraphs.

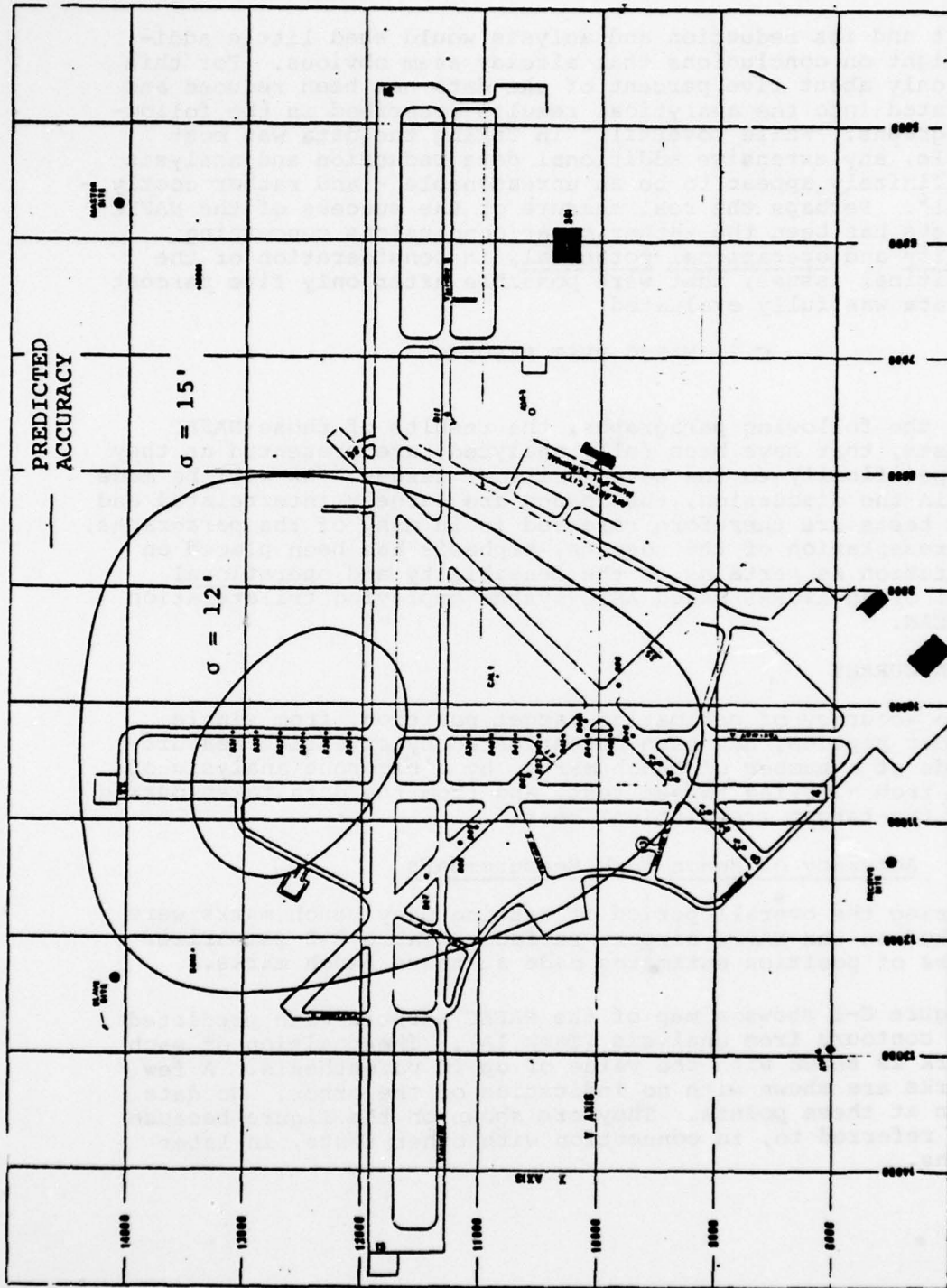


Figure C-1. Benchmark Positional Errors Compared With Predicted Accuracy

TABLE C-2  
RESULTS OF NAFEC FIELD TEST BENCH MARK MEASUREMENTS

BENCH MARK NUMBER	TAPE & FILE NUMBERS	NUMBERS OF SAMPLES	ERRORS IN FEET				
			$\sigma_x$ (a)	$\sigma_y$ (a)	$\sigma_p$ (b)	$\Delta x$ (c)	$\Delta y$ (c)
B-31	5924-1,2,3,5,6	617	6.78	4.33	5.42	43.80	31.03
B-32	5924-7,8,10	30	18.64	17.57	18.10	31.45	22.55
B-33	5924-11,12,13	64	7.41	5.03	6.11	34.36	21.19
B-34	5924-14,15	41	5.13	5.16	5.14	36.64	33.55
B-35	5924-16,17	25	5.28	4.29	4.73	38.08	30.20
B-36	5924-18,19	77	6.34	5.38	5.84	38.71	33.39
B-39	5924-20,21	1808	4.96	6.49	5.67	30.42	29.26
B-40	5924-22,23	145	4.82	6.64	5.66	29.40	26.18
B-41	5924-24,25	433	5.14	7.65	6.27	28.85	25.26
B-42	5924-26	77	4.5	6.7	5.49	31.5	18.3
B-43	5924-27A,27B	1408	5.1	7.06	6.00	24.15	26.19
B-44	5924-28	65	5.0	8.3	6.44	26.9	28.1
B-45	5924-29	812	5.4	9.1	7.01	32.0	21.6
B-46	5924-30	139	6.2	9.5	7.67	26.3	21.6
B-11	1227-15	743	5.7	6.0	5.85	40.1	49.1
B-87	0205-33,34	26	4.47	5.26	4.85	7.21	24.22
B-88	0205-32	32	3.1	5.5	4.13	9.1	20.5
B-89	0205-31	217	3.7	6.1	4.75	10.5	18.3
B-92	0205-28	310	4.1	6.1	5.00	11.3	15.7
B-93	0205-27	375	4.8	7.4	5.96	10.8	16.2
B-94A	0205-25	274	4.7	6.9	5.69	7.9	11.1
C-2	1226-16	108	4.7	11.1	7.22	24.1	21.4
C-3	1026-15	181	4.2	9.2	6.22	1.0	-1.1
C-4	1026-14	65	5.5	11.0	7.73	-0.5	-3.0
C-6	1026-13	108	4.8	9.3	6.68	-3.3	8.7
C-7	1026-12	309	5.5	9.3	7.15	-10.7	0.3

NOTES: (a) These are the standard deviations of the difference between the ASTC values and the phototheodolite values for the total number of data samples taken at each bench mark.

NOTES (Cont'd. from Table C-2)

- (b) Since  $\sigma_x$  and  $\sigma_y$  are orthogonal, they define an error ellipse.  $\sigma_p$  is essentially the mean value of the standard deviation of the positional error. It is the radius of the circle whose area is equal to that of the ellipse with semi-major axes of  $\sigma_x$  and  $\sigma_y$ .
- (c) These are the mean values of the errors between the ASTC estimates and those of the theodolite.

It seems evident from Figure C-1 that the errors derived from the test data is, on the average, less than one-half of that predicted from analysis. This discrepancy is discussed in paragraph C.3.1.4.

C.3.1.2 Accuracy of a Moving Target

Data was taken on a moving test vehicle on October 22, 1975. The vehicle moved west on runway 26. Data was taken with a large area scan at five scans per second. The vehicle velocity at the start was about 35 knots. It slowed to a complete stop at the intersection of runways 26 and 35 and then accelerated back to about 35 knots for the remainder of the run. The overall run lasted 70 seconds with the target moving about 3,060 feet. The full run is shown on Figure C-2. Both the phototheodolite and brassboard DAS tracks (raw data) are shown. Also shown on Figure C-2 is a 15-foot positional error contour - the predicted value from analysis (see Appendix A). Along most of the track the predicted error was about 14 feet.

The standard deviation of the positional error (between the measured DAS position and that reported by the phototheodolite) was calculated for successive 4-second segments of the track. These values are plotted on Figure C-3 versus time from the start of the run. The varying velocity is also shown. The dashed line indicates a one sigma error of 6.2 feet which also calculated from all data points where the velocity was in excess of 55 feet per second. The dotted line was derived from all data points with velocity below 55 feet per second. Several conclusions are obvious:

The average error was definitely less than 50 percent of the predicted from theory.

The error was essentially independent of the target velocity (and acceleration).

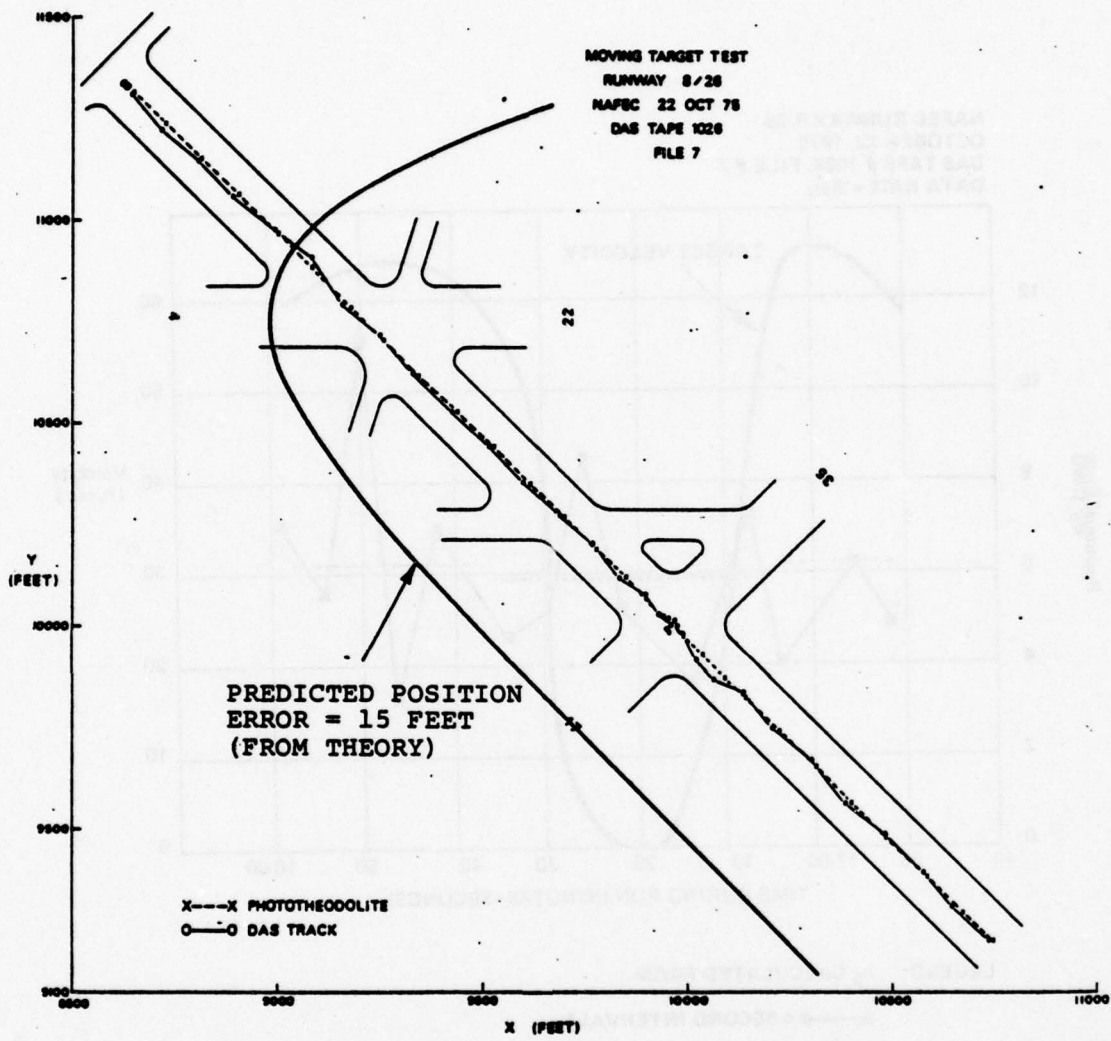
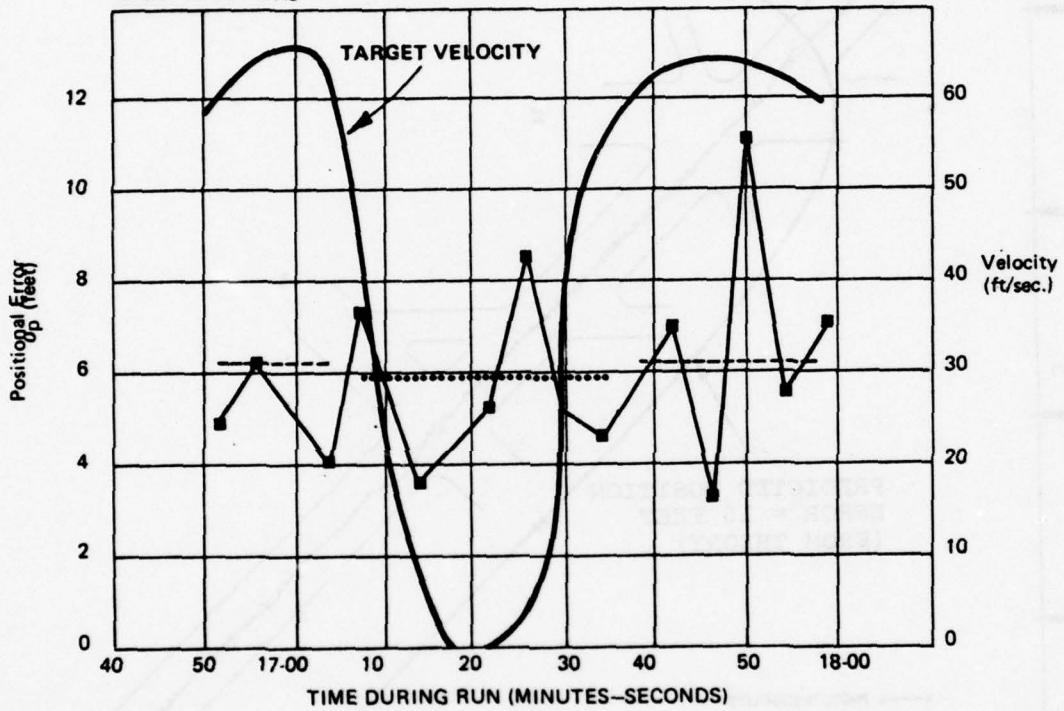


Figure C-2. Raw DAS Data Vs Theodolite Track  
 For Moving Target Test

NAFEC RUNWAY 8/26  
 OCTOBER 22, 1975  
 DAS TAPE # 1026, FILE # 7  
 DATA RATE = 5Hz



LEGEND:  $\sigma_p$  CALCULATED FROM

■ 4 SECOND INTERVALS

--- ALL DATA POINTS FOR VELOCITY > 55 FT/SEC

..... ALL DATA POINTS FOR VELOCITY < 55 FT/SEC

Figure C-3. Positional Error and Velocity  
 During Moving Target Test

Figure C-4 shows an expanded view of approximately the initial seven seconds of the run. In addition to the theodolite and the raw DAS data a track of smoothed DAS data is also shown. A simple alpha-beta tracking algorithm was assumed ( $\alpha = 0.5$ ,  $\beta = 0.2$ ). Although no effort was made to optimize the tracking parameters, it is obvious that the average deviation from the theodolite track has been reduced. Also shown on Figure C-4 are the three-sigma error boundaries, assuming an average one sigma value of six feet.

#### C.3.1.3 Accuracy From a Two Target Test

Data was taken on two targets separated by 130 feet. This data, recorded on Tape 0205, File 5, involved a small area scan and was part of a series of data runs made to evaluate resolution. Error contours for the two targets were calculated from the data and are shown on Figure C-5. Error eclipses are shown since the data was recorded in an orthogonal coordinate (X-Y) system. The following expression was used to calculate the one sigma position errors.

$$\sigma_p = (\sigma_x \sigma_y)^{1/2}$$

The error values found using this equation for the two targets are shown in Table C-3.

TABLE C-3  
POSITION ERROR FOR TEST VEHICLE AND  
CALIBRATION TRANSPONDER MEASUREMENTS

TARGET	POSITION ERROR (1 $\sigma$ )
Test Vehicle	6.63 feet
Calibration Transponder	6.15 feet

#### C.3.1.4 Conclusions About Accuracy

The accuracy results described above indicates that the typical positional error at NAFEC had a one sigma value of about 5-7 feet. This is less than one-half the values that were predicted during the analysis that preceded the field tests. The predicted error curves are shown on Figure C-1. Consideration of

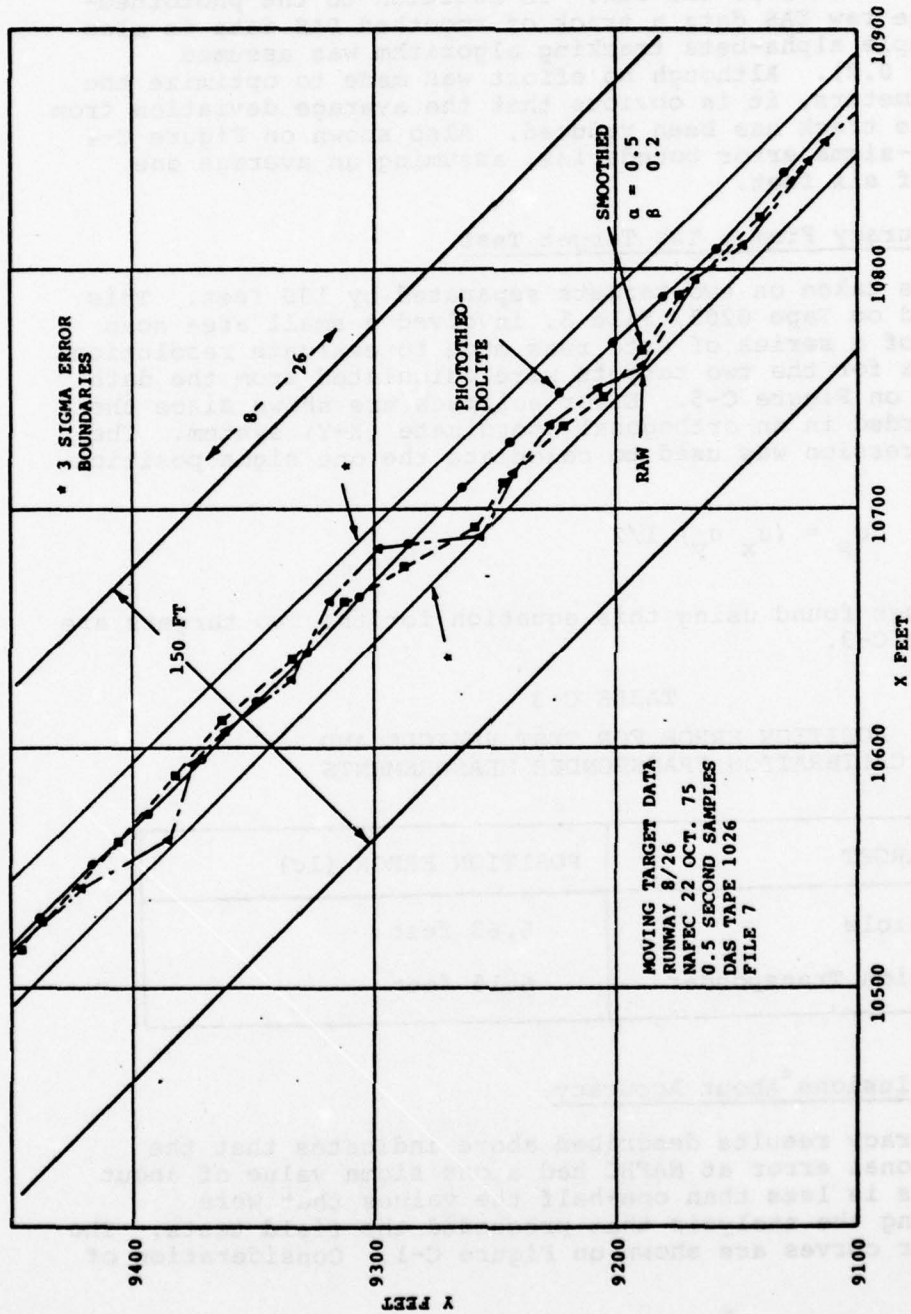


Figure C-4. Portion of Moving Target Track

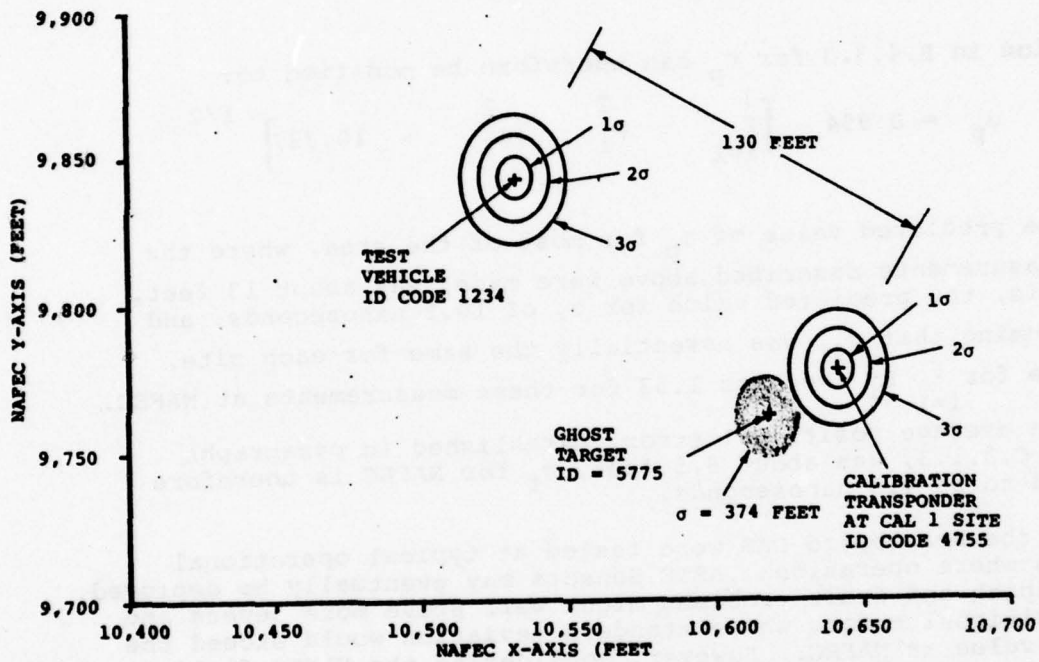


Figure C-5. Two Target Resolution Test Results.  
 DAS Tape 0205, File 5

the expression for  $\sigma_{TOA}$ , as a function of range and transponder height, developed in Appendix B for a NAFEC DAS, gives a strong indication of the probable source of this discrepancy. The average ranges for all of the measurements were below 6,000 feet and the height of the vehicle transponder antenna - used for all of these tests - was 6 feet. Using these values, the expression for  $\sigma_{TOA}$  becomes:

$$(\sigma_{TOA})^2 = (\sigma_f)^2 + 10.33$$

Expression in B.4.3.3 for  $\sigma_p$  can therefore be modified to:

$$\sigma_p = 0.984 \left[ \sum_{i=1}^3 P_i^2 (\sigma_f^2 + 10.33) \right]^{1/2}$$

The predicted value of  $\sigma_p$  for most of the area, where the NAFEC measurements described above were made, was about 13 feet. Using this, the predicted value for  $\sigma_f$  of 10.2 nanoseconds, and also assuming that  $\sigma_{fi}$  was essentially the same for each site, the value for  $\sum_{i=1}^3 P_i^2$  becomes 1.53 for these measurements at NAFEC.

Since the average positional error, established in paragraphs C.3.1.1, C.3.1.3, was about 6.5 feet,  $\sigma_f$  for NAFEC is therefore estimated to be 4.3 nanoseconds.

If the brassboard DAS were tested at typical operational airfields where operational ASTC Sensors may eventually be deployed, the multipath and fruit problems might well prove more severe and yield positional errors whose standard deviation would exceed the 6.5 foot value at NAFEC. However, considering the NAFEC field test results and the fact that an operational ASTC sensor would undoubtedly include design improvements to reduce the contributions of hardware errors, it seems most reasonable to expect that the one sigma positional accuracy of operational sensors will be better than 10 feet.

### C.3.2 SURFACE COVERAGE

The issue of surface coverage essentially involves the following two questions:

Are the ASTC interrogation signals, received by transponders located at surface points of interest, of adequate strength to effect replies from those transponders?

Are the transponder replies from surface points of interest, as received by each ASTC DAS receiving station, of sufficient strength to ensure detection of all pulses in the reply and provide the desired accuracy of TOA measurement?

These two questions really involve a determination of the propagation loss between the interrogator and transponder antennas. The analysis of this parameter indicated that its expected value,  $L_p$ , is given by:

$$L_p = \frac{H_T^2 H_I^2}{R^4}$$

If the above expression is correct, the signal-to-noise ratio of the reply pulses received at the ASTC stations should agree with equation in B.4.3.2. For most of the estimates of positional accuracy, as presented in paragraph C.3.1, the values  $H_I$ ,  $H_T$ ,  $G_I$  and  $R$  were 6 feet, 10.7 dB, and 6,000 feet, respectively. Thus, the predicted signal-to-noise ratio - assuming the above relationship for  $L_p$  - would be about 33 dB. This would imply a value for  $\sigma_n$ , in the equation for  $\sigma_{TOA}$ , of 1.42 nanoseconds. In the actual testing at NAFEC, the received signals were deliberately attenuated 10 dB at the antenna output. This was done since it was expected that most of the testing would not involve the maximum range for which the brassboard DAS was designed and it was felt that this action would eliminate some of the "long range fruit". For evaluation purposes, this was a reasonable thing to do since an operation DAS design would undoubtedly employ a directive antenna for reception and computer controlled range gating to reduce the effects of external interference. Thus, in order to make the brassboard system operate closer to a production design - and thereby to provide a better insight into the operational potential of the basic techniques being evaluated - the inclusion of 10 dB of attenuation was believed desirable.

The effect of the 10 dB of attenuation would reduce the predicted value of the signal-to-noise ratio of the processed receive signals to 23 dB. This value would mean that the parameter  $\sigma_n$ , in the equation for  $\sigma_{TOA}$  would equal 4.48 nanoseconds. But the overall value of  $\sigma_{TOA}$  was determined to be about 5.2 nanoseconds from the accuracy data. Therefore, this would mean that the variance of all other contributions to  $\sigma_{TOA}$  would be about 7.0. Considering the error components listed in Table B-4, the variance of the clock quantization error alone is 2.9, and this value is indisputable for a 100 MHz clock. It is also certain that the other

error components listed in Table B-4 cannot all be zero.

The above discussion leads to an obvious conclusion. The assumed expression for  $L_p$  is certainly conservative for NAFEC and probably conservative for other airports. Therefore, the two questions posed at the start of the discussion of surface coverage can most certainly be answered in the affirmative on the basis of the AFEC tests, and the theoretical treatment of the subject of surface coverage - in particular the matter of vertical multipath (or "fade loss") - should be accepted as conservative.

### C.3.3 RESOLUTION AND INTERROGATION CELL SIZE

The interrogation cell is a parallelogram shaped area on the airport surface with each "width" being the product of the range from an interrogator station and a small angle. Thus, for an interrogation cell width of 150 feet at 6,000 feet, the angle must be 0.025 radians or 1.43 degrees. The analysis of this subject showed that this angle is a function of the ratio of the power levels of the received  $P_2$  and  $P_1$  pulses at the transponder. Figure B-19 in Appendix B shows the probability that a transponder will not be suppressed (and, therefore, that it will reply if the  $P_1$  and  $P_2$  signal levels exceeded the Minimum Triggering Level of the transponder) versus the  $P_2/P_1$  signal level. This curve was developed in consideration of the National Standard requirements for all transponders and is therefore a good estimate of the average performance of a large sample of transponders. For any single transponder, however, it is known that the suppression probability goes from one to zero with a small variation in the  $P_2/P_1$  ratio (generally some value between zero and minus nine dB) and that the actual value where this action occurs varies over the dynamic range of that transponder. The NAFEC test results were consistent with these known characteristics.

#### C.3.3.1 Two Targets as Seen from the Master Station

Figure C-6 was generated from the results of tests run on two transponders which were placed at points equi-distant from the master station and separated by 75 feet and then by 150 feet. The distance involved was approximately 3,285 feet and the slave station was not in operation at the time. Thus, this test was intended to demonstrate the resolution capability of a single ASTC interrogator station. The identities assigned to the two transponders were 1234 and 4321, respectively. Therefore, when both of them replied to a single interrogation, the code detected by the receiver had to be the garbled value of 5335. The separate

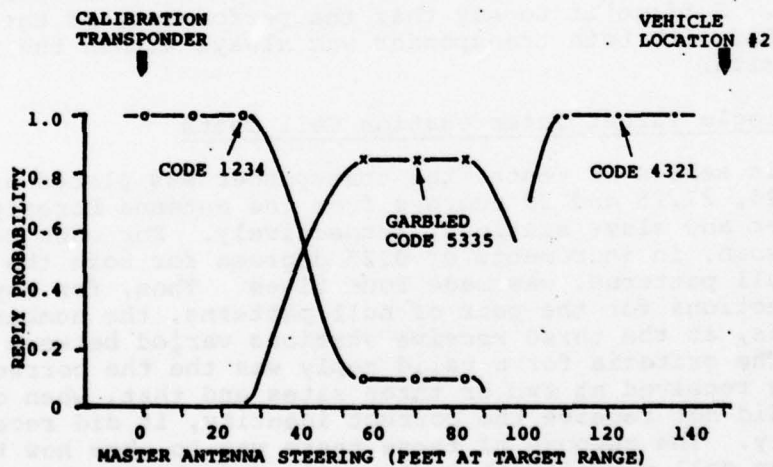
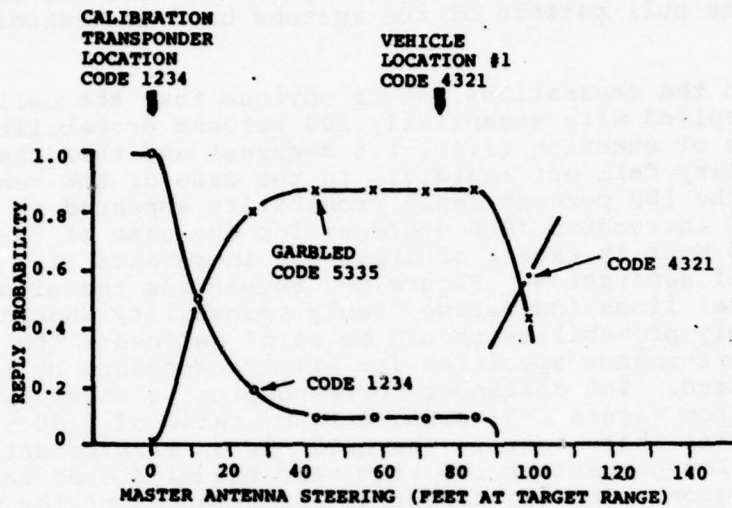


Figure C-6. Two Target Resolution Tests at Point A2  
(Test on 8/22/75;  $P_2/P_1 = 6$  dB)

curves of Figure C-6 show the percentage of correct replies (i.e., from each of the transponders separately) and of the garbled replies versus the variation in the direction (expressed in feet at the range of the pair of targets from the master station) of the null pattern of the antenna used to transmit the  $P_2$  signal.

For both the separations, it is obvious that the calibration transponder replied with essentially 100 percent probability for six increments of steering (i.e., 1.5 degrees) and then the reply probability fell off rapidly. In the case of the vehicle transponder, the 100 percent reply probability appeared to extend over about 3.2 increments (0.8 degrees) for the case of 75-foot separation and over an extent of about 6.8 increments (1.7 degrees) for 150 feet of separation. Figure C-7 summarizes the situation. The two vertical lines indicating "reply probability should be >90%" and "reply probability should be zero" delineate the extremes of performance specified for all transponders by the National Standard. The distances corresponding to these two lines were derived from Figure C-7, using a  $P_2/P_1$  ratio of 6 dB - the value used during these tests. The calibration transponder replied approximately 100 percent of the time near the middle of this performance region. The two differing performances of the vehicle transponder imply a region of response corresponding to the hatched area. Although this entire area fell within the acceptable limits of the National Standard, there is no plausible explanation for the change in performance between 75 and 150 feet of separation. The fact that the data has been evaluated long after the test was made unfortunately prevents a further investigation of this apparent discrepancy. Suffice it to say that the performance of the brassboard DAS with both transponder was always within the National Standard limits.

#### C.3.3.2 Single Target Interrogation Cell Tests

In this series of tests, the transponder was placed at benchmark B84, 27.75 and 20 degrees from the antenna boresights of the master and slave stations, respectively. For each test a large area scan, in increments of 0.25 degrees for both the master and slave null patterns, was made four times. Thus, for any set of steered directions for the pair of null patterns, the number of valid replies, at the three receive stations varied between zero and four. The criteria for a valid reply was the the correct identity was received at two or three sites and that, when one of the sites did not receive the correct identity, it did receive a garbled reply. The purpose of these tests was to show how the interrogation cell varied with  $P_2/P_1$  ratio and whether or not multipath effects produced sporadic replies at angles well outside of the interrogation cell.

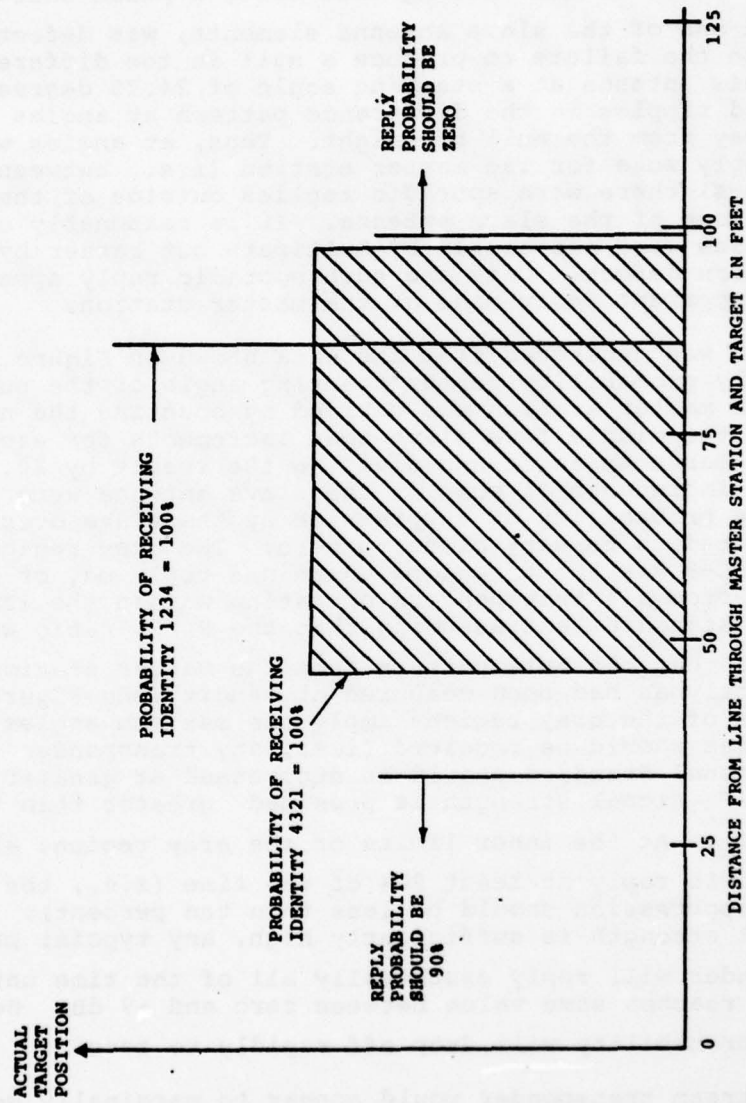


Figure C-7. Two Target Resolution Tests at Point A2  
 (Regions within which each Target replies with  $P_2/P_1 = 6$  dB)

Figure C-8 shows a matrix of the number of valid replies received for the four scans versus the scan angles of the two null beams. For this test, a Gulfstream aircraft was used and the  $P_2/P_1$  ratio was set at 7 dB. During this test, a phase shifter, associated with one of the slave antenna elements, was defective. This resulted in the failure to produce a null in the difference pattern from this antenna at a steering angle of 24.75 degrees. It also produced ripples in the difference pattern at angles considerably away from the null boresight. Thus, at angles within the apparent reply zone for the master station (i.e., between 26.0 and 29.75 degrees) there were sporadic replies outside of the expected reply zone of the slave antenna. It is reasonably certain that these replies were not caused by multipath but rather by the difference pattern defect. Only one such sporadic reply appeared outside of the apparent reply zone of the master station.

Figure C-9 was generated from the data shown on Figure C-8. The plot of reply probability versus steering angle of the null pattern from the master station was derived by counting the number of replies from the middle five slave scan increments for each increment of master scan angle and dividing the result by 20. The center five increments of scan of the slave antenna were used because the probability of suppression by the slave over this region was expected to be very close to zero. The grey regions shown on Figure C-9 are those regions wherein a reply may or may not be expected from all transponders operating within the limits of the National Standard<sup>1</sup> and assuming that the  $P_2/P_1$  ratio was exactly 7 dB and that the null pattern from the master station antenna was exactly as had been measured at Bendix (see Figure B-1). The outer limits of the grey regions imply the maximum angles from which replies should be received (i.e., any transponder meeting the National Standard should be suppressed at greater angle where the  $P_2$  signal strength is presumed greater than that of the  $P_1$  signal). At the inner limits of the grey region, all transponders should reply at least 90% of the time (i.e., the probability of suppression should be less than ten percent). If the  $P_1/P_3$  signal strength is sufficiently high, any typical production transponder will reply essentially all of the time until the  $P_2/P_1$  ratio reaches some value between zero and -9 dB. Beyond this point the probability will drop off rapidly to zero.

The Gulfstream transponder would appear to marginally meet the National Standard requirement that suppression must be 100% when the  $P_2$  signal level exceeds that of  $P_1$ . The fact that a reply probability of 45% appears outside of the limit at 29.75

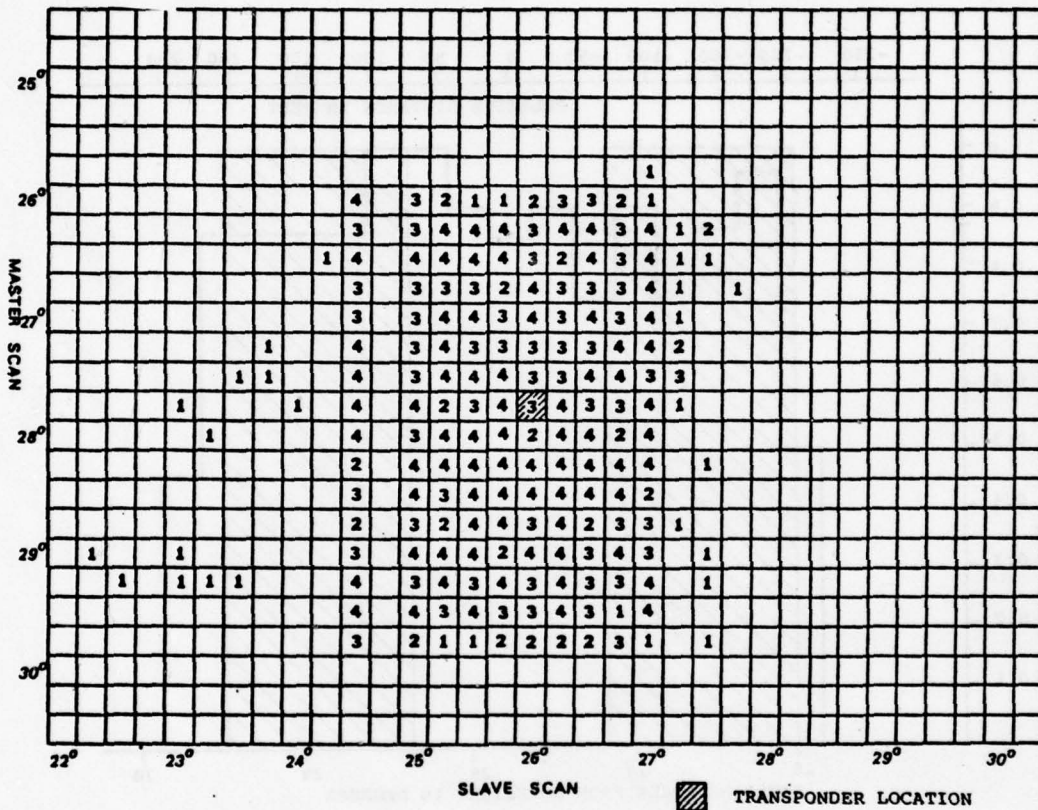


Figure C-8. Reply Count for Four Scans Versus Pairs of Steering Directions from Master and Slave Stations  
 Steering Increments of 0.25 Degrees  
 Gulfstream Aircraft Located at Point B84  
 (Data from Tape 3339, File 9)

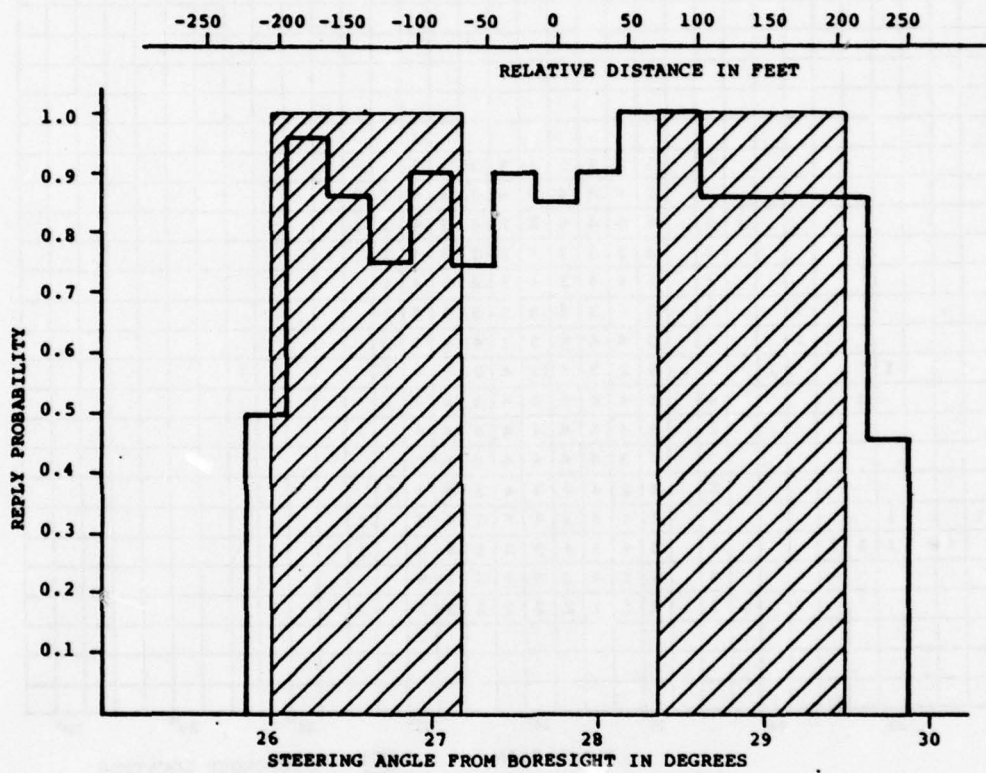


Figure C-9. Histogram of Reply Probability for the Master Station with a Gulfstream Aircraft at Point B84 and  $P_2/P_1 = 7$  dB (Tape 3339, File 9)

degrees could involve the quantization of steering, the fact that the maximum steering error is known to be about 0.15 degrees,  $P_2/P_1$  ratio slightly less than 7 dB, or a minor deviation from the measured antenna pattern. The fact that the reply probability was not at least 90 percent over most of the response curve is mainly attributable to non-valid replies caused by fruit interference with at least two of the received replies (i.e., less than two of the three receive stations reported the correct ID).

Figure C-9 also includes a scale in feet that indicates that the interrogation cell size (for the Gulfstream) was about 400 feet wide as seen from the master station. It also indicates that an identical transponder offset about 250 feet from the Gulfstream would have been resolved by separate interrogations in the directions of the two transponders.

Figure C-10 was also derived from the data shown on Figure C-8, except that the reply count was made for each steering angle increment of the slave antenna using only the reply counts from the center five steering increments from the master station. The  $P_2/P_1$  ratio for the slave station was 3 dB. Figure C-10 shows a performance skewed somewhat relative to the shaded areas. This was probably caused by the defect in the slave antenna steering system described previously. The zero response level at a steering angle of 24.75 degrees also reflects this condition. The distance scale on Figure C-10 indicates an interrogation cell width (for the Gulfstream) of about 100 feet as seen from the slave station.

Figure C-11 is another histogram wherein the test vehicle was used rather than the Gulfstream. The vehicle was placed about 100 feet southwest of point B84 and a  $P_2/P_1$  ratio of 5 dB was used with the master station. The transponder's response is shown to be within the grey area corresponding to the National Standard.

The cell size is seen to be in the 450-475 foot range, somewhat larger than was the case with the Gulfstream as shown on Figure C-9. The lower value of  $P_2/P_1$  should generate a larger cell and the suppression characteristics of the different transponder could, of course, cause some difference.

#### C.3.3.3 Typical Two Target Test

Figure C-5 showed the performance of the brassboard DAS with two targets separated by 130 feet. The performance capability was derived from the data on DAS tape 0205, File 5.

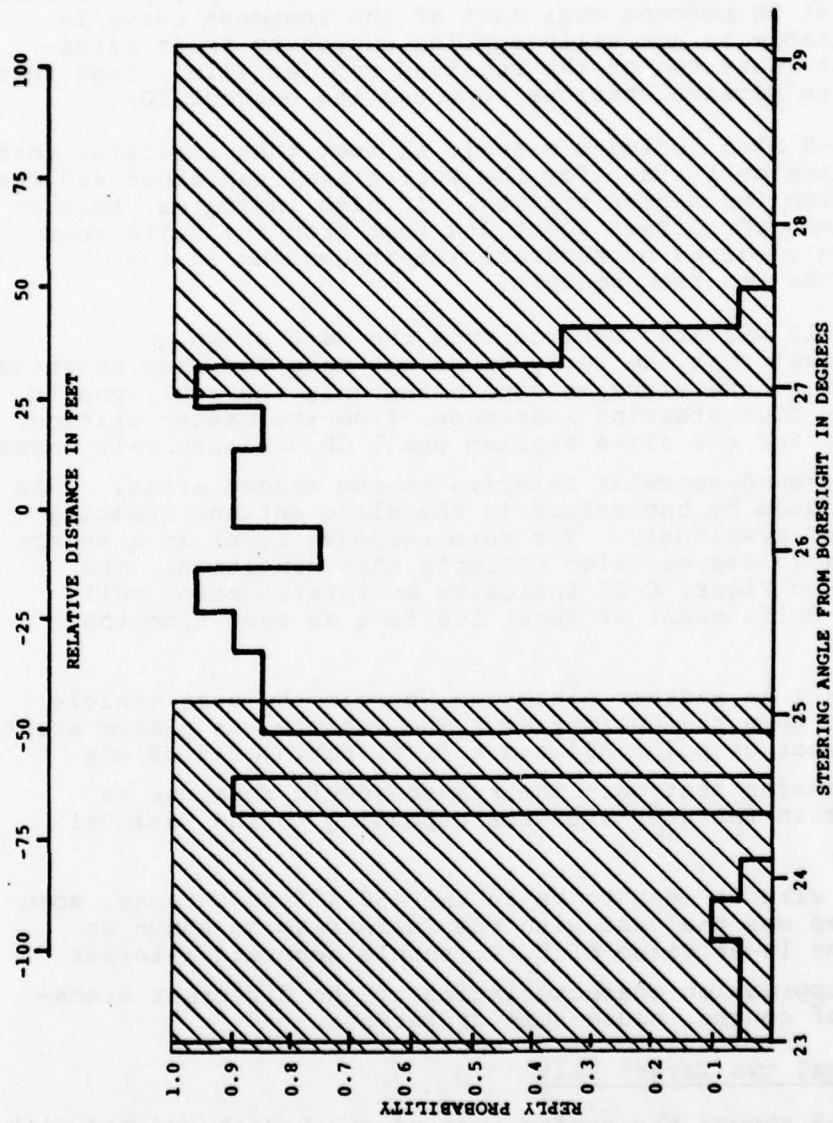


Figure C-10. Histogram of Reply Probability for the Slave Station with a Gulfstream Aircraft at Point B84 and  $P_2/P_1 = 3$  dB (Tape 3339, File 9)

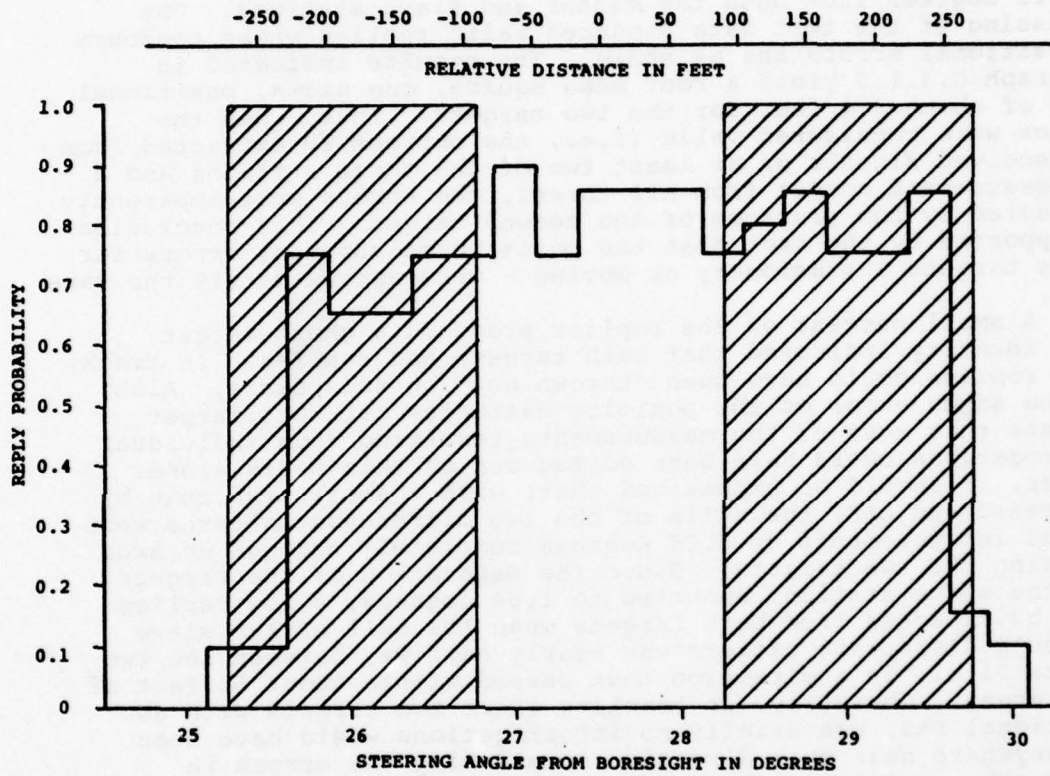


Figure C-11. Histogram of Reply Probability for the Master Station with a Test Vehicle 100 Feet Southwest of Point B84 and  $P_2/P_1 = 5$  dB (Tape 3339, File 9)

In this test, the calibration transponder was situated at the CAL 1 site on the NAFEC airport - 5,175 feet from the master station and 4,500 feet from the slave station. The second transponder, in the test vehicle was located approximately on the line from the master station through the CAL 1 Site. Thus, resolution was provided by the signals transmitted from the slave station. The test parameters involved a small area scan in increments of 0.25 degrees from both the master and slave stations. The processing of the test data produced valid replies whose contours of positional errors are as shown. The results indicated in paragraph C.3.1.3 yield a root mean square, one sigma, positional error of about 6.4 feet for the two targets. Thus, when the replies were considered valid (i.e., the correct ID extracted from the received signals of at least two of the three stations and a TOA measurement output from all three), the errors were apparently unaffected by the presence of the second target. This conclusion is supported by the fact that the position measurement errors for single targets - stationary or moving - were approximately the same value.

A small percent of the replies produced a ghost target whose identity indicated that both targets had replied. In track, these replies could have been "thrown out" on this basis. Also, the one sigma error of the position estimates for this target indicate that most of the measurements resulting from individual interrogations could have been edited out on this basis alone. Further, it should be emphasized that, with a small area scan by the brassboard DAS, the nulls of the two difference patterns were steered in increments of 0.25 degrees completely through an area enclosing the two targets. Since the separation of the targets, from the slave station, amounted to 1.66 degrees, a few replies could be expected from both targets when the null of the slave station's difference pattern was nearly half way between the two targets (i.e., in a direction that passed within about 65 feet of each target. Obviously, in tracking these two targets with an operational DAS, essentially no interrogations would have been made anywhere near this direction considering the errors in knowing the actual position of each target. Thus the probability of having no reinterrogate because of synchronous garble involving the two targets (i.e., the resolution problem) would be insignificant and probably much smaller than that caused by a relatively high level of fruit.

#### C.3.3.4 Conclusions About Resolution and Interrogation Cell Size

The interrogation cell, as seen from either the master or slave station, must satisfy the following two conditions if the ASTC DAS is to be considered suitable as a potential operational sensor:

1. It must be possible to maintain the dimension of the cell, wherein the  $P_1$  signal strength is 9 dB in excess of that of the  $P_2$  signal (as seen at any transponder whose operational characteristics are within the National Standard), of sufficient width that the target can be tracked. This means the one-half cell width must exceed the errors of knowing the target's position plus the error in placing the null of the antenna difference pattern in the predicted direction of the target.
2. The dimension of the cell, wherein the  $P_1$  and  $P_2$  signal strengths are equal, should be sufficiently small to ensure resolution of the two transponders operating within the specified characteristics of the National Standard. One-half the cell width must exceed the sum of the desired resolution, the error in knowing the position of the target being interrogated, and the error in placing the null of the antenna difference pattern in the predicted direction of the target.

In considering the operational potential of the brassboard DAS as regards the above two conditions, the following limitations of the brassboard must be kept in proper perspective:

The minimum steering increment of 0.25 degrees

The accuracy (repeatability) of steering. This is known to never exceed 0.15 degrees for the brassboard.

Difference patterns limited by the selection of 16 or 6 operating antenna elements. This determines the width of the null in the difference pattern.

The lack of any automatic (i.e., computer-controlled) capability to dynamically adjust the selection of the  $P_2/P_1$  ratio, the steering angle and the aperture size. Any operational ASTC Sensor would obviously have this capability.

The half-width of the interrogation cell is given by:

$$W_{1/2} = \frac{6076.1R}{2} \times \frac{\pi\alpha}{180} \times \frac{16}{N_E \cos\delta}$$

$$W_{1/2} = \frac{848R\alpha}{N_E \cos\delta} \text{ feet}$$

Where:  $R$  = range in nautical miles

$\alpha$  = width of null of difference pattern at point where cell size is defined, as shown on Figure B-1, in degrees

$N_E$  = number of antenna elements actually employed

$\delta$  = angle from the array boresight (master or slave antenna) to the target.

Figure C-12 was developed from the expression above and the two curves on Figure B-1 in the following manner:

1. Using the curve corresponding to  $P_1 = P_2 + 9$  dB from Figure B-1, an initial value of  $W_{1/2}$  was calculated for a range of two nautical miles,  $N_E = 16$ ,  $P_2/P_1 = 12$  dB, and boresight. A value of 12 dB for the  $P_2/P_1$  ratio is considered the maximum practical value for the brassboard because of the effects of multipath.
2. A line is drawn from this point toward the origin until it crosses the value of 30 feet for the half-cell width. The value of 30 feet was considered a very conservative value to maintain track on any transponder operating in accordance with the National Standard considering that the average value of the one sigma error in predicting position during the NAFEC field test fell in the 6-8 foot range.
3. At the range where the intersection with the 30-foot line occurs, (0.96 nautical miles on Figure C-12), a new value for  $W_{1/2}$  is calculated using a value for  $\alpha$  corresponding to a  $P_2/P_1$  ratio of 9 dB. This increases the one-half cell width to 42 feet. A line is drawn from this point toward the origin until it intersects the 30-foot line (at 0.70 nautical miles).
4. The above procedure is repeated for  $N_E = 16$  elements until the  $P_2/P_1$  ratio is 3 dB. This is considered the lowest value for practical operation with the difference beam.
5. The intersection of the "3-dB line" with the 30 foot line on Figure C-12 occurs at 0.34 nautical miles. At

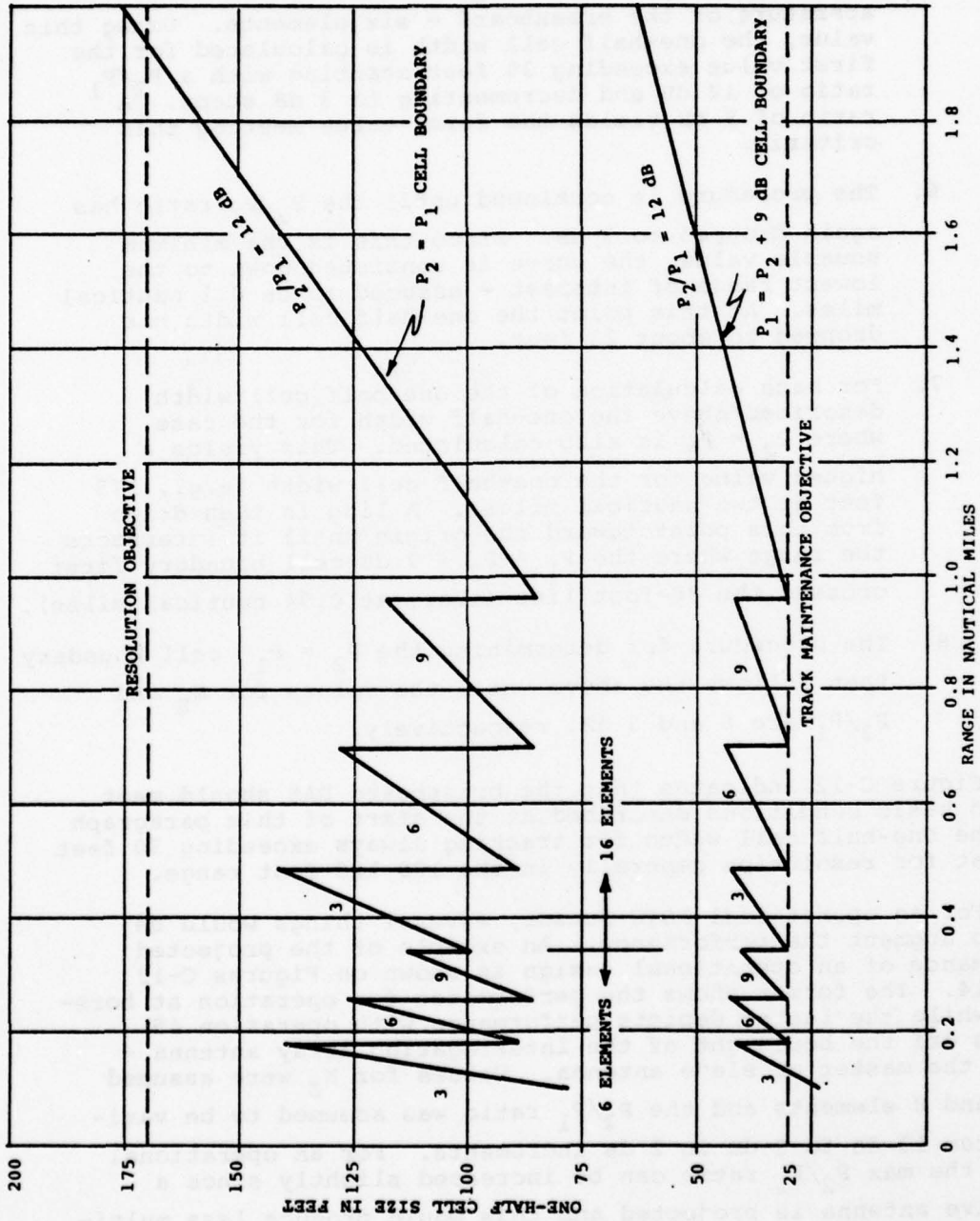


Figure C-12. Brassboard DAS Interrogation Cell Boundaries  
(Operation at Boresight)

this point the value of  $N_E$  is reduced to the small aperture of the brassboard - six elements. Using this value, the one-half cell width is calculated for the first value exceeding 30 feet starting with a  $P_2/P_1$  ratio of 12 dB and decrementing in 3 dB steps. A ratio of 9 dB yields the first value meeting this criteria.

6. The procedure is continued until the  $P_2/P_1$  ratio has again dropped to 3 dB. Since this is the minimum usable value, the curve is continued down to the lowest range of interest - assumed to be 0.1 nautical miles. At this point the one-half cell width has dropped to about 23 feet.
7. For each calculation of the one-half cell width described above the one-half width for the case where  $P_2 = P_1$  is also calculated. This yields a higher value for the one-half cell width (e.g., 175 feet at two nautical miles). A line is then drawn from this point toward the origin until it intersects the range where the  $P_1 = P_2 + 9$  dB cell boundary first crosses the 30-foot line (i.e., at 0.94 nautical miles).
8. The procedure for determining the  $P_2 = P_1$  cell boundary then follows the above until the values for  $N_E$  and  $P_2/P_1$  are 6 and 3 dB, respectively.

Figure C-12 indicates that the brassboard DAS should meet the two basic conditions described at the start of this paragraph with the one-half cell width for tracking always exceeding 30 feet and that for resolution generally in the 100-125 foot range.

For an operational ASTC Sensor, several things would be done to augment the performance. An example of the projected performance of an operational design is shown on Figures C-13 and C-14. The former shows the performance for operation at bore-sight while the latter depicts performance with operation 45 degrees off the boresight of the interrogating array antenna - either the master or slave antenna. Values for  $N_E$  were assumed as 22 and 8 elements and the  $P_2/P_1$  ratio was assumed to be variable from 13 dB to 3 dB in 2 dB increments. For an operational design the max  $P_2/P_1$  ratio can be increased slightly since a directive antenna is projected and this would produce less multi-

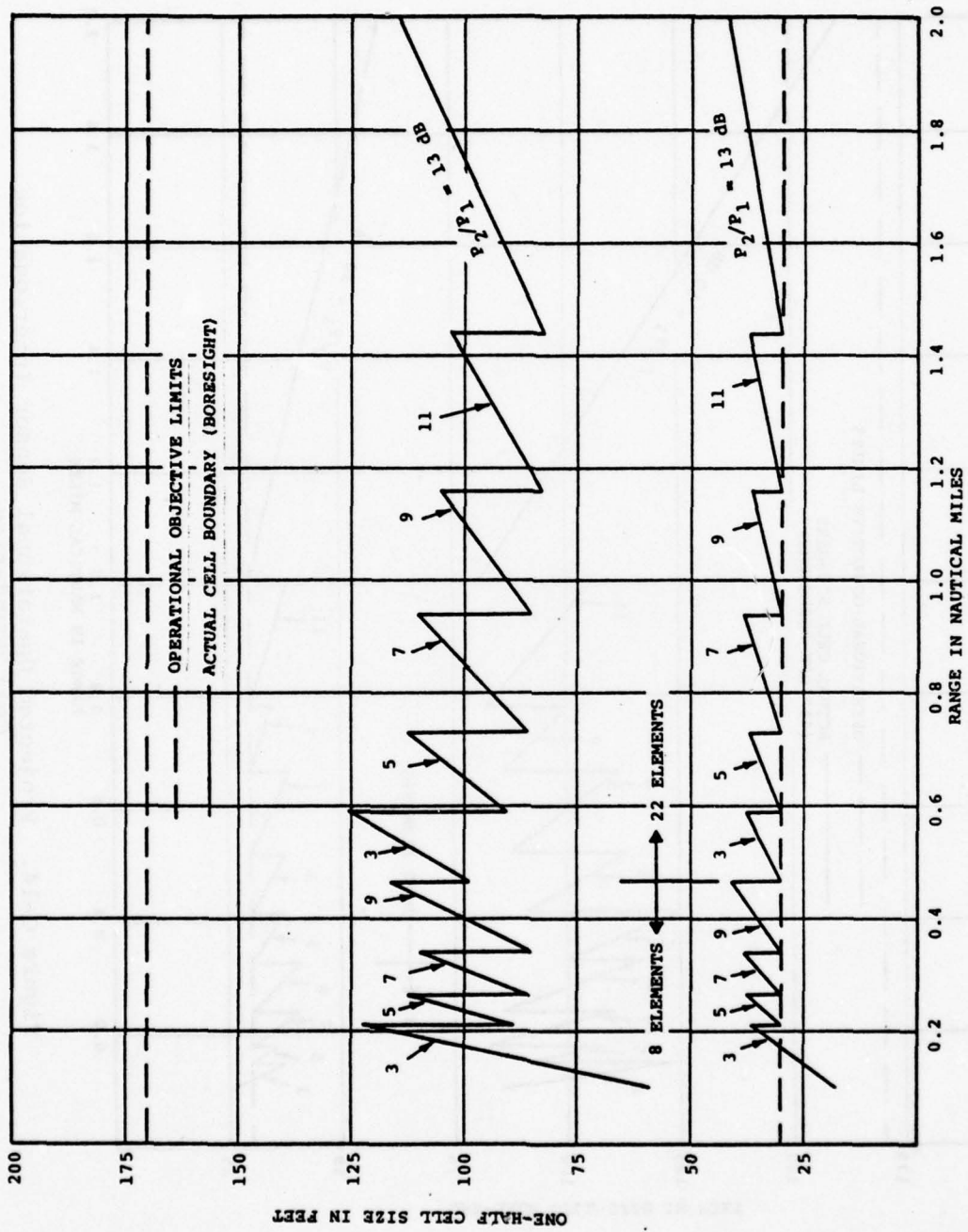


Figure C-13. Projected Operational Sensor Interrogation Cell Boundaries

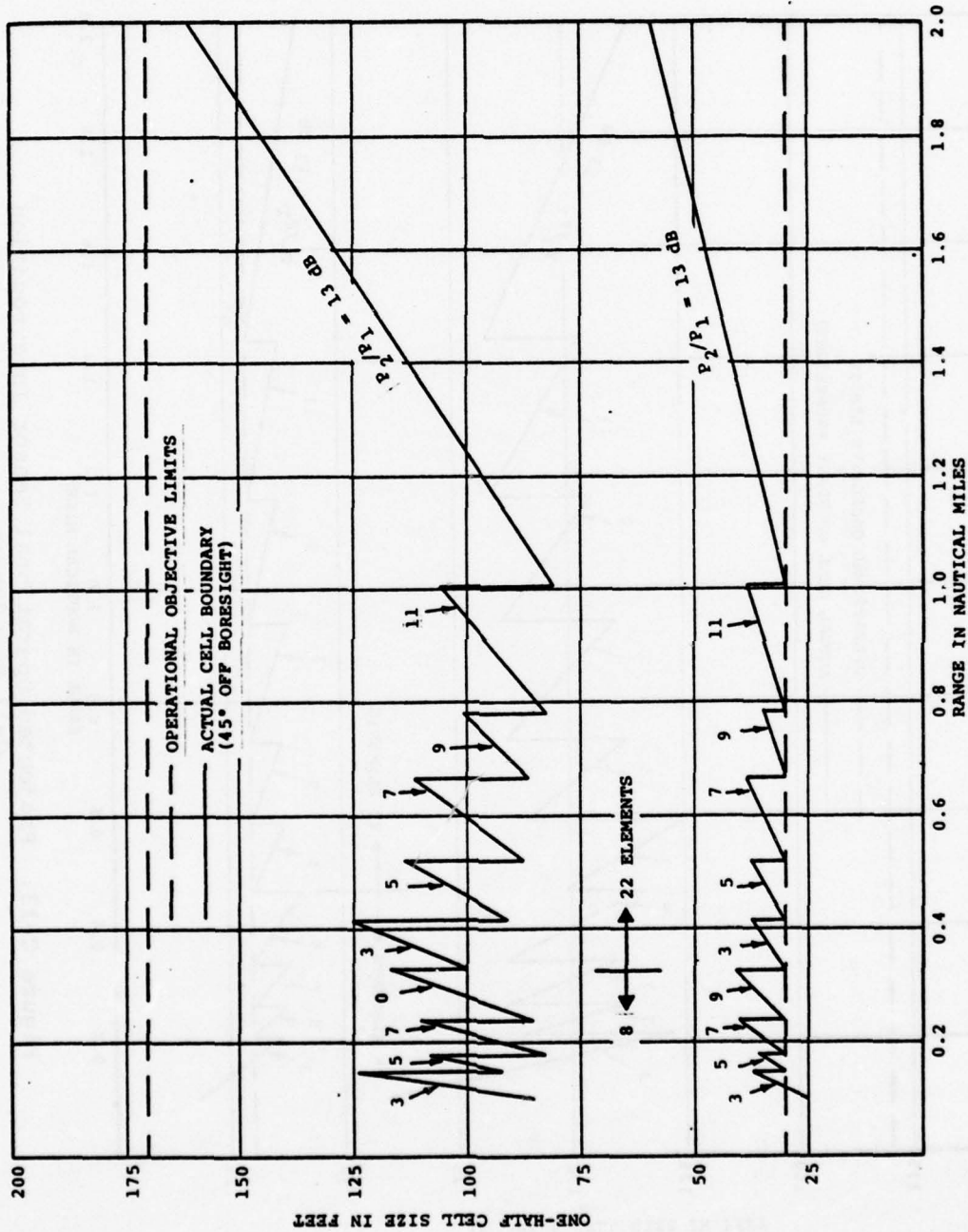


Figure C-14. Projected Operational Sensor Interrogation Cell Boundaries

path problems in operating with a high  $P_2/P_1$  ratio.

Figures C-13 and C-14 would seem to indicate that in achieving the one-half interrogation cell width deemed appropriate for the brassboard DAS to achieve track maintenance, the operational design described would yield a resolution capability of better than 125 feet unless the range exceeds 1.56 nautical miles with an angle off boresight of 45 degrees.

Two factors were not included in the above projections of operational sensor design. These are the quantization and the accuracy of steering the null of the difference pattern. For the brassboard, these values are 0.25 and 0.15 degrees, respectively. A vigorous analysis of the performance of a projected design would include one-half of the quantization value plus the maximum steering error. In considering these factors and others that would affect the performance of an operational sensor, it is concluded that the parameters and characteristics of an operational design would typically involve the following:

An aperture selection of 22 or 8 active elements

The ability to adjust the  $P_2/P_1$  ratio in one-dB increments

Quantization of the null pattern steering in 0.125 degree increments (at boresight)

Maintaining the steering error within a maximum value of  $\pm 0.1$  degree.

Logic in the software that includes control of the  $P_2/P_1$  ratio and the aperture selection adaptively with changes in range and the angle off the array boresight, an appropriate prediction algorithm for track maintenance, and an algorithm for reacquisition in case of a lost track.

All of the curves of Figure C-12 through C-14 were predicted the assumption that the sensor would always be operated in a manner that presumes that any transponder must be assumed as operating anywhere within the characteristics described in the National Standard. It may well be that operational algorithms could eventually be developed that would take into consideration the actual distribution of the pertinent characteristics of a large sample of operational transponders. This could result in the achievement of better resolution while still maintaining some desired probability of track mainten-

ance. The subject of reacquisition would obviously be appropriately incorporated into these improved algorithms.

The overall conclusion to be drawn from the analysis of the interrogation cell size and the resolution capability achieved by the brassboard DAS during the NAFEC field tests in that there is no question of feasibility in this regard and the capability required of an operational sensor should be achieved with a reasonable augmentation of the brassboard hardware supplemented by computer control employing suitable algorithms.

#### C.3.4 MULTIPATH

Discussed here are the results of lateral multipath testing, vertical multipath being covered under surface coverage, paragraph C.3.2. Lateral multipath (hereafter referred to as multipath) effects on TOA accuracy and identity (ID) decoding accuracy have been investigated directly by multipath signal level measurements and indirectly as implied by the accuracy levels achieved in benchmark testing, etc.

##### C.3.4.1 Multipath Signal Level Measurements

During the NAFEC test program a series of multipath tests were conducted. These tests involved measurement of the direct and reflected signals from test vehicle transponders searching a representative portion of the runway/taxing network. Particular attention was paid to those areas in the vicinity of large hangers, buildings and parked aircraft where the probability of severe specular multipath is greatest. The region covered is shown in Figure C-15. Oscilloscope photographs were taken of the resulting video signals developed at the master station receiver's log video test connector to document such multipath signals as were found.

Figure C-16 is a calibration photo taken by double exposure of a 10 dB step in RF input attenuation. This was taken on taxiway B and is representative of typical multipath levels, down 15-20 dB or more. Multipath evaluation points M1 through M6 had peak multipath signal levels in the -3 dB to -6 dB range. All other points found were -6 dB or below except for M10 at the center of an area where a severe multipath signal was found. Careful location of the test vehicle allowed recording the multipath signal at its -3 dB point although a peak of +3 dB was observed. This +3 dB level could not be photographed because the multipath was so position sensitive that the test vehicle could only pass through these regions. Efforts to push the small van used as a test vehicle into position and photograph the +3 dB level were unsuccessful. While stopped, a mild breeze of 5 Kn or less shifted the vehicle's body on it's springs enough to remain largely out



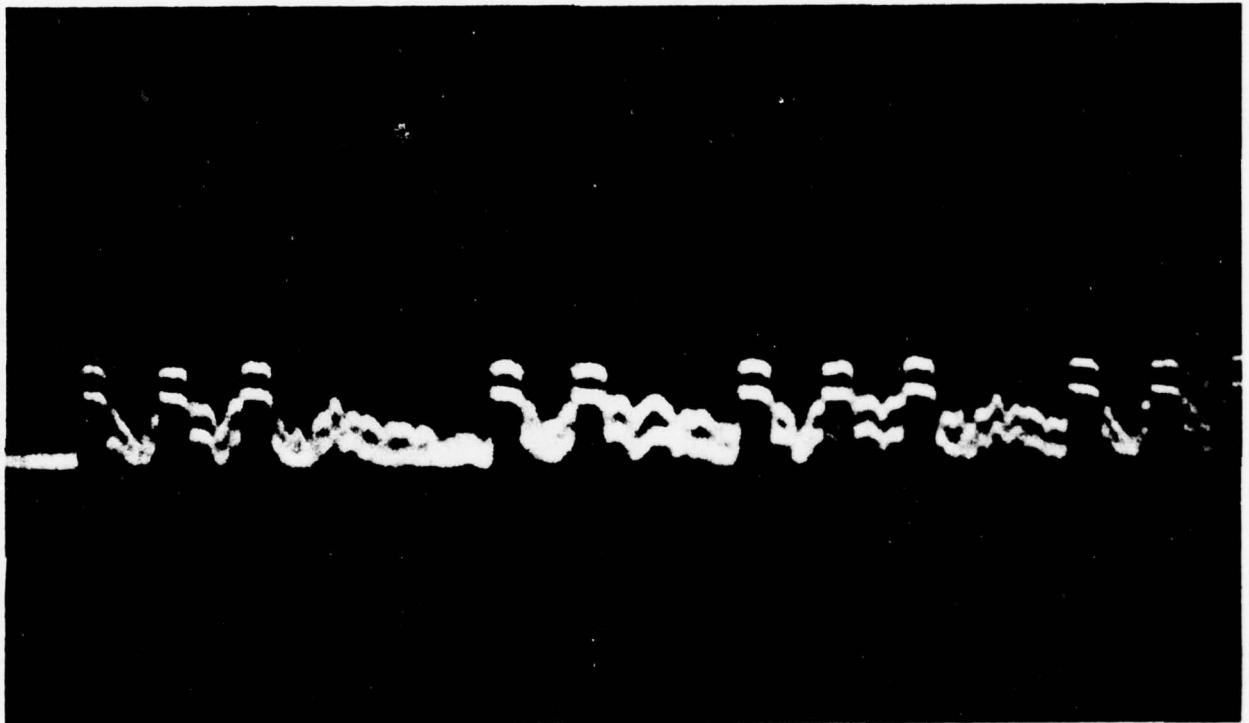


Figure C-16. Calibration Photo Log Video Showing  
10 dB Step in Input Attenuation

of the +3 dB region.

At test point M9 about 35 feet away the multipath was below -3 dB. Test point M8, 65 feet away showed multipath levels below -6 dB, see Figure C-17.

During multipath testing it was found that the effects of multipath both on interrogation and on TOA could not be documented by observing received waveforms. A statistical evaluation of multipath must be relied upon to provide meaningful insight into their effects on resolution and position accuracy (see paragraphs C.3.1 and C.3.3).

#### C.3.4.2 Conclusions About Lateral Multipath

Multipath levels measured at NAFEC are summarized in Table C-4 below. This data is plotted in Figure C-18.

TABLE C-4  
NAFEC MULTIPATH DATA

Multipath Signal		Coverage Area Affected	Effect on TOA	Effect on ID
Amplitude	Delay <sup>a</sup>			
>20 dB down	3 $\mu$ s	91%	None	None
-9 to -20 dB	1 $\mu$ s	8%	None	None
-3 to -9 dB	.1 $\mu$ s	1%	None	None
+3 to -3 dB	.2 $\mu$ s	0.01%	None Measurable	Measured <sup>b</sup>

<sup>a</sup>Typical.

<sup>b</sup>Loss of ID at one of three sites during this condition.

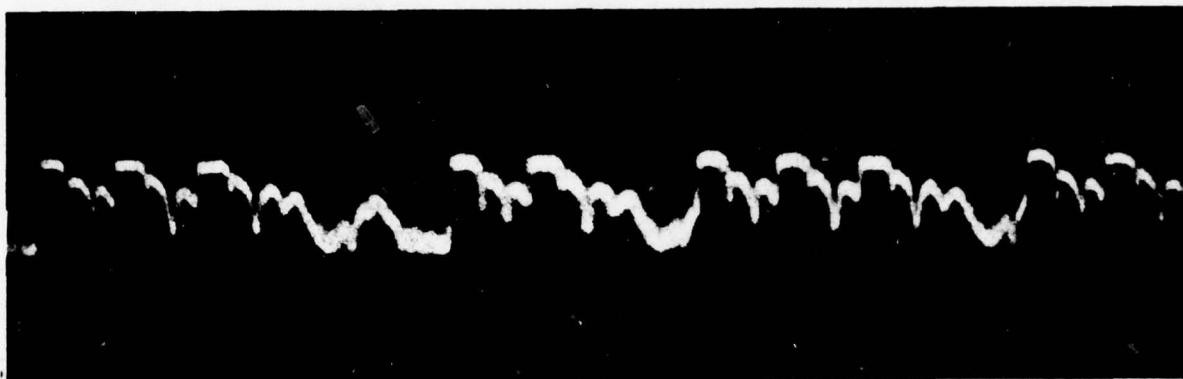


Figure C-17. Master Station Reply Video Form  
Test Point MB Showing Multipath Levels

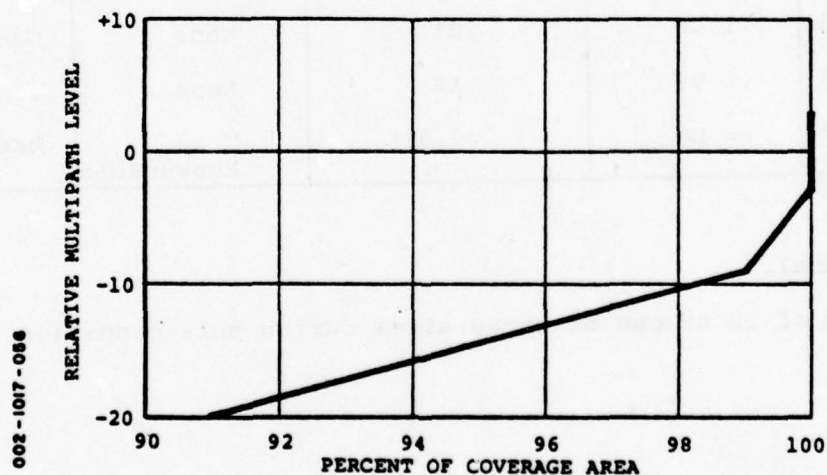


Figure C-18. Multipath Levels Versus Percentage of Coverage  
Area as Measured at NAFEC

This distribution of multipath is used to generate a plot of the probability of at least two out of three correct ID's, using the measured NAFEC ASTC round reliability of 0.89. This plot is presented in Figure C-19.

The source of the strong multipath signal found at point M10 was analyzed to determine if it was the result of a specular reflection from a large vertical surface as predicted. Referring to Figure C-20, which shows only the F1 and its multipath signal from M10, the multipath is delayed by approximately .76 microsecond. An ellipse of constant .76 microsecond delay is constructed between source M10 and the master station receiver, see Figure C-15. The ellipse passes close to the Atlantic City Terminal and ASR-7 facility but only the NAFEC tower complex (C the figure) lies on the ellipse. Examination of the photomap of NAFEC reveals that the NAFEC tower, see Figure C-21, is located such as to produce a multipath signal with delay of 0.777 microseconds. This is well within the resolution capability obtained using the M10 multipath photo. Furthermore, the angle on interception of a signal from M10 with the broad face of the tower is within a fraction of a degree of the reflection angle measured to the master station. The angle of interception from M10 changes only  $4.25^\circ$  to M9 where the multipath was down below -3 dB and  $8.5^\circ$  to M8 where it was below -6 dB.

The following conclusions relative to multipath testing at NAFEC may be made:

Multipath levels in excess of the nominal assumed level of -6 dB did exist but were limited to a small percentage of the coverage area.

Multipath from each specular reflector which is greater than -3 dB exists only in a small region, within a few degrees of maximum, the amplitude changing rapidly from good to bad as one moves through this region.

Effect on TOA was minor, the assumed 7.5 ns  $1\sigma$  value assumed in analysis well in excess of the measured effect (see paragraph C.3.1).

Effect on ID was measurable but the -3 dB PAE threshold amplitude setting and use of the "at least two out of 3" valid ID criteria should provide a .95 probability of correct ID over 99% of the NAFEC surface.

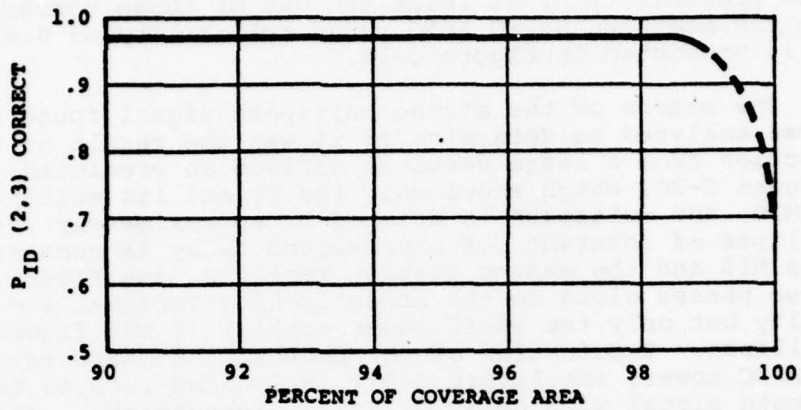


Figure C-19. Probability of at Least Two Out of Three Valid ID's Based on Multipath Data Taken at NAFEC

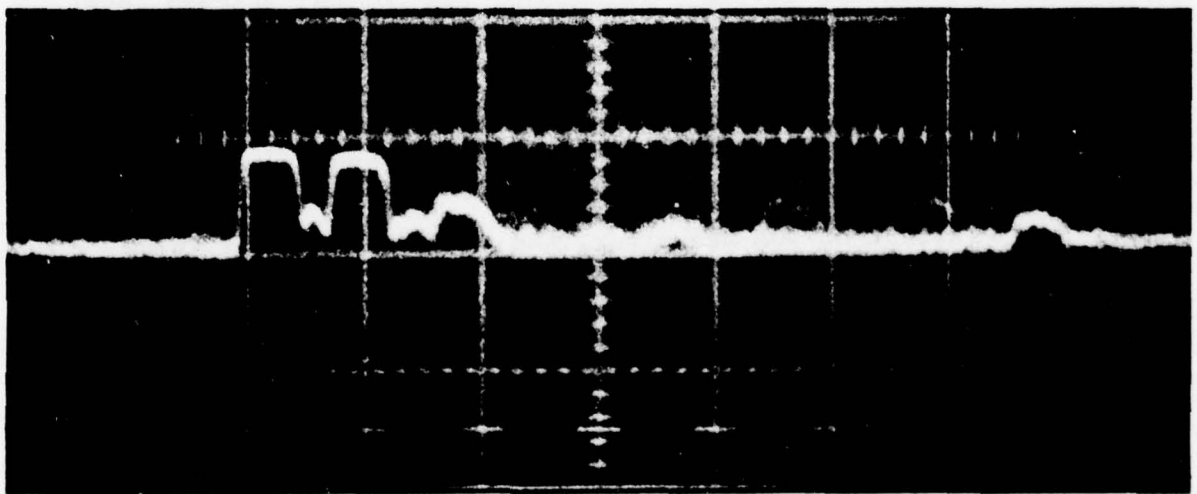


Figure C-20. F1 Pulse and the Resulting Multipath Signal From MIO, 1 Microsecond per Division



Figure C-21. NAFEC Tower

### C.3.5 UPDATE RATE

#### C.3.5.1 Conventional Sensors

For most surveillance systems, the update rate is equal to the scan rate. For typical TCS ASR/ATCBI's, the scan period is 4 seconds, giving a 0.25 Hz update rate. For ASDE radars, it is typically one Hz. These sensors are characterized by the following:

- a. All targets in track are updated at the same rate. This rate may be more or less than adequate depending on the operational problem. The only way to alter the rate is to change the antenna scan period (or possibly us back-to-back antennas, etc.).
- b. Search has the same update rate as track. Thus, new targets will usually be detected with delay that is somewhat less than the inverse of the update rate. Acquisition into track generally requires at least two scans. This assumes some automated tracking algorithm.
- c. The problem of track coast or reacquisition of a lost target is also limited by the scan period. This obviously proves inadequate in many instances.
- d. The hits per scan (a radar) or the interrogations per update period (a beacon) typically run 15-20. The number depends on the antenna beamwidth, the PRF, the scan period, and the target range (this determines whether detection is effected over the antenna patterns 3 dB width, 10 dB width, etc.). Thus, though the average number of replies from a given target for a TCA ATCBI may be 5 per second, the update rate is still 0.25 Hz. These sensors are therefore rather inefficient in terms of the average number of interrogations to achieve a satisfactory update rate. One bad result, for beacons, is that the fruit generated by a single interrogator is proportional to the higher number. This is a good reason for providing these antennas with a monopulse capability.

#### C.3.5.2 The Brassboard DAS

The brassboard DAS at NAFEC was capable of update rates that were quite low to a maximum value that could approach the PRF of the sensor to which it was synchronized - the NAFEC ASR-4's ATCBI, whose PRF is 380. Consider the following two extremes:

- a. A large area scan test could be set up wherein both the master and slave antennas scanned +32 degrees in 0.25 degree increments. With a PRF of 380, the

duration of the total scan would be:

$$\text{Scan duration} = \left( \frac{64}{0.25} \right)^2 \times \frac{1}{380} = 172.5 \text{ seconds}$$

Depending on the target location and the  $P_2/P_1$  ratio employed during the test, the number of valid replies during this interval could be typified by the numbers shown on Figure C-6 divided by four (that test involved the replies over four scans). Assuming there had been no defect in the phase shifter (as discussed in paragraph C.3.3.2), the reply region could reasonably be described as bounded by the overlap of angular sectors of 24.5 - 27.25 degrees from the slave station and 26 - 29.75 degrees from the master station. This involves a 12 x 16 matrix of scan positions. Within this reply region, assuming the performance for the 24.75 degrees slave column (the "blank" column) had averaged that of the two adjacent columns, an average of 147 valid replies would have occurred during the 172 second scan. Even though the brassboard scan involves a "sweep" from the master station for each steering increment of the slave station antenna, and the 147 replies would have appeared in 12 groups, the effective update rate would still have been about once every 172 seconds since the 12 groups would have occurred consecutively during a total scan involving 256 beam positions.

- b. For a single fixed target, the brassboard "scan" could have been set up to consist of a single interrogation cell that included the known target location. Thus, the average update rate could have equalled 380 (the PRF) multiplied by the Round Reliability. If the center 7 x 7 raster of scan positions from Figure C-6 had shown a value of "four" in each cell (i.e., the Round Reliability had been 1.00), it is easily determined that the actual Round Reliability was about 0.89 (a simple count of the numbers in the 7 x 7 matrix divided by 4 x 49). Thus, under the external interference conditions existing at the time the test was run whose results are shown on Figure C-6, the update rate on a single target would have been about 338 Hz.

The above two extreme cases lead to the rather obvious conclusion that update rate had no real meaning for the tests run at NAFEC. For example, the moving target test described in

paragraph C.3.1.2 involved a 5 Hz update rate that was uniquely established by the manner in which the brassboard hardware was operated during that test. Thus, any meaningful discussion of update rate, in relation to the NAFEC field tests, must involve a discussion of how an operational ASTC Sensor would be used to perform the functions of search, acquisition, track, reacquisition (of lost targets), etc.

### C.3.5.3 Update Rate of an Operational ASTC Sensor

The brassboard DAS tested at NAFEC consisted of two line arrays (at the master and slave sites) that provided the capability to steer the nulls of the respective difference beam patterns. However, the brassboard DAS did not include computer control with a sophisticated scheduling algorithm. Thus, the key difference between an operational ASTC Sensor and the brassboard DAS would be that the former would most certainly be computer controlled and the principal feature of the control would be sophisticated scheduling algorithm. With such an algorithm, the expression update rate would have the following significance:

- a. The update rate would vary with the operational function. Search, track, acquisition, etc. would all have different update rates.
- b. For any specific operational function, more than one update rate would likely be employed. Thus, for track, a typical operational ASTC Sensor would have data rates varying from 0.5 Hz to 8 Hz in binary steps.
- c. The tracking algorithm would dynamically alter the update rates of individual tracks in accordance with the requirements to maintain track (a function of such parameters as the interrogation cell size, the error in estimating target position, the desired probability of maintaining track, target velocity and acceleration) and the requirements of the user (e.g., a target holding short of a runway might require an 8 Hz data rate to ensure that any sudden acceleration would be recognized in time to effect an appropriate ATC action).
- d. Round Reliability is a most important parameter in the determination of the number of interrogations required to maintain a desired update rate in track. Reinterrogations would be automatically scheduled when no reply (or a non-valid reply) is reached in track.

In any discussion of update rate for an operational ASTC Sensor, two expressions are of particular significance relative to

the multiple target track problem. The number of interrogations required in an attempt to achieve a single track data point (i.e., an update) is given by:

$$n_i = 1 + (1-\overline{RR}) + (1-\overline{RR})^2 + \dots + (1-\overline{RR})^{n_r} \quad (C-5)$$

The probability that a given number of attempted track update efforts will be successful is given by:

$$P_{SU} = \left[ 1 - (1-\overline{RR})^{n_r+1} \right]^{n_T n_u} \quad (C-6)$$

In the above expressions, the parameters are defined as follows:

- $n_i$  = Maximum of interrogations required in an attempt to achieve a single track update
- $P_{SU}$  = Cumulative probability of achieving  $n_T n_u$  successful update.
- $n_T$  = Number of targets in track
- $n_u$  = Average update rate per target in track
- $\overline{RR}$  = Round Reliability
- $n_r$  = Maximum number of reinterrogations permitted before a reacquisition attempt is made (i.e., the target is presumed "lost").

Figure C-22 shows plots of expression C-5 for 200 track update attempts as function of Round Reliability and the maximum number of reinterrogations permitted. Figure C-22 clearly indicates that, for any reasonable value of Round Reliability, the total number of interrogations per second is about 285 to attempt an update rate of 200 per second with a maximum of four reinterrogations allowed per update attempt. The figure of 200 means 200 targets updated an average of once per second, 100 targets updated an average of twice per second, etc. It is apparent that the difference between one and four reinterrogations does not significantly affect the total number of interrogations for any given value of Round Reliability. The figure of four is not intended to imply that no more reinterrogations would ever be attempted. A higher number might well be warranted to achieve some desired

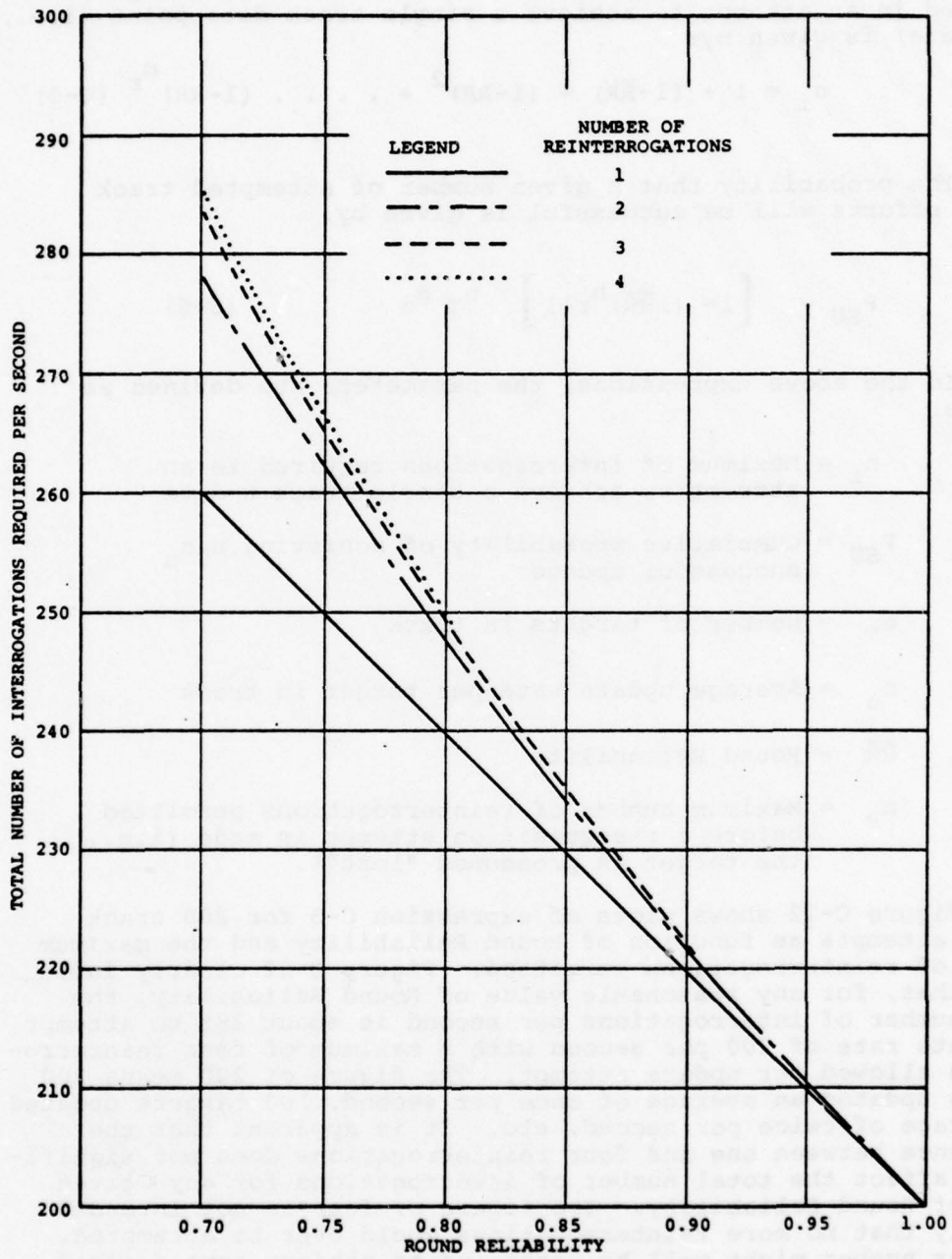


Figure C-22. Total Number of Interrogations Required to Achieve 200 Updates per Second

probability of successful update before resorting to a reacquisition attempt. Obviously, additional reinterrogations would have little impact on the total number of interrogations. For the brassboard at NAFEC, where the Round Reliability was apparently about 0.89 (see paragraph C.3.5.2b), a maximum of about 222 interrogations per second would have been required to maintain a one Hz update rate on 200 targets - if the brassboard had been designed to perform automatic computer-controlled tracking with adaptive reinterrogation. Thus, if the maximum PRF of the ASTC DAS had been fixed at 380 (the PRF of the ATCBI to which the brassboard DAS was synchronized at NAFEC), there would have been about 158 interrogations per second available for search or any other operational function other than track and reinterrogation.

Relative to the subject of reinterrogation, it is envisaged that, in an operational ASTC Sensor, this function would be totally adaptive - to the extent that a reinterrogation would automatically be scheduled during the next period of the ATCBI to which the ASTC Sensor is synchronized. Thus, if the PRF were 400 and a maximum of four reinterrogations were scheduled, the "shift in time" of the update point would never exceed 0.01 seconds from the nominal time. This would constitute a maximum deviation, from a desired one Hz rate, of one percent (or two percent maximum from a two Hz rate, etc.).

Figure C-23 shows plots of expression C-6 for 200 and 100 updates per second and varying values of the maximum number of permissible reinterrotations. If the ASTC DAS at NAFEC had had the capability to perform as an operational sensor, with the previously established value of 0.89 for the Round Reliability of NAFEC, 200 targets could have been updated each second with a probability of success (for the full second's operation) of 99.7 percent with a maximum of four reinterrogations per target update. The crux of the subject of operational potential of the brassboard DAS, relative to the matter of target update (in track), is fully depicted in Figure C-23.

### C.3.6 ATCRBS INTERFERENCE

#### C.3.6.1 ATCRBS Interference Measurements During NAFEC Testing

During the period from August 18 to November 18 five test days were allocated for interference tests to verify the compatibility of the ASTC data acquisition subsystem with existing ATCRBS, ARTS III and NAS stage A equipment. These interference tests are identified in Table C-5. This table shows the days of which interference tests were performed and all pertinent information related to the operation of the DAS interrogators and any special conditions employed in the performance of each test

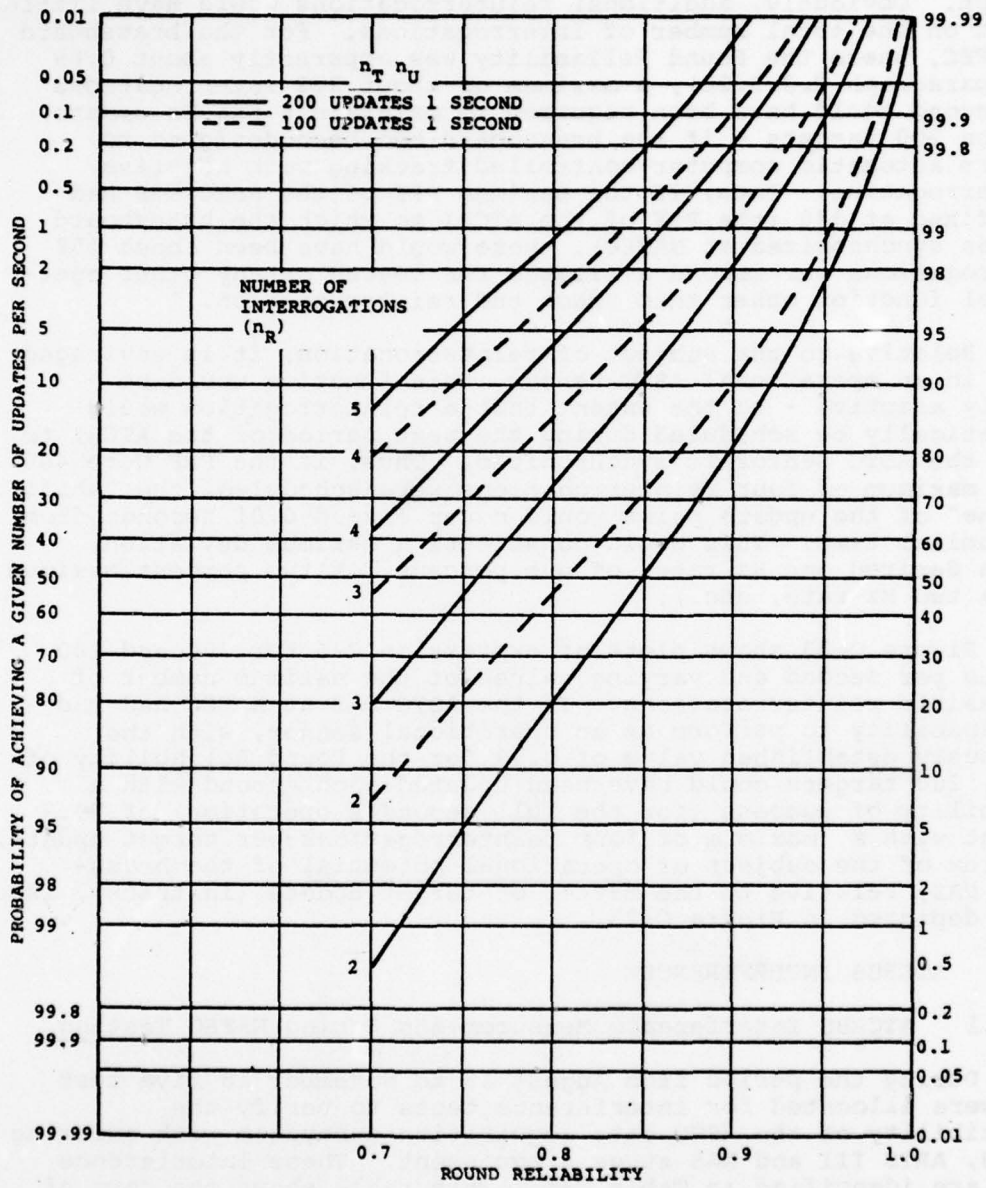


Figure C-23. Probability of Achieving a Given Update Rate ( $n_T n_U$ ) Versus Round Reliability and Number of Reinterrogations

TABLE C-5  
TEST SCHEDULE

DATE	RUN NUMBER	ASTC OPERATION				NAFEC INTERROGATOR ENVIRONMENT			DEDICATED AIRCRAFT				COMMENTS
		P1 POWER	P2 POWER	PRF X ASR-4	BEACON SYNC	ASR-4	ASR-5	ASR-7	N-46	N-377	N-49	N-376	
9/18	1	35.0W	140.0W	1	ASR-4	on	off	on					No dedicated aircraft were used on these runs, only aircraft-of-opportunity. Slave interrogator not operational.
	2	3.5W	14.0W	1	ASR-4	on	off	on					
	3	25.0W	100.0W	1	ASR-4	on	off	on					
	4	100.0W	400.0W	1	ASR-4	on	off	on					
	5	350.0W	2750.0W	1	ASR-4	on	off	on					
9/29	1	35.0W	140.0W	1	ASR-4	on	off	on					No dedicated aircraft was used for these runs, only target-of-opportunity.
	2	3.5W	14.0W	1	ASR-4	on	off	on					
	3	25.0W	100.0W	1	ASR-4	on	off	on					
	4	100.0W	400.0W	1	ASR-4	on	off	on					
	5	350.0W	1400.0W	1	ASR-4	on	off	on					
	6	350.0W	2750.0W	1	ASR-4	on	off	on					
	7	100.0W	400.0W	1	ASR-4	on	off	on					
	8	350.0W	2750.0W	1	ASR-4	on	off	on					
9/30	1	35.0W	140.0W	1	ASR-4	on	off	on					Not performed Not performed Runs 3 through 8 are repeats of runs 3-8 on 9/22.
	2	3.5W	14.0W	1	ASR-4	on	off	on					
	3	25.0W	100.0W	1	ASR-4	on	off	on					
	4	100.0W	400.0W	1	ASR-4	on	off	on					
	5	350.0W	1400.0W	1	ASR-4	on	off	on					

TABLE C-5  
TEST SCHEDULE  
(CONTINUED)

DATE	RUN NUMBER	ASTC OPERATION			NAFEC INTERROGATOR ENVIRONMENT		DEDICATED AIRCRAFT			COMMENTS				
		P <sub>1</sub> POWER	P <sub>2</sub> POWER	PRF X ASR-4	BEACON SYNC	ASR-4	ASR-5	ASR-7	N-46		N-377	N-49	N-376	
9/30	6	350.0M	2750.0M	1	ASR-4	on	off	on						
	7	100.0M	400.0M	1	ASR-4	on	off	on						
	8	350.0M	2750.0M	1	ASR-4	on	off	on						
10/29	1	100.0M	400.0M	1	ASR-4	on	on	on						N-376 instrumented to count airborne SLS rate
	2	350.0M	2750.0M	1	ASR-4	on	on	on						A/C flying vertical profile on 260° radial
	3	100.0M	400.0M	2	ASR-4	on	on	on						
	4	350.0M	2750.0M	2	ASR-4	on	on	on						
	5	25.0M	100.0M	4	ASR-4	on	on	on						
	6	100.0M	400.0M	4	ASR-4	on	on	on						
	7	350.0M	2750.0M	4	ASR-4	on	on	on						A/C flying constant altitudes of 5000 ft.
11/18	1	350.0M	1400.0M	1	ASR-4	on	on	on	1000'	A/C flying on ACM 260° at 11,000 ft. 0-25 nmi	A/C flying on ACM 260° at 5,000 ft. 0-25 nmi	A/C flying on ACY 260° at 15,000 ft. 0-50 nmi		N-46 instrumented to count airborne SLS rate
	2	350.0M	1400.0M	2	ASR-4	on	on	on	1000'					
	3	350.0M	1400.0M	2	ASR-4	on	on	on	3000'					
	4	350.0M	1400.0M	4	ASR-4	on	on	on	3000'					
	5	350.0M	1400.0M	4	ASR-4	on	on	on	7500'					

TABLE C-5  
TEST SCHEDULE  
(CONTINUED)

002-1017-075.3

DATE	RUN NUMBER	ASTC OPERATION			NAFEC INTERROGATOR ENVIRONMENT			DEDICATED AIRCRAFT			COMMENTS	
		P <sub>1</sub> POWER	P <sub>2</sub> POWER	PRF X ASR-4	ASR-4	ASR-5	ASR-7	N-46	N-377	N-49		N-376
11/18	6	350.0W	1400.0W	4	on	on	on	7500' <sup>a</sup>	A/C flying on ACT 170° at 11,000 ft.	A/C flying on MIV 150° at 10,000 ft.		
	7	350.0W	1400.0W	4	on	on	on	500'	at 0-25 nmi			Repeat of Run #7 on 10/29

a - M-46 at constant altitude for each run.

b - M-46 on the 260° for all runs except Run #6 which was on the 170° radial.

such as the use of dedicated aircraft and their flight plans. With the exception of the September 29 and 30 tests, interference tests were performed at approximately one month intervals. Each interference test is described in the following paragraphs.

The ASTC DAS interrogators were operated at NAFEC for the first time on August 18. During the time this equipment was operated, ASTC interference was monitored at Washington and Philadelphia Terminal areas, the New York and Washington ARTCC and NAFEC. The DAS was operated in a single interrogator configuration since the slave interrogator had not yet been installed. Initially, the interrogator was operated and a low power of only 35 mW. For this first series of tests, the PRF was held constant at 380 and the power increased in five steps to a maximum of 350 watts.

The September 29 and 30 test series were essentially repeats of earlier tests performed on August 18 with the exception that both master and slave site interrogators were operational and these interrogators were turned on and off on alternate one minute intervals. Each test at a given interrogator power level was run for a total of ten minutes thus providing five minutes of data with the ASTC system on and five minutes of data with the ASTC system off.

This test series consisted of performing eight runs; each with specified master and slave site interrogation and suppression power levels and a specified NAFEC interrogator environment. The  $P_1$  power was varied over an range from 35 milliwatts to 350 watts, while  $P_2$  power was varied from 140 milliwatts to 2.75 KW. ARTS III data were collected during these tests at the Philadelphia and Washington TRACONS and at NAFEC using the ASR-5 and ASR-7 site beacon interrogators. NAS Stage A data were collected at the New York and Washington Air Route Traffic Control Centers. Site monitors were again present at all locations and were in communications with the test director at NAFEC. In addition, to provide verification that the ASTC interrogators were in fact transmitting interrogation and suppression signals and at the power levels measured at the master and slave sites, a mobile test van deployed on the NAFEC airport surface was used to measure the radiated power level of the ASTC interrogators and the interrogation and suppression rates experienced by a surface transponder under these conditions.

A fourth set of interference data was collected on October 29, 1975. These tests were similar to those performed on September 29 & 30 using a similar set of test procedures. The major difference was in the PRF Values selected for the DAS interrogators. For these tests the DAS interrogators were operated at PRFs of 1, 2

and 4 times that of the ASR-4 and at power levels of  $P_1 = 100$  watts,  $P_2 = 400$  watts and  $P_1 = 350$  watts,  $P_2 = 2.75$  KW. In addition, the ASTC suppression rate was measured for an airborne aircraft flying a prescribed flight pattern. Since earlier tests indicated that very few targets-of-opportunity were present within approximately 15 nmi of NAFEC, the test aircraft was used to provide a target for the NAFEC ARTS III systems in this area as well as to obtain a feel for the maximum range for which the ASTC suppression signals could be received. The suppression counts were obtained using a portable transponder attached to the aircraft transponder antenna.

A fifth set of interference data was collected on November 18, 1975. These tests were again similar to those previously performed. For these tests the DAS interrogators were operated at PRFs of 1, 2 and 4 times that of the ASR-4 and at a power level of  $P_1 = 350$  watts,  $P_2 = 1400$  watts. Since earlier tests indicated that very few targets-of-opportunity were present within approximately 15 nmi. of NAFEC, four test aircraft were used to provide targets for the NAFEC ARTS III systems. The flight paths selected for these aircrafts were such that aircraft targets would be available at various ranges and altitudes at all times. That is, each aircraft was assigned a specified altitude and VORTAC radial on which to fly. During the tests, each aircraft then flew back and forth on their assigned radial and at their assigned altitude. One aircraft was instrumented with a portable transponder attached to the aircraft transponder antenna. This instrumented aircraft was used to measure ASTC suppression rates as a function of range and to determine range dependence on altitude. Since this aircraft was the key element in this test, the ASTC system remained active during the outbound leg of the flight. When the instrumentation indicated loss of ASTC suppression signals, the inbound leg was initiated and during this period the ASTC interrogators were turned on and off on alternate one minute intervals.

In summary, interference data were collected on five separate occasions representing a total of 33 test runs and providing a total of 26 hours during which data were collected. Data were obtained for targets-of-opportunity in the vicinity of NAFEC for various conditions of traffic densities as well as with the use of as many as four simultaneously dedicated aircraft. In addition, data were collected at two operational TRACON facilities (Washington and Philadelphia), two operational enroute facilities (Washington and New York), two non-operational ASR facilities (NAFEC ASR-5 and ASR-7) and one operational ASR facility to which the ASTC system was synchronized in order to prevent interference (NAFEC ASR-4).

### C.3.6.2 Interference Test Results

The analysis of data concentrated principally on those runs made at the maximum ASTC power level of  $P_1 = 350$  watts, and a PRF of 4 times the ASR-4 (1520 interrogations per second). The ASTC interrogators were turned on and off on alternate one minute intervals for a period of ten minutes thus providing five minutes with the ASTC "on" and five minutes with the ASTC "off". ARTS III performance indexes such as probability of detection, probability of strong target report, target run and hit lengths, and transponder round reliability were determined for the average of the ASTC "on" samples and the average of the ASTC "off" samples. A comparison of the two sets of values then provided an indication of any interference impact on overall ARTS III performance at Philadelphia, Washington, and NAFEC; particularly with respect to the masking of replies to these interrogation sites by ASTC suppression of airborne transponders. In addition, for some tests, on identical set of ARTS III parameters was obtained for the test aircraft. Since this aircraft was flying a prescribed pattern and was being tracked by the NAFEC ARTS III systems, the analysis of these data when correlated with the ASTC suppression rate measurement made in the test aircraft has provided an in depth examination of the potential for ASTC reply masking to interrogations from a selected interrogator. The probability of detection for targets-of-opportunity in the Atlantic City sector the Islip and Leesburg enroute centers were also determined using listings obtained from the NAS stage A equipment at these facilities. For all tests, observers were stationed at the Philadelphia and Washington TRACONS and the Islip and Leesburg enroute centers. These observers were in communication with the test director at NAFEC such that immediate feedback of any observed qualitative interference could be relayed to NAFEC. The following statements summarize the results of the analysis.

1. Power level measurements made on the field at NAFEC have provided supporting evidence that the DAS interrogators were operating as planned.
2. At a DAS power of  $P_1 = 350$  watts,  $P_2 = 2.75$  KW and a PRF of  $4 \times$  ASR-4 (1520/sec), no quantitative degradation to the ARTS III target detection and tracking functions for targets-of-opportunity was found in the Philadelphia, Washington or NAFEC ARTS III system. This was true for a wide distribution of target ranges and azimuths at all sites where data were collected and analyzed.
3. No quantitative degradation to the ARTS III target

detection or tracking of any of the test aircraft was observed when the ASTC interrogators were activated at a power levels of  $P_1 = 350$  watts,  $P_2 = 2.75$  KW and a PRF of 4 x ASR-4 (1520/sec). This was true for test aircraft ranges varying from 0 miles to 60 miles from NAFEC and for flight paths placing the aircraft within either or both of the scanning limits of the master or slave interrogators.

4. At a DAS power of  $P_1 = 350$  watts and a PRF of 4 xASR-4 (1520/Sec), the data appears to be inconclusive with respect to actual degradation of target hit lengths. A slight reduction in hit length ( $\sim 1$  hit/scan) appears to be present in the data for both the targets-of-opportunity and test aircraft, however, this loss is too small to substantiate statistically valid conclusions. It is therefore recommended that additional interference tests be performed at PRFs of 6 x and 8x to investigate effects on the hit length as the PRF is increased above 4x. This test should be performed using the aircraft flying similar patterns to those previously used and should be made with all beacon defruiters activated at NAFEC to represent an operational situation. In addition, it is recommended that in all future tests an interval timer be used to control the ASTC on-off cycles. In some cases data had to be discarded due to uncertainties with respect to the ASTC equipment operation.
5. ASTC suppression counts measured in the test aircraft indicate that the maximum range over which the ASTC signals can activate airborne transponders is 15 to 40 nmi depending on altitude. Although ASTC suppression counts measured in the test aircraft indicate that the system does contribute to the suppression rate experienced by airborne transponders, the overall suppression rate experienced by airborne transponders in the ASTC environment remained below the threshold where significant degradation to the target hit lengths and target detection probability occur (see number 4 above). It is important to recognize that although the ASTC contribution to the airborne suppression rate did not exceed the threshold in the NAFEC interrogator environment and therefore significantly degrade target hit lengths and detection probability, other locations must be evaluated based on testing at those locations.

6. A comparison of ASR-5 and ASR-7 with ASR-4 data at NAFEC (the ASTC suppressions and interrogations were synchronized to occur during the ASR-4 dead-time) reveals that there is no discernible degradation to any of the beacon systems whether or not the system is synchronized to the ASTC system. The results therefore indicate that even nearby unsynchronized ASR or ARSR beacon interrogators will not experience significant degradation from the ASTC system when operated at the PRF and lower level specified above.
7. For the DAS parameter settings specified above, no degradation was introduced to the target detection probability at the New York and Washington ARTCCs. This determination was based on analysis of DART and COMDIG listings from both sites as well as range length and range distribution histograms of the Leesburg's Suitland beacon data.
8. Observers stationed at the Washington and Philadelphia TRACONS and the New York and Washington Centers reported that no qualitative interference was observed by controllers at these sites for any of the test runs.

In conclusion, the analysis indicates that interference should not preclude the successful implementation of the ATRBS - based ASTC system if the ASTC interrogator power level is no greater than  $P_1 = 350$  watts and the ASTC PRF remains below 1520 interrogations per second. It is recommended that additional tests be performed in connections with Option 2 testing at Logan Airport (Boston) to ascertain the maximum limits at which the ASTC system can be operated within the ATRBS environment.

#### C.3.6 VEHICLE EFFECTS

The vehicle, normally an aircraft, is a part of the ASTC environment and will, to some degree, affect the system performance. Earlier tests at NAFECs investigated the effect of shadowing or signal strength loss due to line-of-sight blockage by airframe landing gear, flaps, doors, etc. The value of the loss in signal strength was found to be typically 5-7 dB with a 15 dB maximum for the DC-6, Gulfstream I, and Aerb Commander aircraft. During DAS testing at NAFEC, a series of tests were conducted to acquire data to measure the effect in terms of variations in system accuracy, errors, and lost or false targets. These tests, designated L-O-S Blockage in Table C-1, used the DC-6 and CV-580 aircraft loacted at various benchmarks, rotated to different headings with flaps up/flaps down configurations.

Only a small portion of the data taken was analyzed due to the limited funds available. A typical test consisted of positioning a CV-580 aircraft at point B95 (about 0.85 nmi from the Master Station) and interrogator power set of 7dB above the theoretical Minimum Triggering Level (MTL) value for a nominal transponder at that range to allow for nominal azimuth shadowing loss. The aircraft was rotated essentially in place. A round reliability of greater than 90% was observed with a continuous update rate of about four samples per second during the complete turn. During other moving target and approach monitor tests, vehicle effects did not prevent obtaining continuous data from a Gulfstream aircraft taxiing down runway 4-22 or from a Cessna 172 taxiing along runway 8-26.

These results were essentially as predicted. The effect of azimuth shadowing added to the signal strength loss due to vertical multipath is within the range of the system performance budget established by analysis. Vehicle effects will not prevent the successful use of the existing transponder on the surface by a beacon based ASTC DAS. While much more data on representative types of aircraft is required for a thorough analysis and determination of complementary DAS performance specifications, the ultimate systems analysis trade-off will be cost (gain of each DAS antenna and number of stations required) versus coverage given a defined population of aircraft types. Rare or unusual aircraft possessing particular problems would be cost-effectively handled as special cases where it would be known to the controller that surveillance coverage would not be provided in specific areas of the airport.

APPENDIX D:

SUMMARY OF WORK ACCOMPLISHED

UNDER CONTRACT OPTION 1

Contract Option 1 for Logan and O'Hare Test planning and DAS hardware augmentation design, was exercised on 15 May 1975. In addition to preparing field test plans, a design study was conducted to determine the most effective manner of augmenting the DAS with a capability for real-time performance evaluation. The modified DAS would provide semi-automatic tracking of a limited number of surface targets and eliminate the manual control and programming used during NAFEC testing. The phased array antennas would be modified to provide greater resolution at maximum range. Most important under the proposed augmentation would be real time engineering display. This display would be operated in parallel with the recording of data on magnetic tape for off-line computer processing. These changes would be amenable to future upgrading of the DAS without redesign of existing hardware to provide fully automatic operation.

An application for temporary operation of the brassboard DAS at Logan was submitted and has been approved by the FAA. This application included proposed DAS site locations, obstruction clearances, and an evaluation of radio/radar navigation and communication interference. Preliminary meetings with Massachusetts Port Authority representatives have been held and the Logan installation can proceed as funds for option 2 are made available.

APPENDIX E

REFERENCES

1. Trilateration Data Acquisition Subsystem (DAS) Analysis and Test Outline Report, Interim Report, Bendix Communications Division Report 489A01, 1 August 1974.
2. Task 1A Critical Issues Working Paper, Interim Report, Bendix Communications Division Report 489A02, Revision A, 6 March 1975.
3. A Beacon Trilateration Data Acquisition Subsystem: Interim Design Report, Bendix Communications Division Report 489A04, Revision A, 28 February 1975.
4. Department of Transportation, Federal Aviation Administration Order 1010.51A, U.S. National Aviation Standard for the Mark X (SIF) Air Traffic Control Radar Beacon System (ATCRBS) Characteristics, 8 March 1971.
5. J. D. Vinatieri, Experimental Measurements of Beacon Antenna Radiation Patterns for Surface Aircraft, Test Report, MITRE Corporation Report MTR-2780, 26 February 1974.
6. ATCRBS Surface Interrogation and Interference Measurement Program (Measurement at Logan Airport), Test Report, MITRE Corporation Report MTR-2736; Vol. I, 12 December 1973; Vol. II, 28 March 1974.
7. Measurement of ATCRBS Surface Interrogation Environments at Chicago-O'Hare and Los Angeles International Airports Report No. DOT-TSC-FAA-76-17, May 1976.
8. NAFEC Tests of the ATCRBS Based Surface Trilateration System Compatibility with ATCRBS/ARTS III DOT-TSC Report in Preparation.
9. Airport Surface Traffic Control Concept Formulation Study, Report No. FAA-RD-75-120, July 1975.
10. Report of Work Performed Under Option 1 of Contract DOT-TSC-769, Final Report, Bendix Communications Division Report 489A06, October 1975.

APPENDIX F - REPORT OF INVENTIONS

After a diligent review of the work performed under this contract, no innovation, discovery, improvement, or invention was made. The effort was one of investigating existing techniques, phenomena, concepts and building, field testing, and analyzing the results of an experimental system capable of supporting airport surface surveillance. The use of spatial interrogation technique GEOSCAN<sup>®</sup> was developed and patented before the award of this contract (DOT-TSC-769).

## APPENDIX G - DEFINITION OF TERMS

**Airport Surface Traffic Control (ASTC)** - The exercise of commands to promote the safe and expeditious movement of surface traffic.

**Airport Surveillance Radar (ASR)** - Radar providing position of aircraft by azimuth and range data without elevation data. It is designed for a range of 60 miles. Used for terminal approach and departure control.

**Air Traffic Control Radar Beacon System (ATCRBS)** - The present beacon surveillance system which depends upon a network of ground interrogations and aircraft equipped with transponders. Slant range to all equipped aircraft on a given azimuth from the interrogator site is estimated from the time delays associated with the transponder replies. Most transponders built today reply with ATC assigned identity (Mode A interrogation) and pressure altitude (Mode C interrogation).

**Brassboard** - A working model of a device, subsystem or system which is suitable for field evaluation of functional performance and verification of engineering approach. No constraints exercised on form, fit or packaging other than the minimum constraints required to meet the test objectives. Environmental considerations shall be incorporated in the model to the extent required by the test. Standard or approved parts are not required. Special packaging considerations for test purposes may be incorporated such as special test points, dials, meters etc. not intended for the production items or special cabinetry to provide ease of access during testing.

**Fruit** - See Nonsynchronous Garble.

**GEOSCAN** - A method of interrogating discrete aircraft in order to obtain an ungarbled reply utilizing the aircrafts standard ATCRBS transponder. It is based on using a controlled SLS transmission to form a geographically defined reply zone on the order of the size of the aircraft (Bendix patent 3,870,994).

**Ground Control** - ATC service provided by an airport traffic control tower for vehicles operating on taxiways between the ramp area and the active runways.

**Guidance** - The resultant effect upon a vehicle that moves it in a desired direction; the effect being in response to controls exercised by a person or mechanism inside the vehicle.

Interrogation - Transmission of a signal intended to trigger a transponder.

Interrogator - The ground based surveillance radar beacon transmitter receiver which scans in synchronism with a primary radar, transmitting discrete radio signals which repetitiously request all transponders, on the mode being used, to reply.

Mode 3/A Interrogation - Civil and military interrogation of transponder asking for aircraft identification code.

Mode C Interrogation - Civil transponder interrogation asking for aircraft altitude.

Multipath - Electromagnetic energy arrival at a receiver via indirect path(s) from the source as a result of reflections from either the ground or from other external reflectors such as another aircraft, own aircraft structure, or buildings.

Nonsynchronous Garble - Transponder responses inadvertently picked up by a given interrogator different from the one triggering the response. The result is that the ground station picks up a signal that is not synchronous with the interrogation signal. Also called total fruit.

Primary Radar - That form of radar that depends upon the reception of reflected electromagnetic energy for the detection of objects in the area under surveillance.

Secondary Surveillance Radar (SSR) - The international term for that Air Traffic Control Radar Beacon System (ATCRBS).

Surveillance - The observation, by any means, of an area, place, airspace, lane of approach, or field of activity, in order to be informed of events and actions as they occur in the place under observation.

System/Subsystem - An aggregate of components, software etc. which are functionally related and in which each component or part acts or interacts with the others in accordance with the overall design. A system is frequently comprised of smaller groups of functionally related components which may be separately identified. These sub groups are termed subsystems. The distinction between system and subsystem is one of scope. For example, the Advanced Surveillance System is a subsystem of the Airport Surface Traffic Control System which in turn could be thought of as a subsystem of Air Traffic Control.

Transponder - An airborne automated radar receiver transmitter from which a coded response is triggered by interrogation from a ground transmitter. Response normally contains information on aircraft identification altitude and airspeed, and occasionally, heading, altitude rate and position. See Interrogation.

Triilateration - A system that computes the location of vehicles by utilizing the differences among the times of arrivals at pairs of receiving sites which generate hyperbolic lines of position the intersections of which determine the position of the vehicle.